Smart Mitigation of flow-induced Acoustic Radiation and Transmission for reduced Aircraft, surface traNSport, Workplaces and wind enERgy noise

Acoustic Control And Materials

N. S. Khodashenas, M. D'Elia, T. LAURENCE, F. A. Pires, E. De Bono

ESRs n°3, 4, 5, 10, 12.

M24 SmartAnswer Mid-term Meeting Leuven

THE FRAMEWORK PROGRAMME FOR RESEARCH AND INNOVATION
HORIZON 2020
MARIE CURIE ACTIONS
H2020 MARIE SKŁODOWSKA-CURIE ACTIONS

General introduction

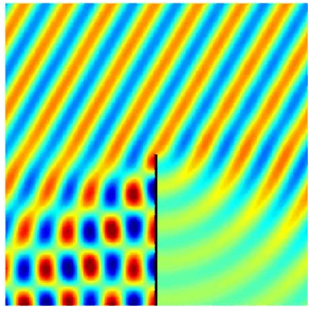

Acoustic Control
And Materials

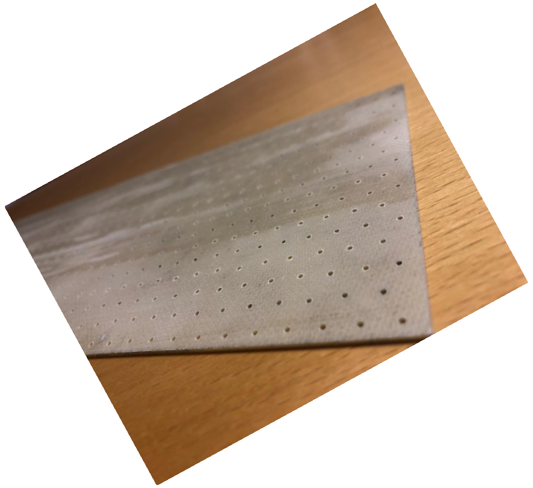

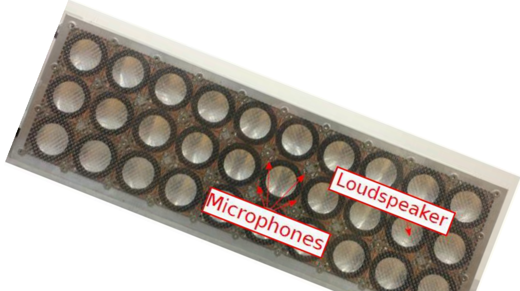

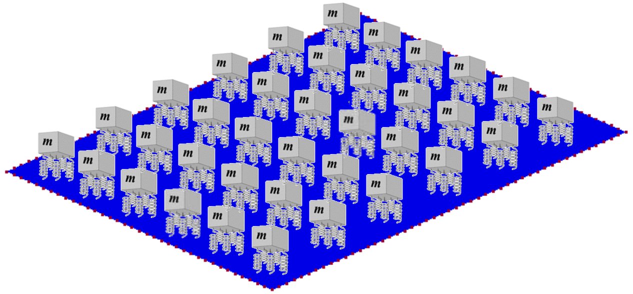

Part 1: Development of Intelligent Lightweight Material Solutions for Improved Vibro-Acoustic Transmission Problems

Felipe Alves Pires

H2020 MARIE SKŁODOWSKA-CURIE ACTIONS

NVH challenges

Noise, Vibration and Harshness challenges

Ecological trend

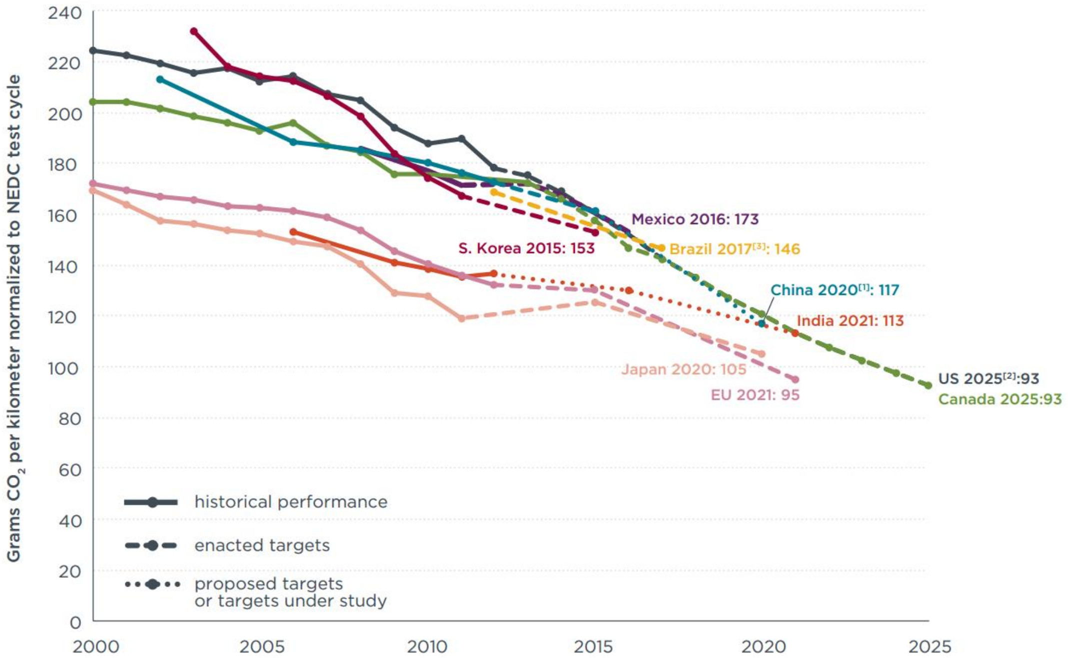

[1] China's target reflects gasoline vehicles only. The target may be higher after new energy vehicles are considered.
[2] US standards GHG standards set by EPA, which is slightly different from fuel economy stadards due to low-GWP refrigerant credits.
[3] Gasoline in Brazil contains 22% of ethanol (E22), all data in the chart have been converted to gasoline (E00) equivalent
[4] Supporting data can be found at: http://www.theicct.org/info-tools/global-passenger-vehicle-standards

Reducing emissions

Reducing fuel consumption

Lightweight design

Worse NVH properties

Novel NVH solutions

Metamaterials

Vibro-acoustic metamaterials

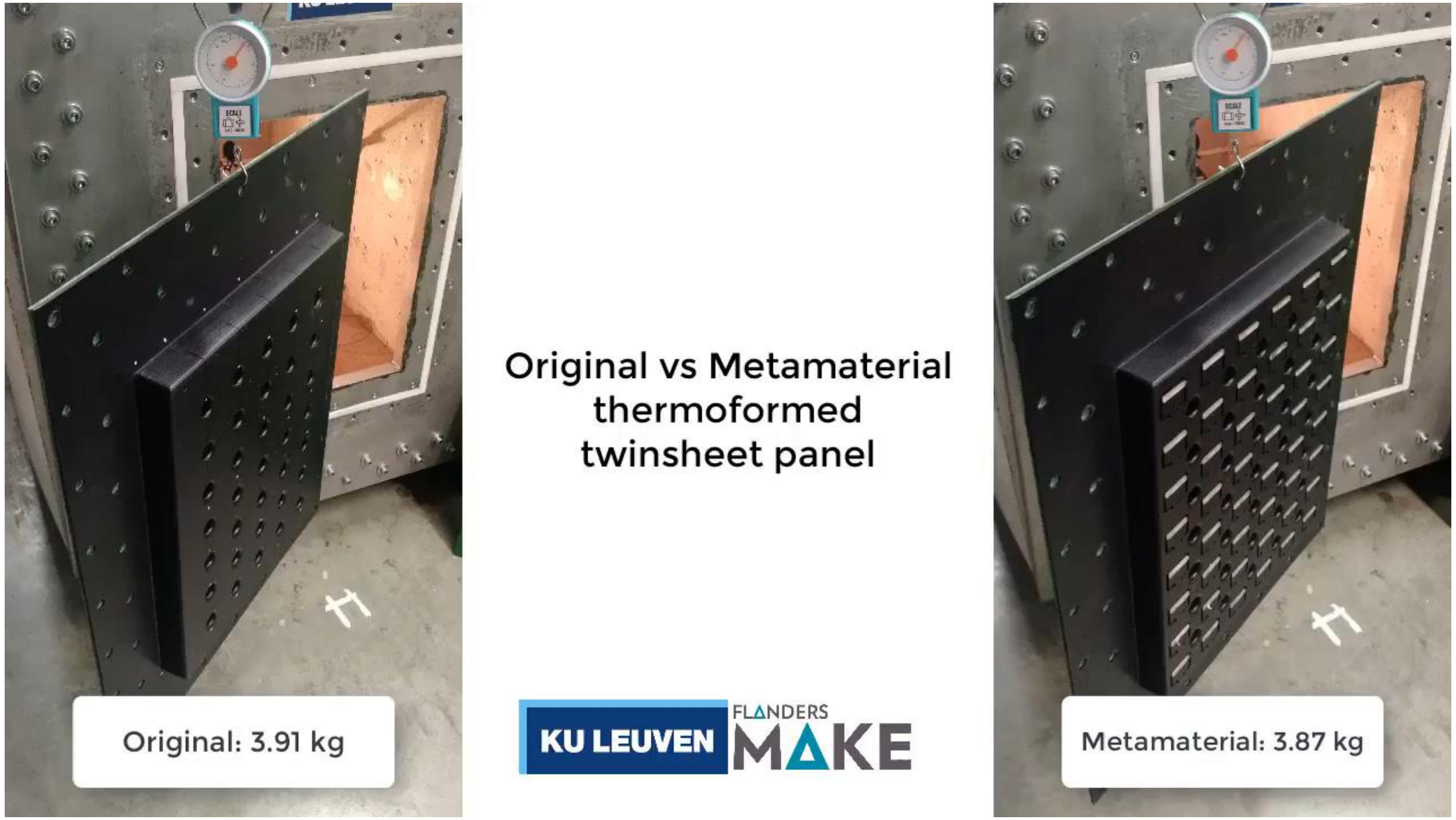

Metamaterials

Vibro-acoustic metamaterials

HOW?

Stop bands

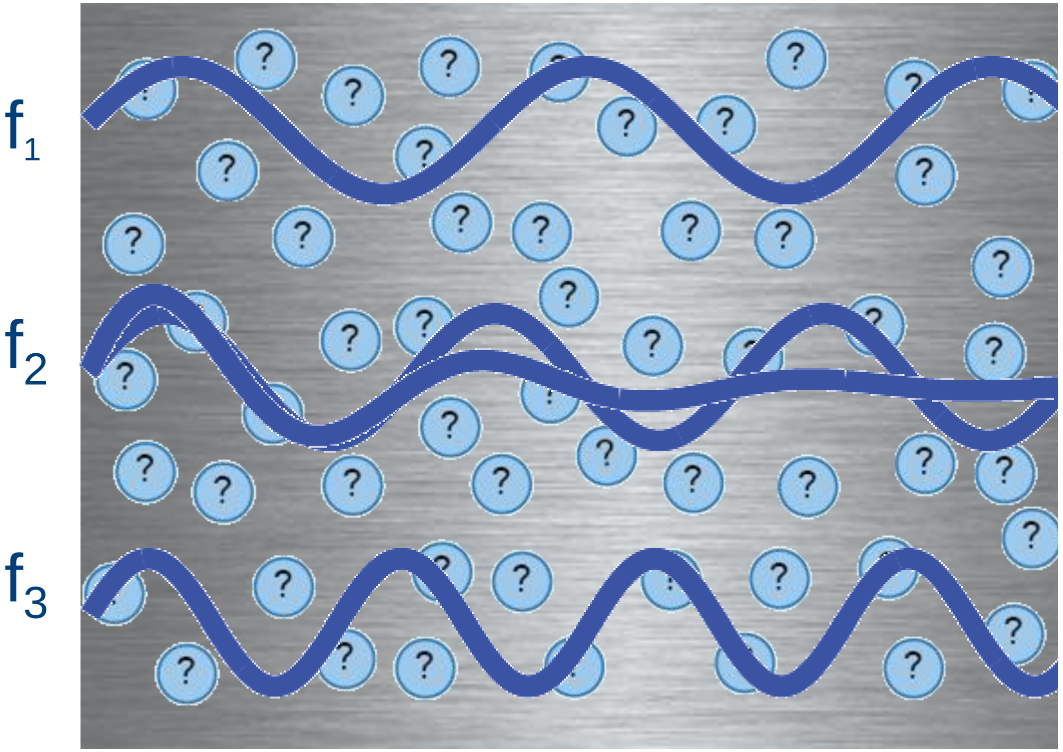

Resonant inclusions on a subwavelength scale

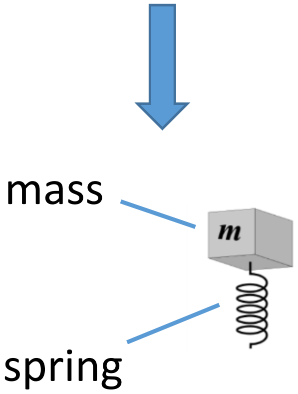

TVA: Tuned vibration absorber

(2)Liu, Z., et al. "Locally resonant sonic materials." science 289.5485 (2000).

Metamaterials

Vibro-acoustic metamaterials

- Stop band prediction
  - ➢Bloch-Floquet Theorem
  - ➢Unit cell modeling utilizing a FE approach

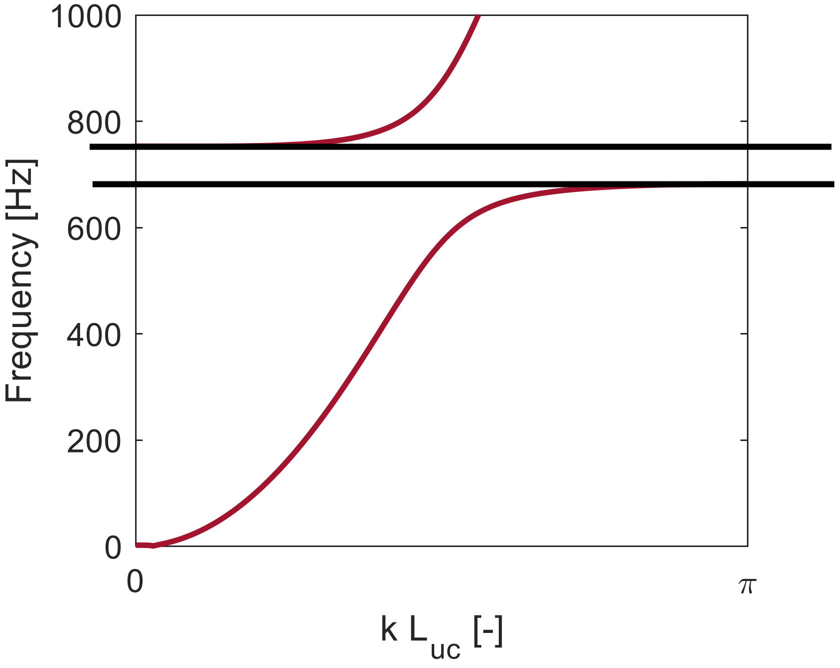

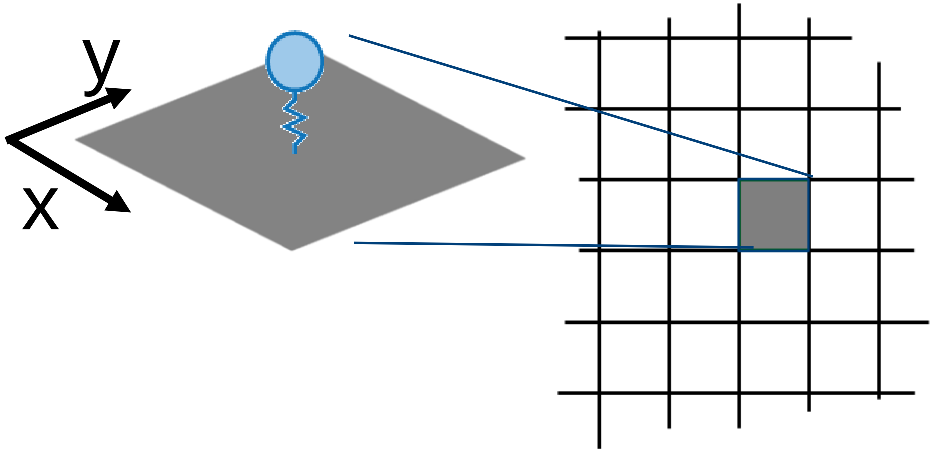

(3)Goffaux, C., et al. Evidence of Fano-like interference phenomena in locally resonant materials. Physical review letters 88.22 (2002).
(4)Brillouin, L. Wave propagation in periodic structures: electric filters and crystal lattices. Courier Corporation, 2003c.
(5)Hussein, I. Reduced Bloch mode expansion for periodic media band structure calculations. Proceedings of the Royal Society of London A: Mathematical, Physical and Engineering Sciences. The Royal Society, 2009.

Metamaterials

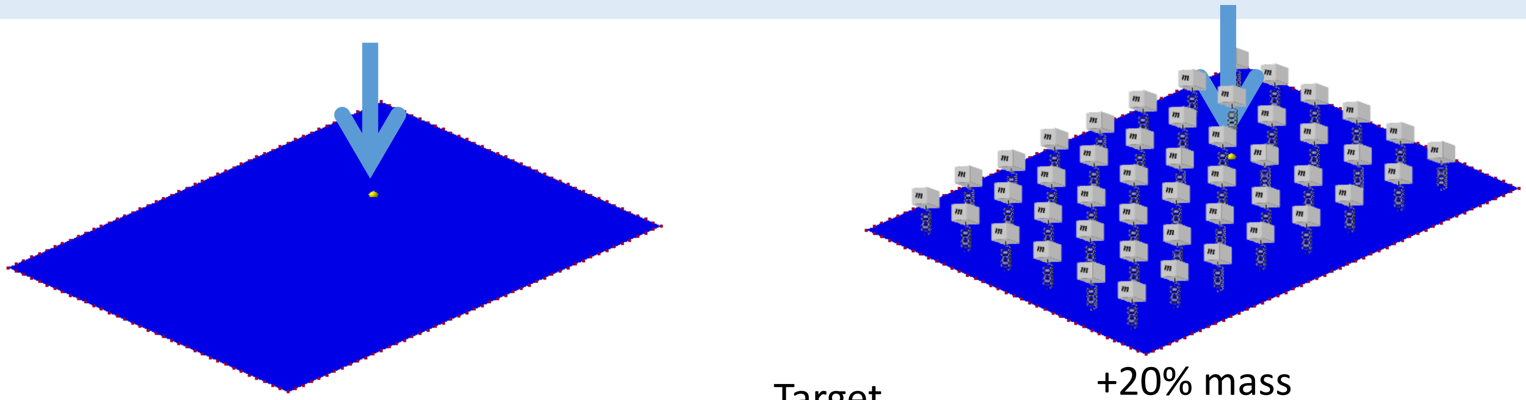

+20% mass

Target

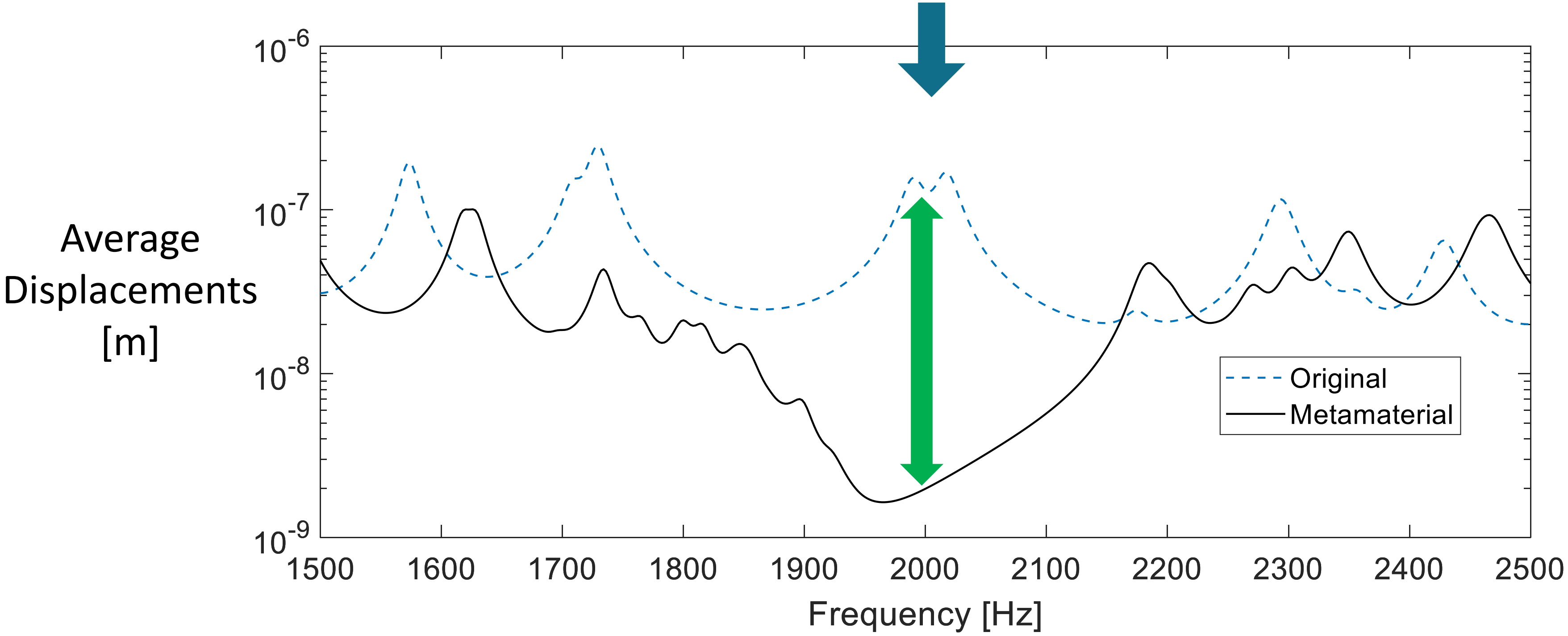

Objectives

Investigate design parameters that influence stop bands

Footprint of resonators

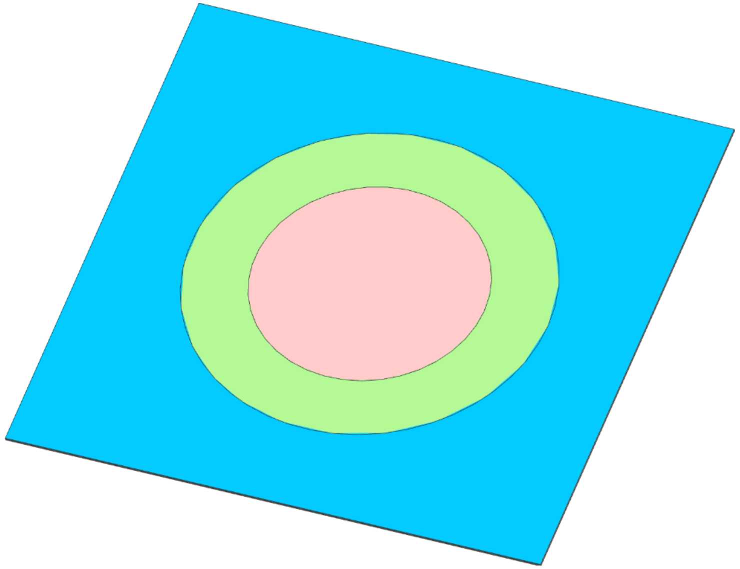

Methodology

- Infinite and Finite problems
  - Using modified TVAs

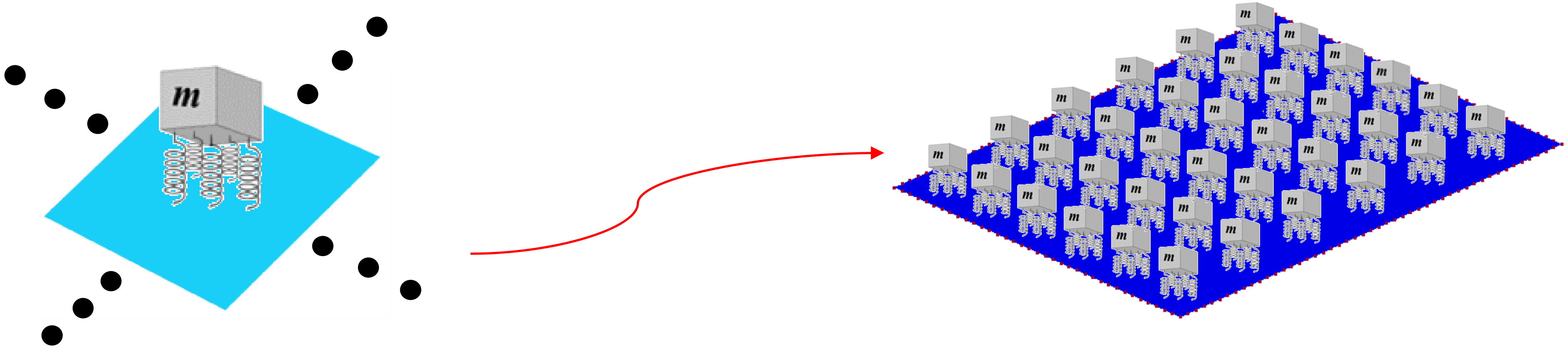

Infinite

Finite

Footprints

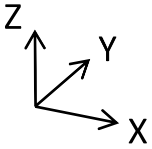

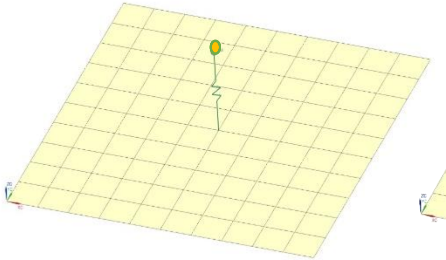
0%

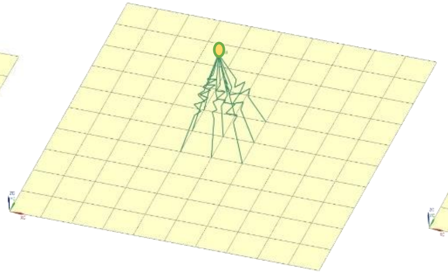
20%

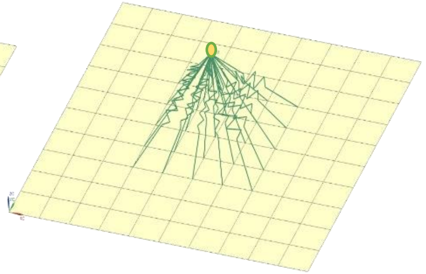
40%

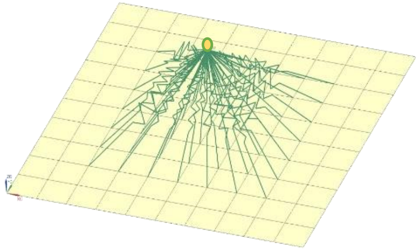
60%

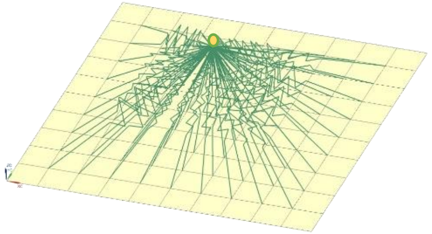
80%

20% mass addition

Change stiffness

Numerical Results

Infinite Plates

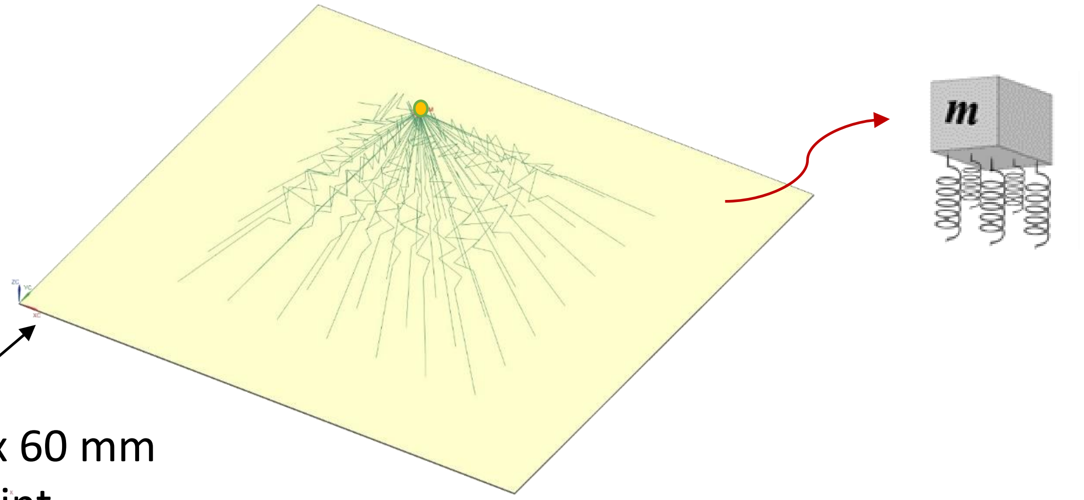

Unit cell: 60 x 60 mm
Bigger footprint

Numerical Results

- Stop bands width x Footprint
  - f_{res} = 2000 Hz

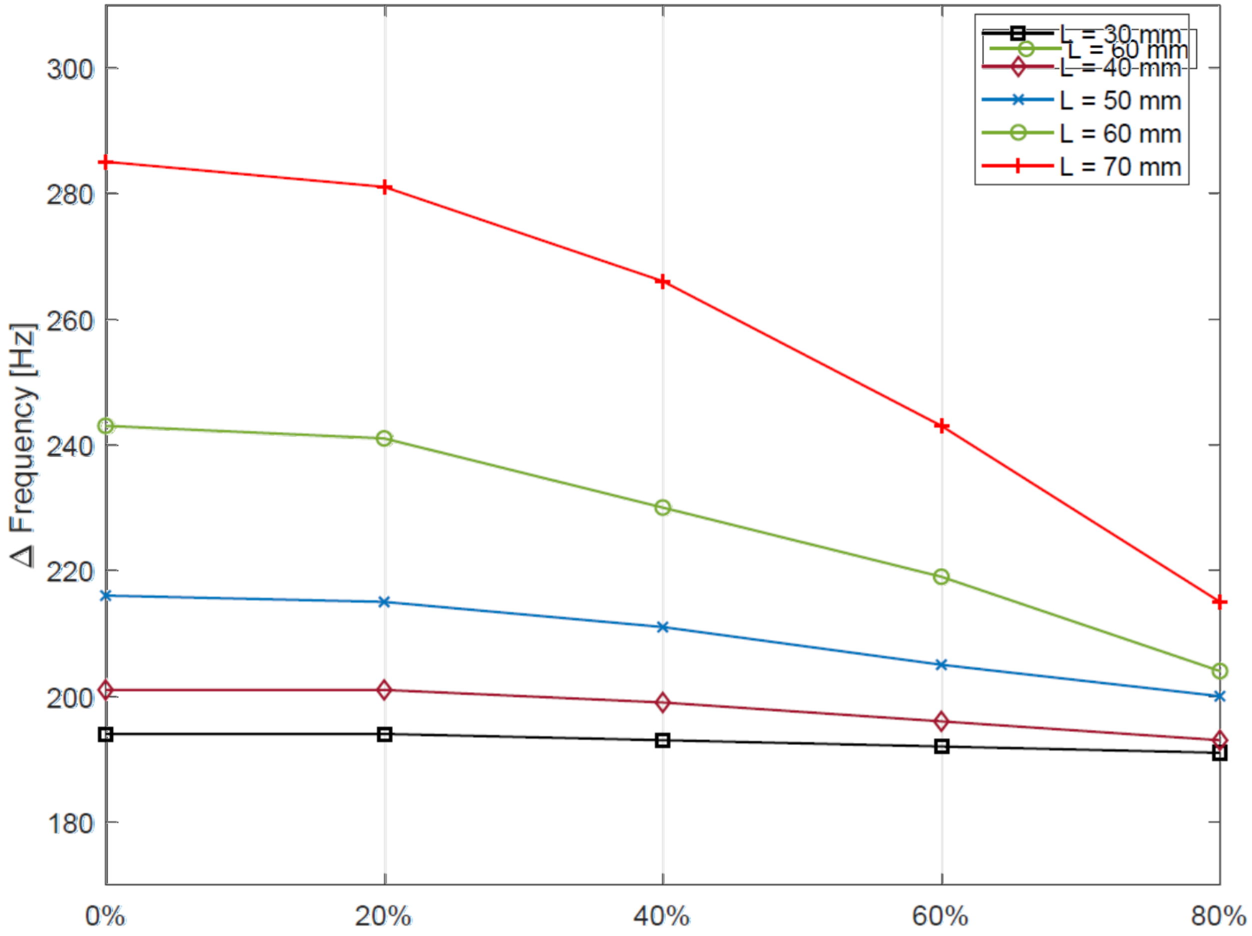

Finite Plates

Displacements

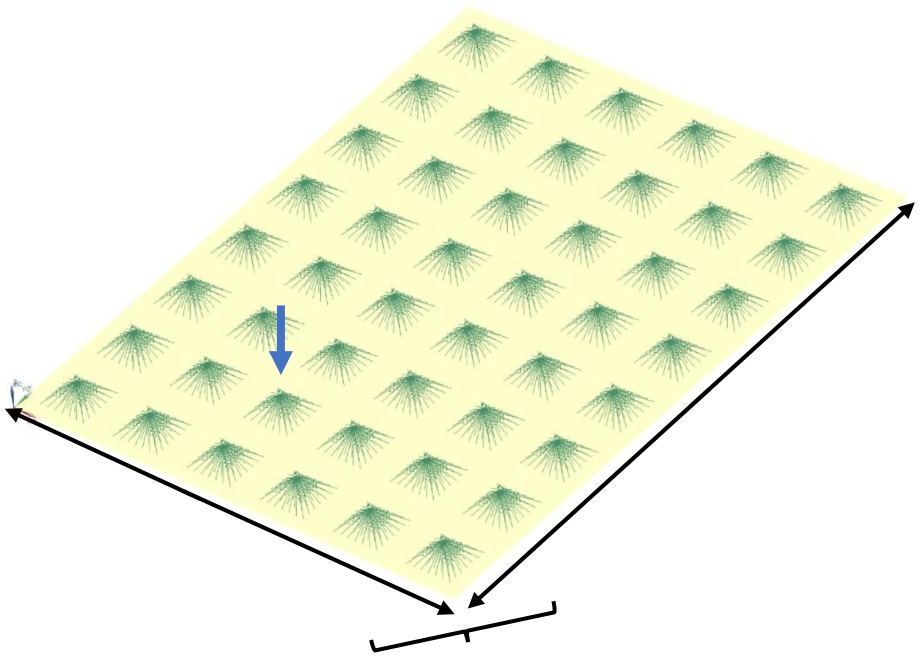

Simply supported

Fahy, Frank J., and Paolo Gardonio. Sound and structural vibration: radiation, transmission and response. Elsevier, 2007.

Numerical Results

- RMS Displacements
  - Resonators tuned to 2000 Hz

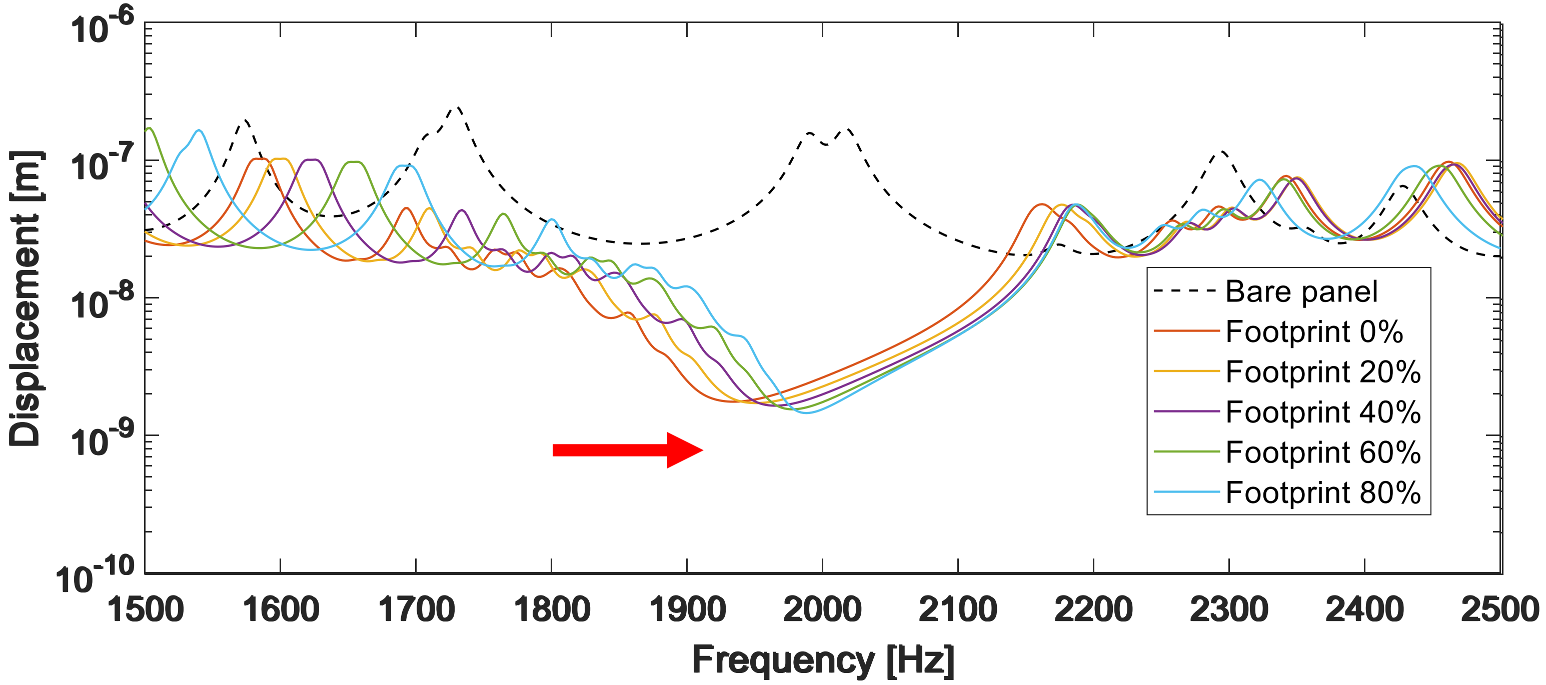

Experimental Validation

Experimental validation

- Finite aluminum beams:

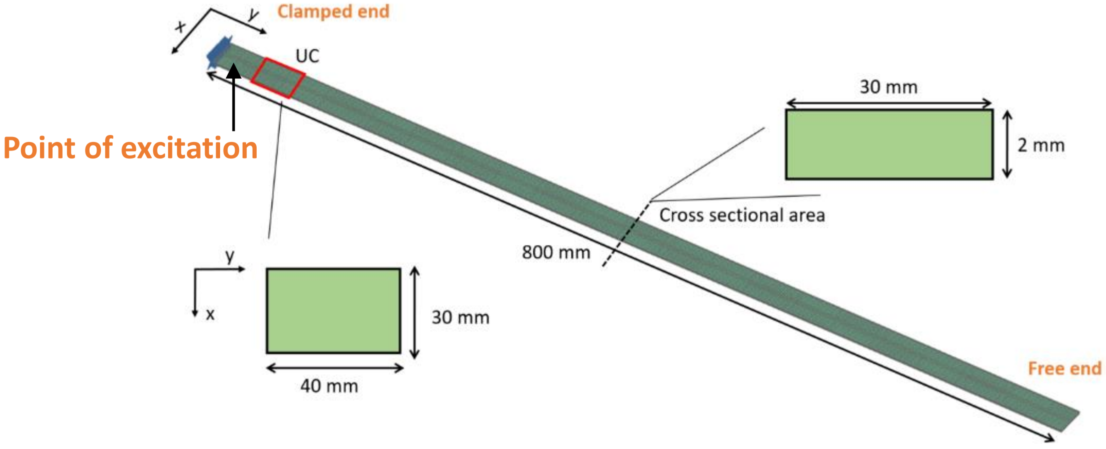

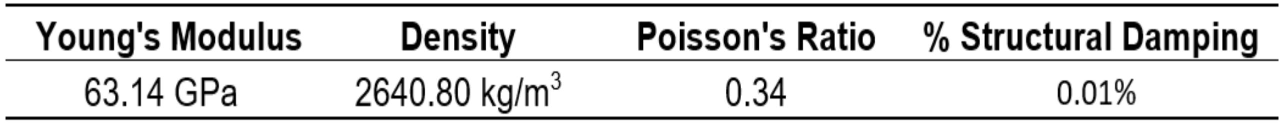

Young's Modulus	Density	Poisson's Ratio	% Structural Damping
63.14 GPa	2640.80 kg/m^3	0.34	0.01%

Material properties of aluminum.

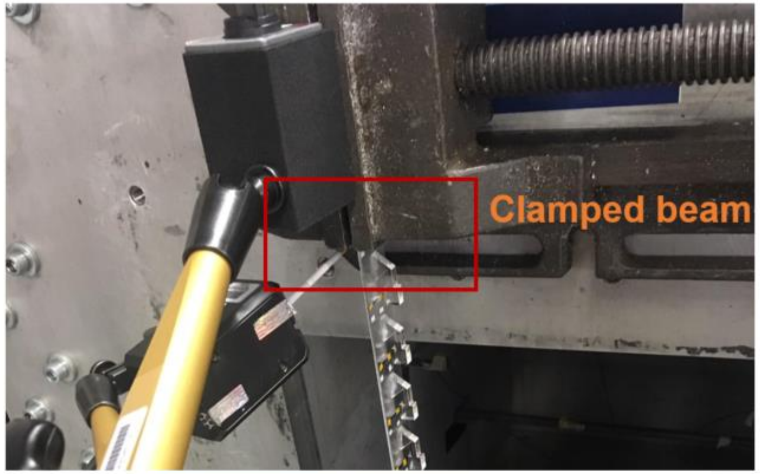

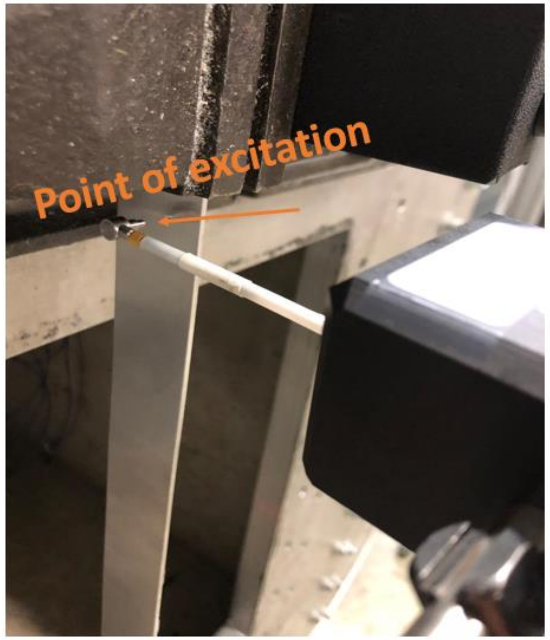

Experimental validation

- Resonators with different footprints:

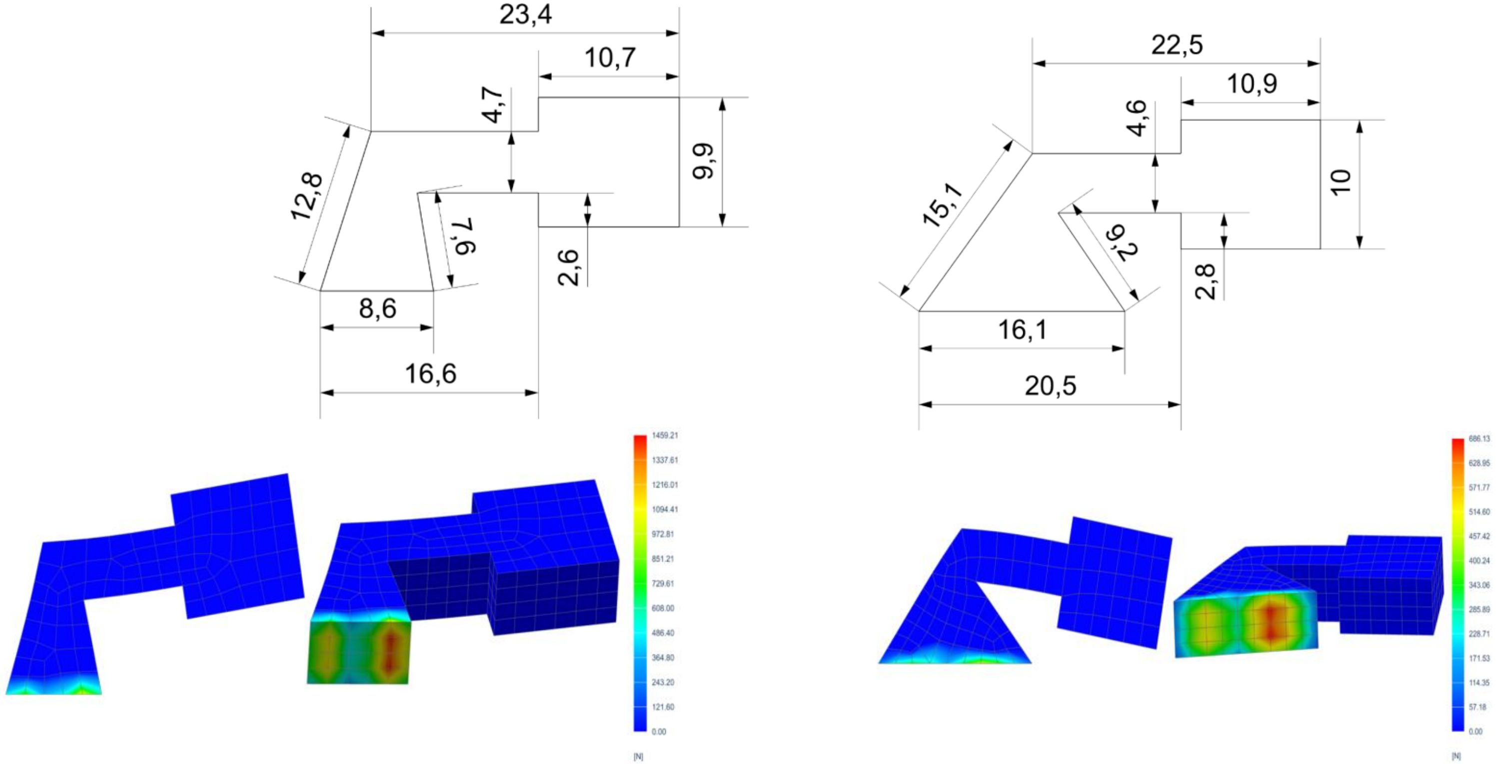

Young's Modulus	Density	Poisson's Ratio	% Structural Damping
4850 MPa	1188.38 kg/m^3	0.31	5%

Material properties of plexiglass.

Experimental validation

- Resonators with different footprints:

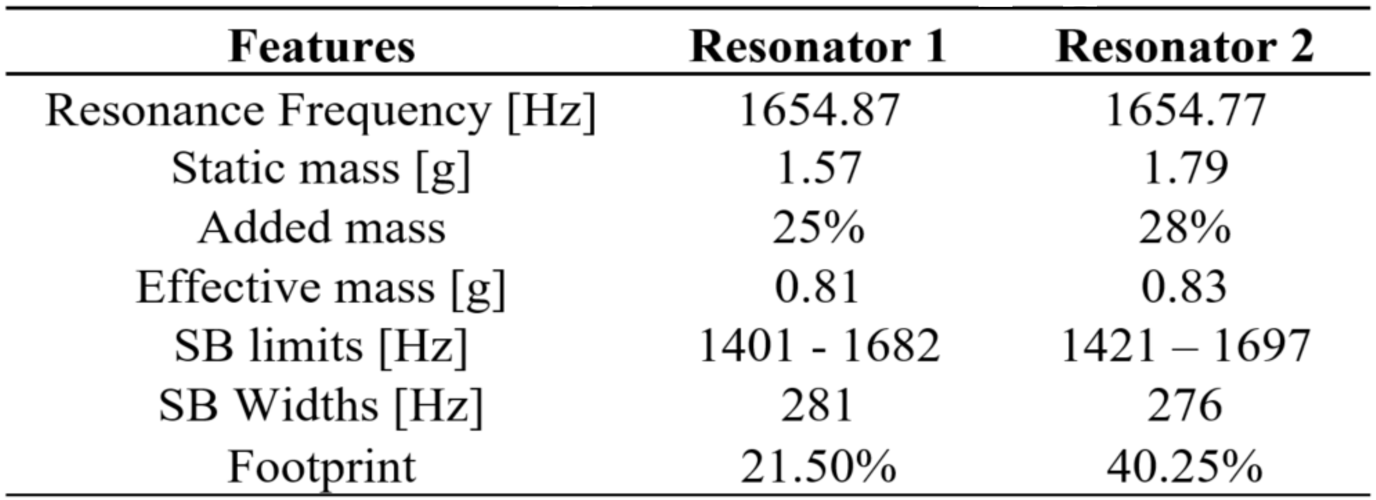

Features	Resonator 1	Resonator 2
Resonance Frequency [Hz]	1654.87	1654.77
Static mass [g]	1.57	1.79
Added mass	25%	28%
Effective mass [g]	0.81	0.83
SB limits [Hz]	1401 - 1682	1421 – 1697
SB Widths [Hz]	281	276
Footprint	21.50%	40.25%

Resonators features numerically acquired.

Experimental validation

- Realized resonators with different footprints:

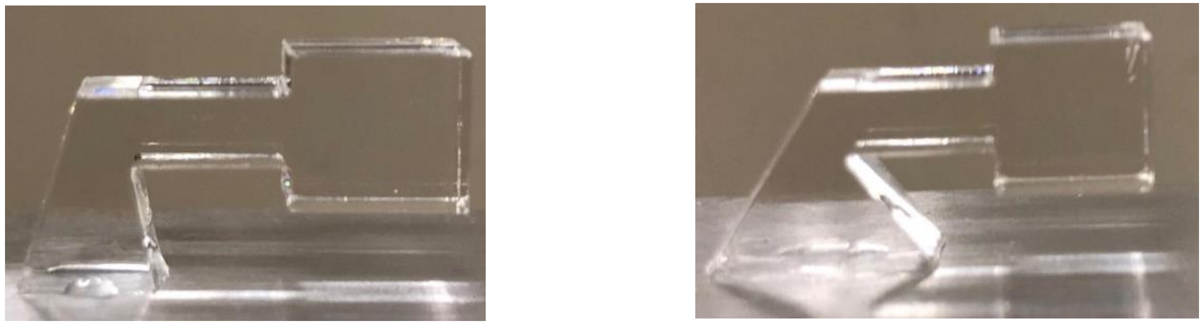

Samples of laser cut resonators (Left) Type 1 (Right) Type 2.

Resonator	Numerical (Hz)	Experimental (Hz)	% Standard Deviation
Type 1	1654.87	1655.20 ± 3.66	0.22
Type 2	1654.77	1654.30 ± 3.64	0.22

Comparison between the simulated and measured resonance frequencies for the 2 types of resonators.

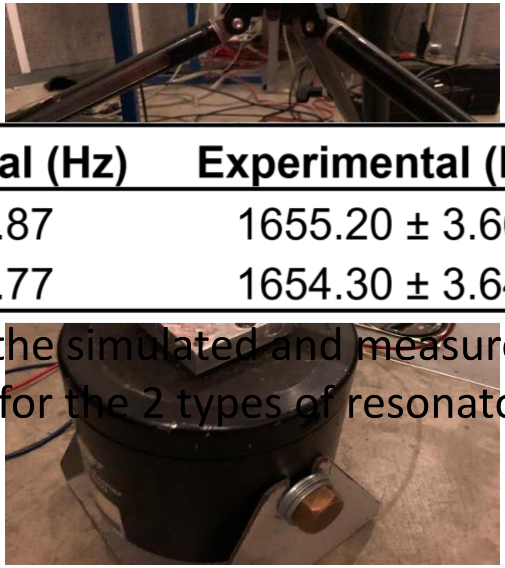

Test set up to retrieve the resonance frequency of the resonators.

Experimental validation

- Predicted stop bands:

1)

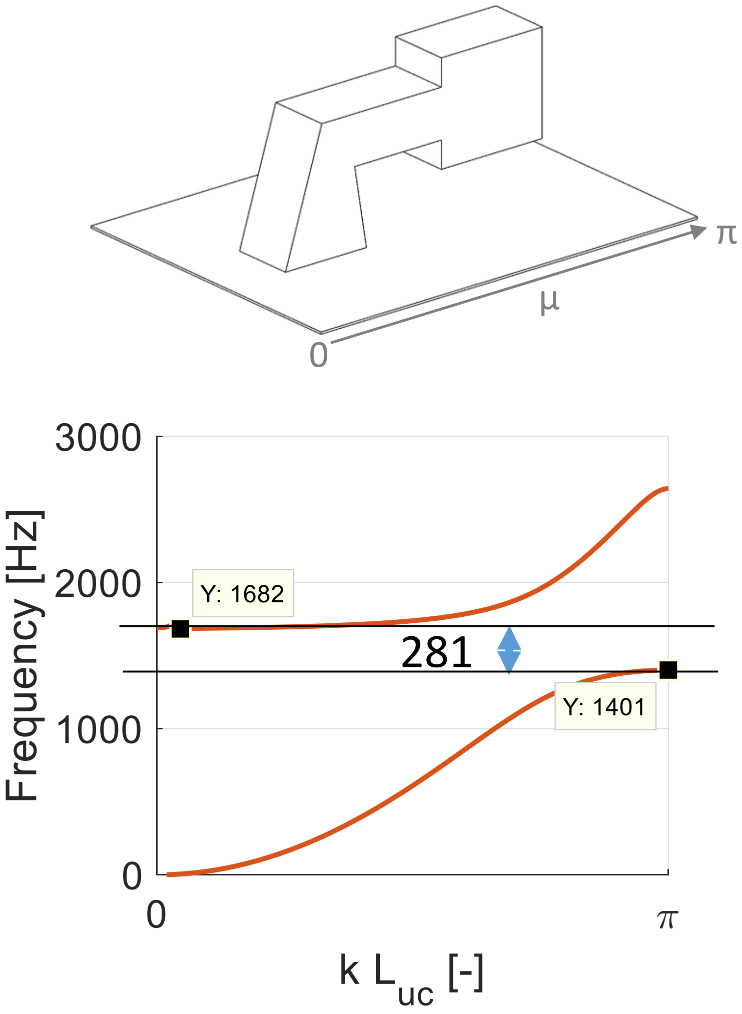

2)

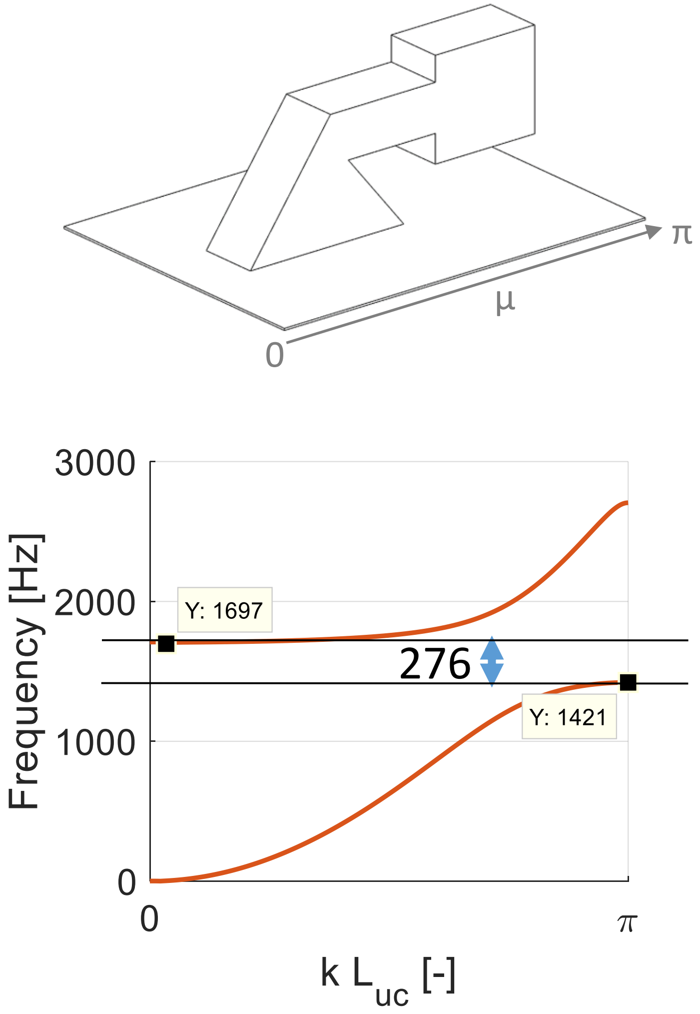

Experimental validation

- Comparison of FRFs of the metamaterial beams:

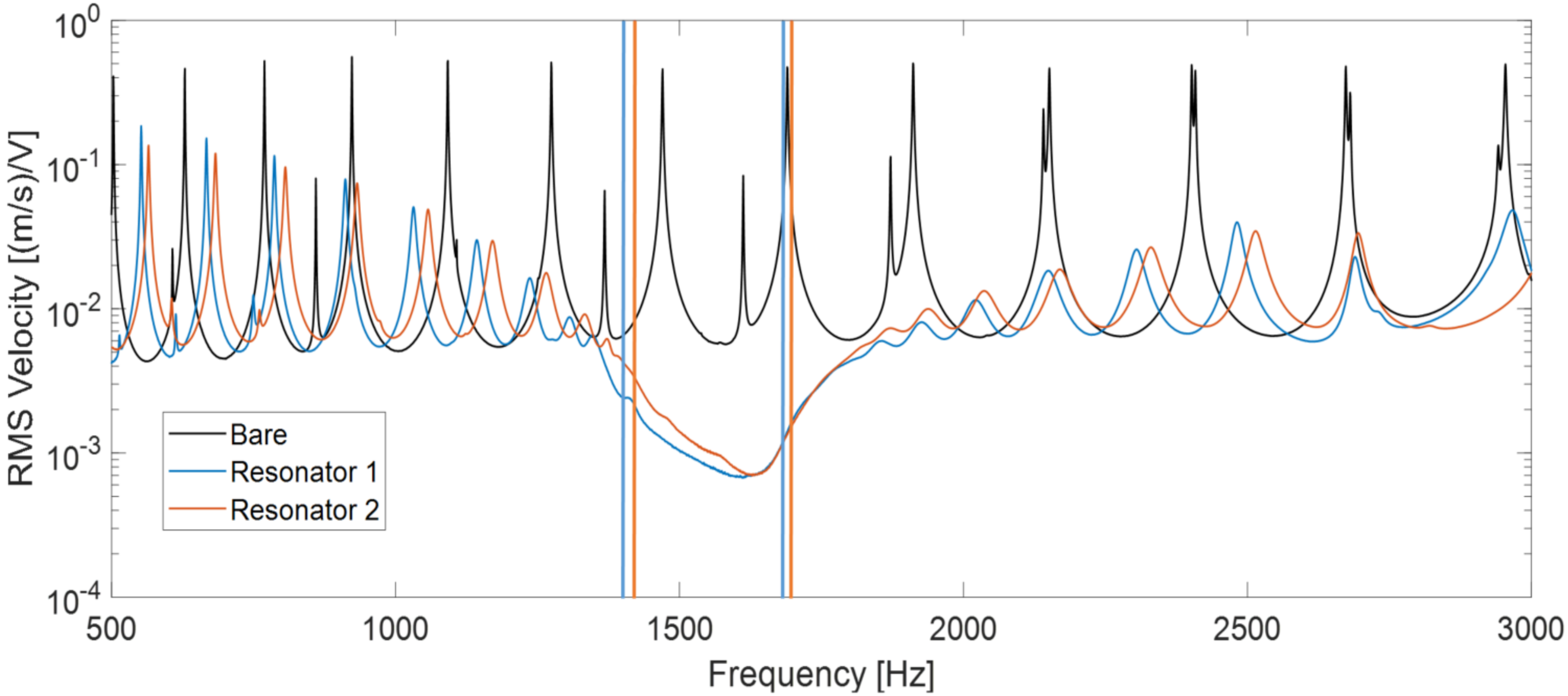

Comparison of experimental FRFs for the bare beam and the beams with resonators.

Concluding remarks

- Novel NVH solution;
- Resonance based stop bands;
- Influence of footprint:
    - Stop bands' widths;
    - Experiments comply with numerical study;
    - Footprint of resonators need to be taken into account.

Future steps

- Experimentally investigate the footprint concept in 2D finite structures
  - Structural vibrations
  - Insertion Loss (IL)

- Design and produce a metamaterial fuselage panel as a demonstrator;

- Test and validate the metamaterial panel on the fuselage setup at ADE.

Smart Mitigation of flow-induced Acoustic Radiation and Transmission for reduced Aircraft, surface traNSport, Workplaces and wind enERgy noise

Part 2: Liner Impedance Control, Stability investigations

Emanuele De Bono

M24 SmartAnswer Mid-term Meeting Leuven

H2020 MARIE SKŁODOWSKA-CURIE ACTIONS

Ultra-High Bypass Ratio turbofan engines

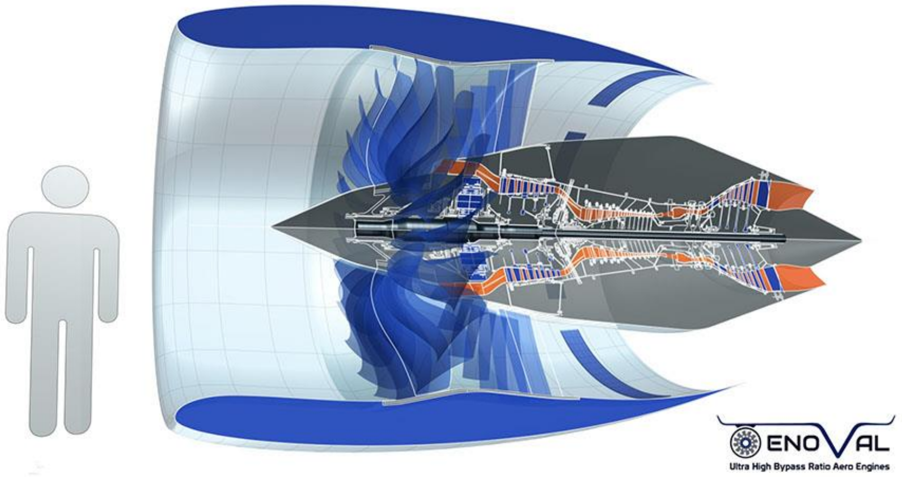

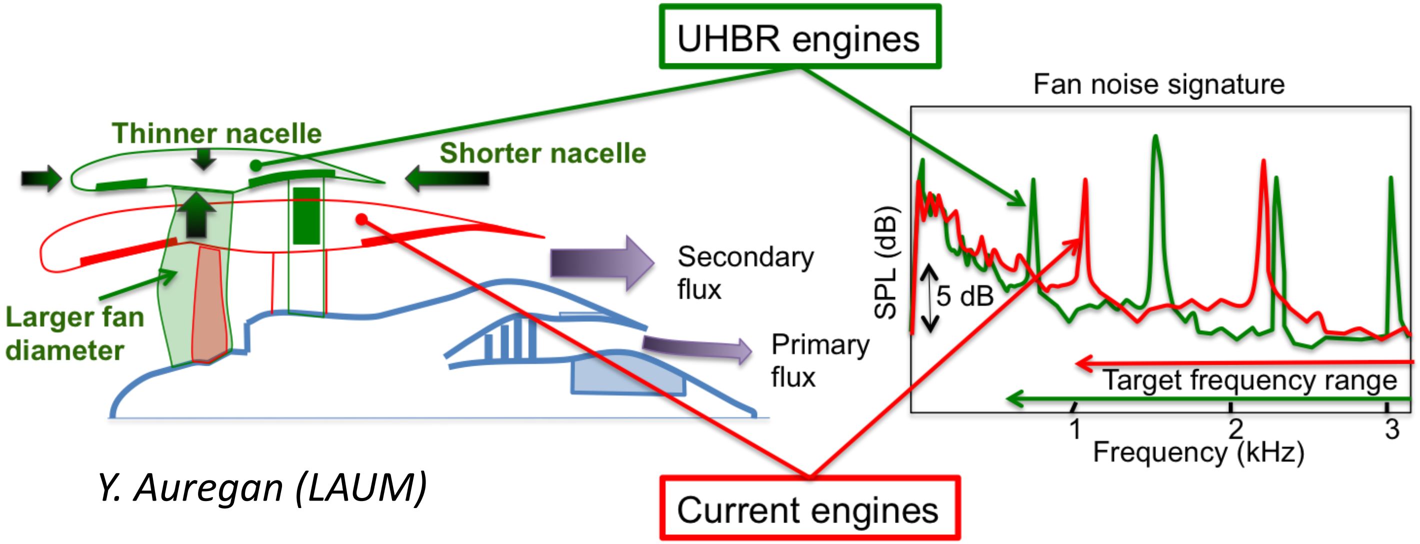

Y. Auregan (LAUM)

Acoustic Liners for Turbofan

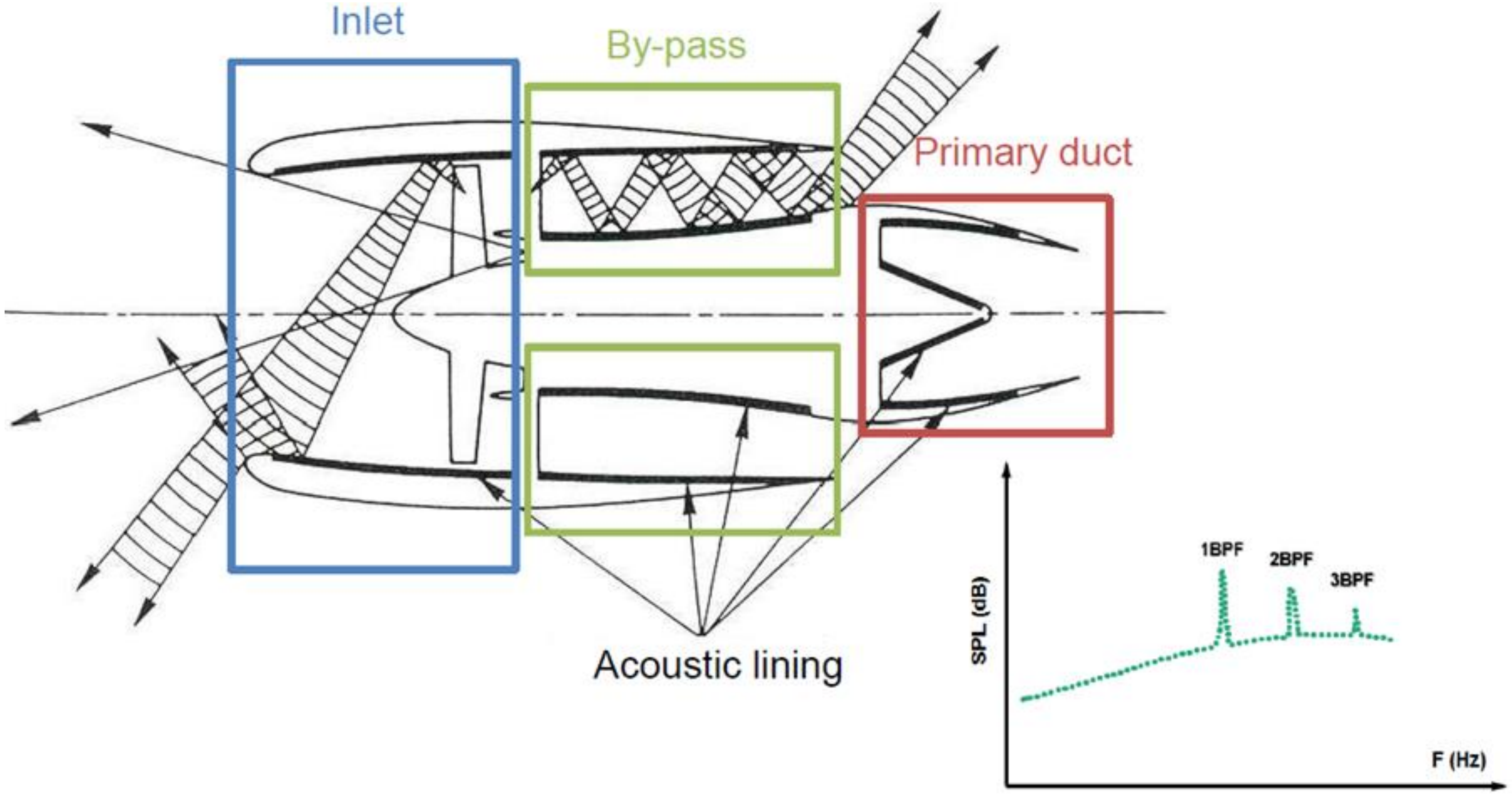

Credits: SAFRAN Nacelles; Karkar et al., Internoise 2015

State of the art in Industrial Application

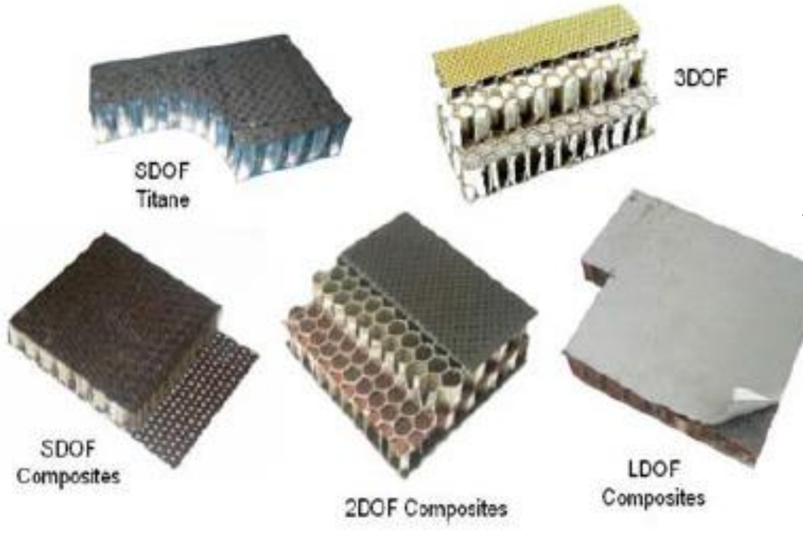

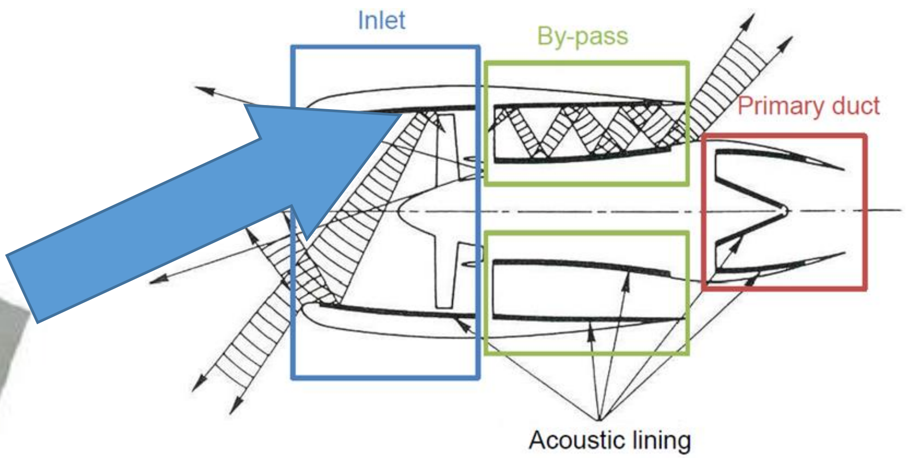

SAFRAN Nacelles

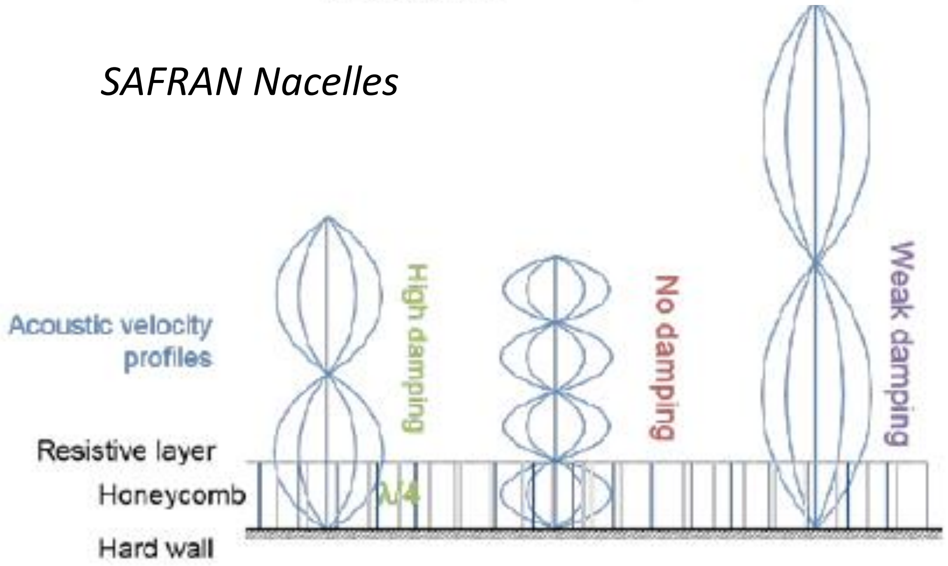

Main limitations:

- Narrow bandwidth.
- Too thick for LF (quarter wavelength resonators)

Need for:

- Wideband concept
- Efficient at lower frequencies
- Reasonable thickness (50mm)

State of the art in Research

“Acoustic Metamaterials”

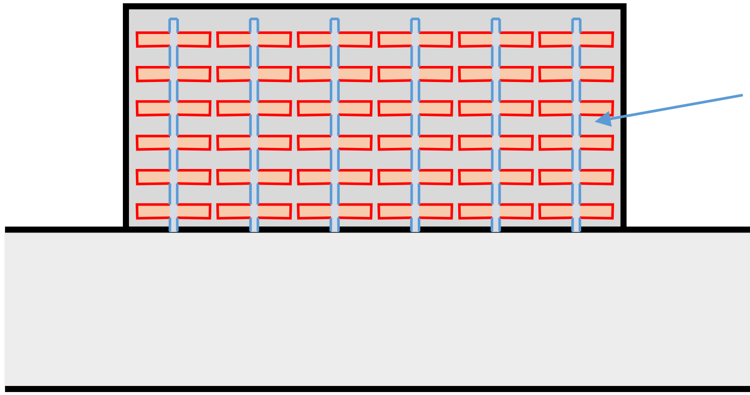

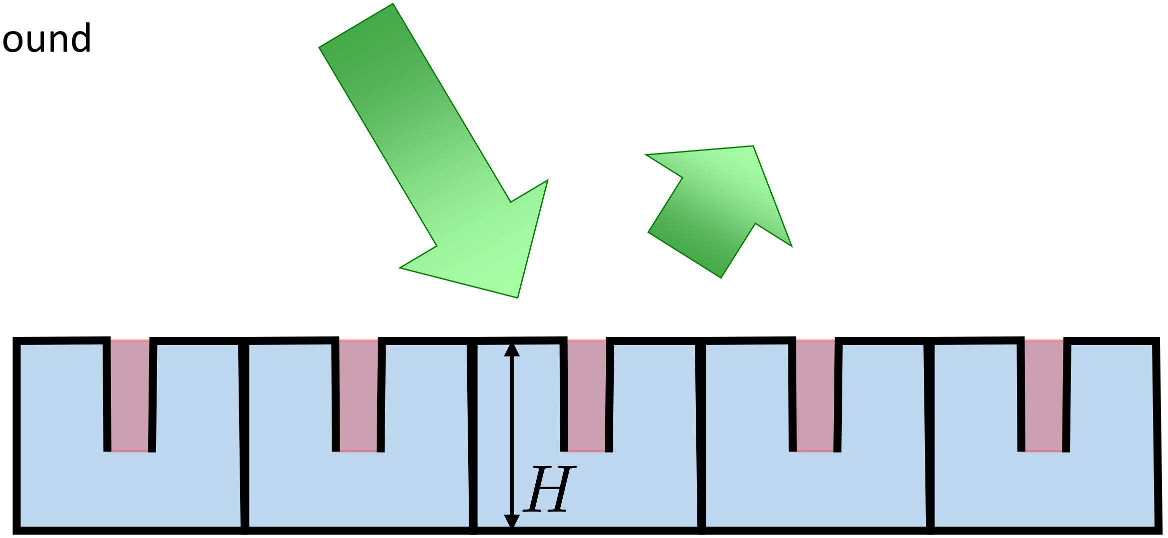

Can be efficient for $H \ll \lambda$

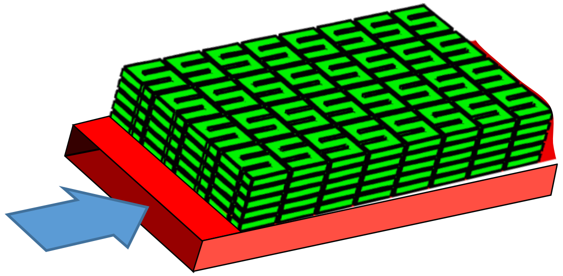

Subwavelength structures

Credits: Y. Auregan (LAUM)

Proposed Active Concept

SAFRAN

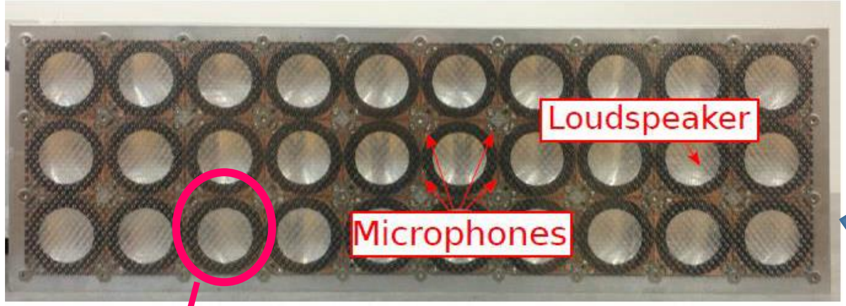

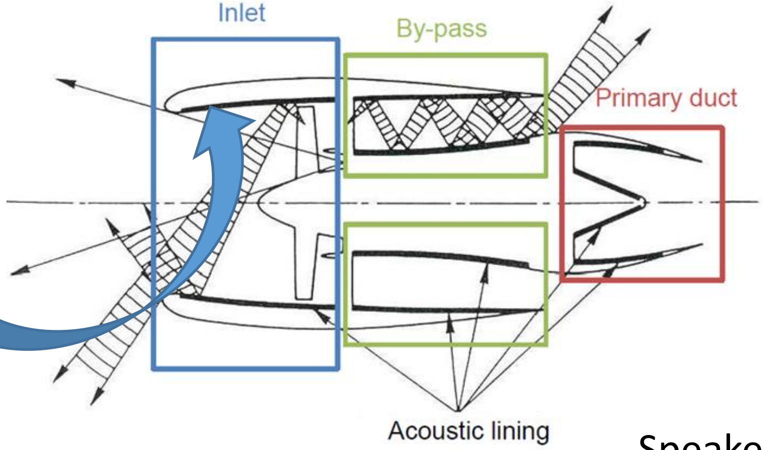

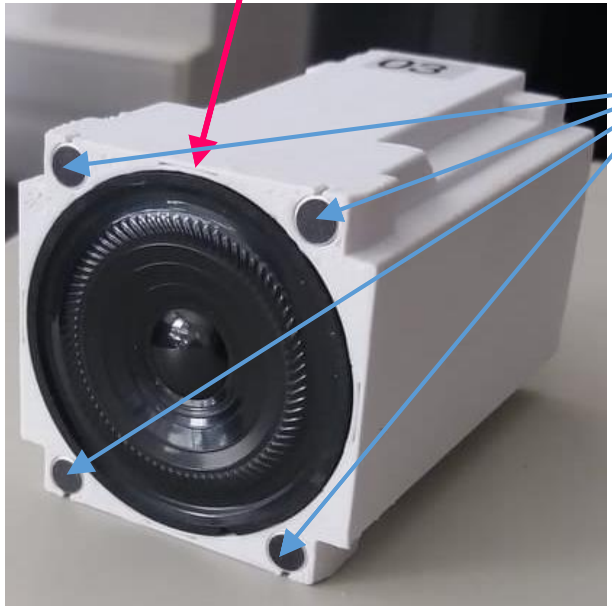

Microphones

Speaker

Electronic card

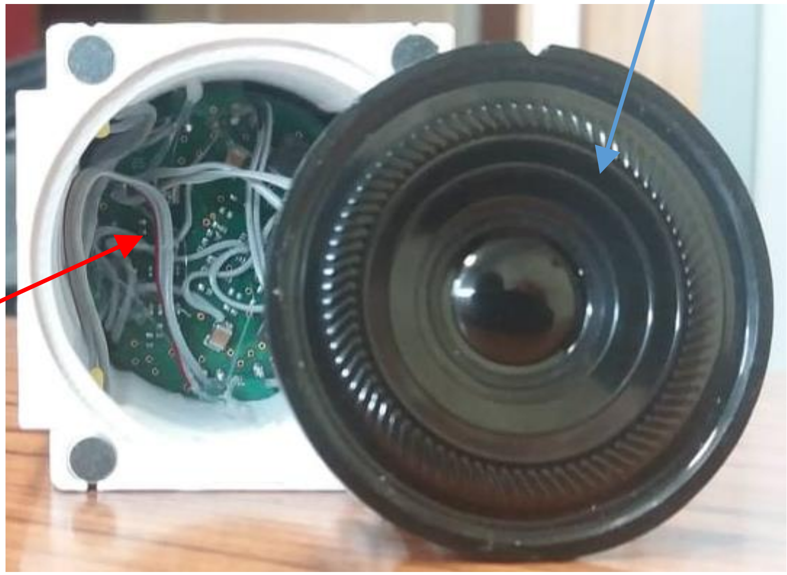

Summary

- The distributed impedance control law:
  - Theoretical stability.
  - The diode effect.
- Local Impedance Control: stability issue.
- Conclusions.

The distributed impedance control law

Control Law on the Boundary:

$$\boxed{-\rho\frac{\partial \boldsymbol{v}(x,t)}{\partial t}=\frac{\partial p}{\partial x}-\frac{1}{\boldsymbol{c_a}}\frac{\partial p}{\partial t}}$$

→ *Evanescent waves toward x>0*

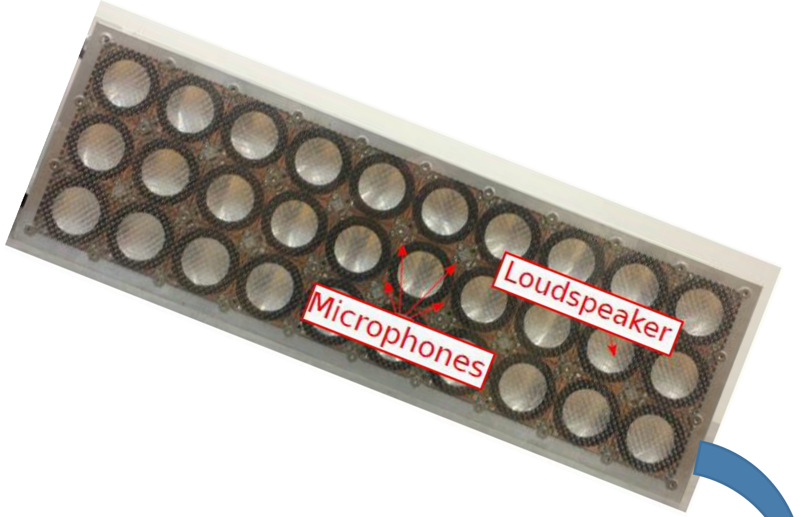

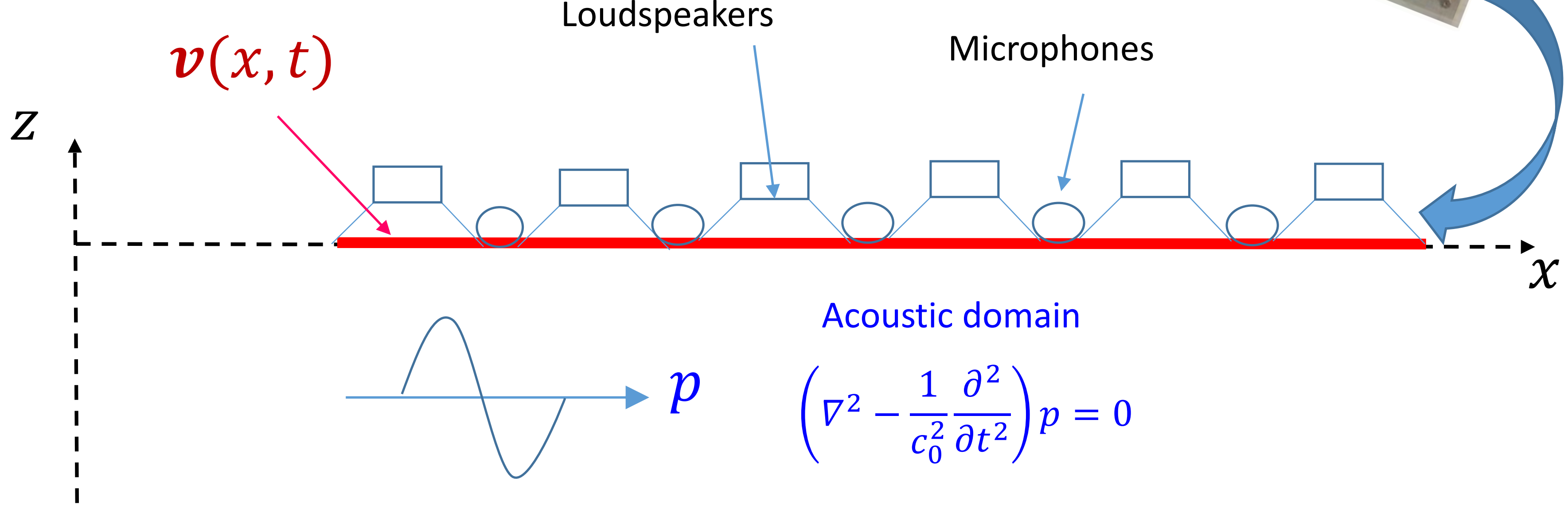

$$\left(\nabla^2-\frac{1}{c_0^2}\frac{\partial^2}{\partial t^2}\right)p=0$$

Collet et al. JASA 2009

Summary

- The distributed impedance control law:
  - Theoretical stability.
  - The diode effect.

- Local Impedance Control: stability issue.

- Conclusions.

The distributed impedance control law: Theoretical Stability

- Open Field Propagation Stability

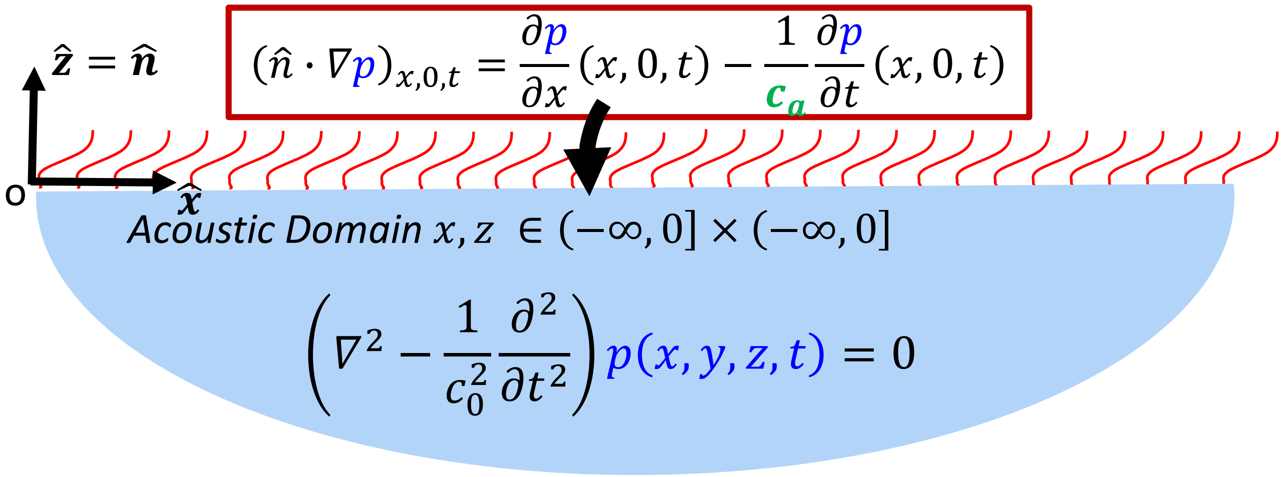

$$(\hat{n}\cdot\nabla p)_{x,0,t} = \frac{\partial p}{\partial x}(x,0,t) - \frac{1}{c_a}\frac{\partial p}{\partial t}(x,0,t)$$

Acoustic Domain $x, z \in (-\infty, 0] \times (-\infty, 0]$

$$\left(\nabla^2 - \frac{1}{c_0^2}\frac{\partial^2}{\partial t^2}\right)p(x,y,z,t) = 0$$

This problem has an analytical solution in the frequency domain in terms of the unkown wave numbers.

Power exchanged at the boundary

$$\boldsymbol{W_b} = Re\left\{v_{(z=0)}\, p^*_{(z=0)}\right\} = \frac{1}{\rho\omega}\left(\boldsymbol{Re}\{\boldsymbol{k_{z_1}}\}\left(|p_1|^2 + p_1 p_2^*\right) + \boldsymbol{Re}\{\boldsymbol{k_{z_2}}\}\left(|p_2|^2 + p_2 p_1^*\right)\right)$$

$$\boldsymbol{k_{z_1}} = \frac{\omega}{2c_a}\left(1 + \sqrt{2\frac{c_a^2}{c_0^2} - 1}\right)$$

$$\boldsymbol{k_{z_2}} = \frac{\omega}{2c_a}\left(1 - \sqrt{2\frac{c_a^2}{c_0^2} - 1}\right)$$

Negative for $c_a > c_0$

The distributed impedance control law:
Theoretical Stability

- Duct mode Propagation Stability

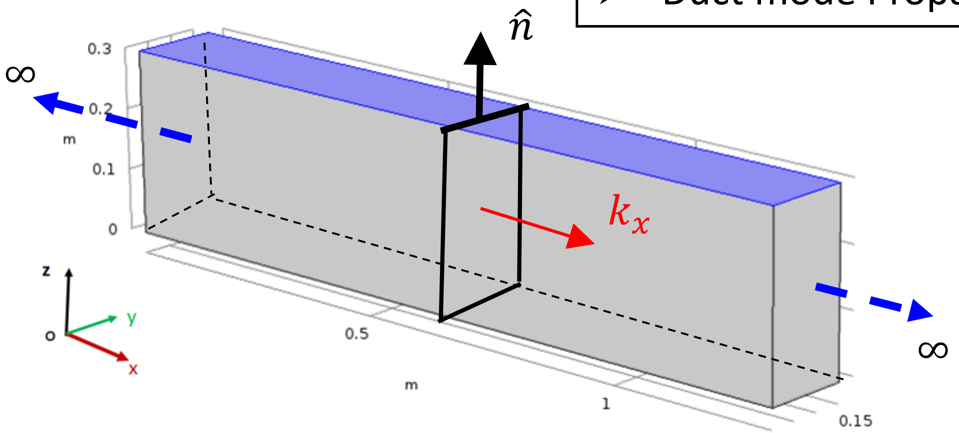

Frequency domain:

$$p(x,y,z,\omega,t) = \tilde{p}\,(y,z,\omega)e^{-j\omega t + jk_x x}$$

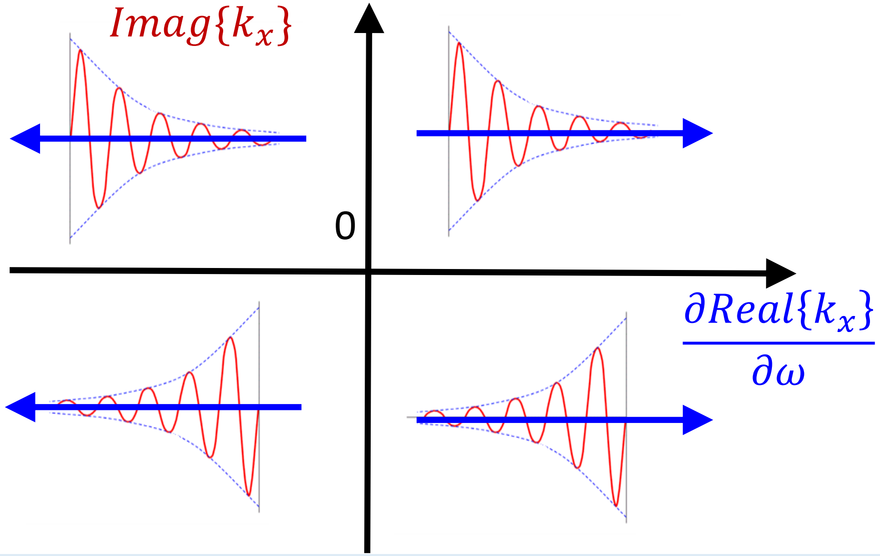

Wave Stability Criteria

$$\frac{\partial Real\{k_x\}}{\partial \omega} \cdot Imag\{k_x\} \geq 0$$

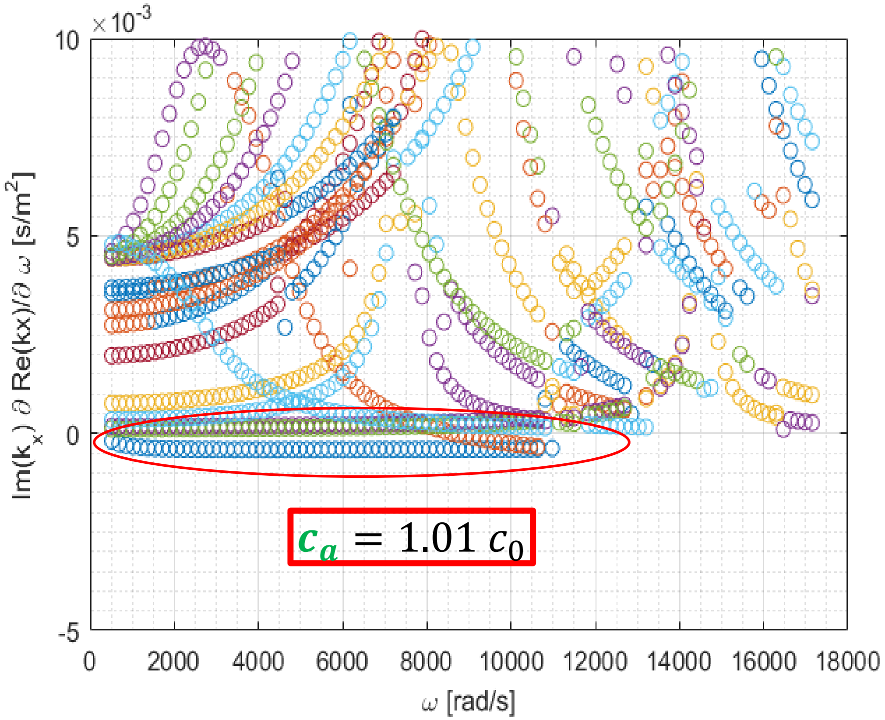

The distributed impedance control law:
Theoretical Stability

➢ Cavity Mode Stability

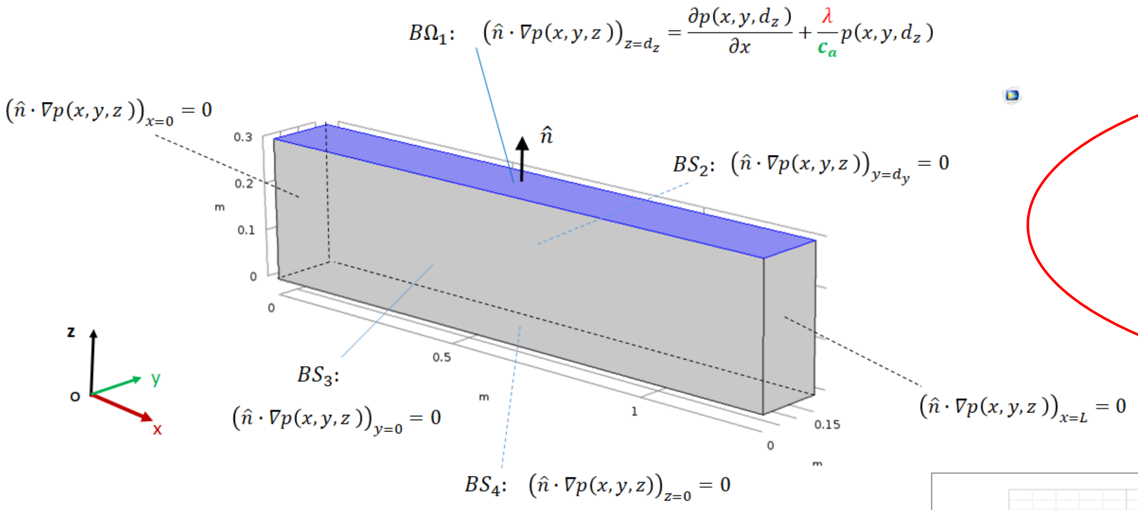

$$B\Omega_1:\quad (\hat{n}\cdot\nabla p(x,y,z))_{z=d_z} = \frac{\partial p(x,y,d_z)}{\partial x} + \frac{\lambda}{c_a}\, p(x,y,d_z)$$

$$(\hat{n}\cdot\nabla p(x,y,z))_{x=0} = 0$$

$$BS_2:\quad (\hat{n}\cdot\nabla p(x,y,z))_{y=d_y} = 0$$

$$BS_3:\quad (\hat{n}\cdot\nabla p(x,y,z))_{y=0} = 0$$

$$BS_4:\quad (\hat{n}\cdot\nabla p(x,y,z))_{z=0} = 0$$

$$(\hat{n}\cdot\nabla p(x,y,z))_{x=L} = 0$$

$$p = \hat{p}\, e^{-\lambda t}$$

If $Re\{\lambda\} < 0$ System Unstable

Cavity mode unstable for $c_a > c_0$

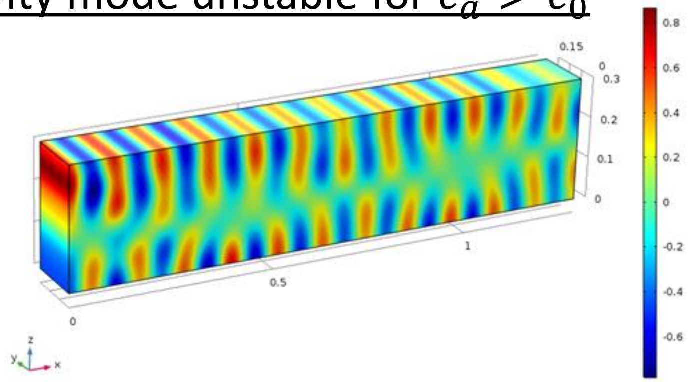

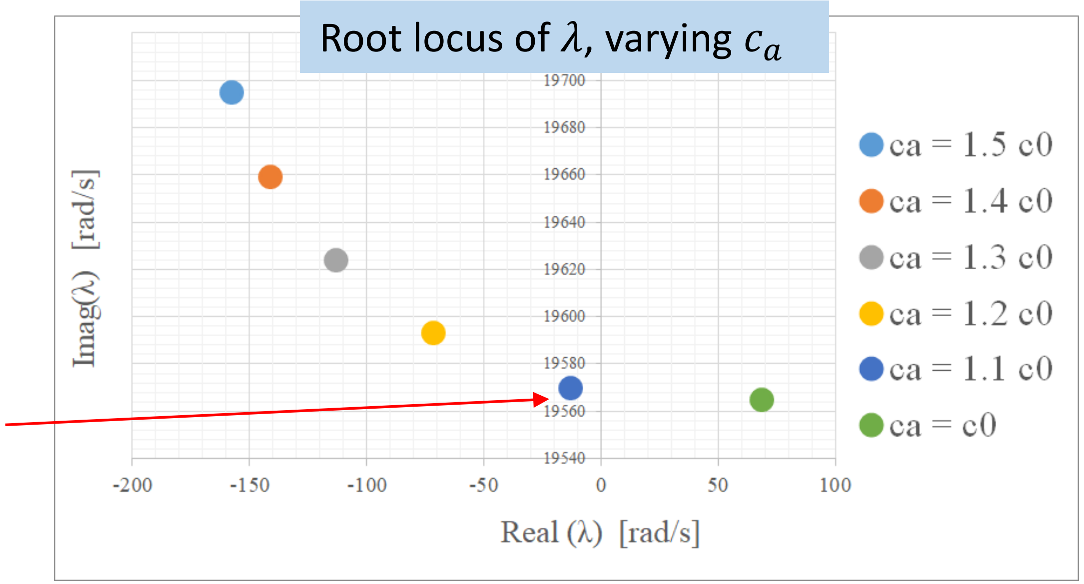

Root locus of λ, varying c_a

Summary

- The distributed impedance control law:
  - Theoretical stability.
  - The Diode Effect.

- Local Impedance Control: stability issue.

- Conclusions.

The distributed impedance control law: The Diode Effect

Dispersion curves relative to sectional duct modes

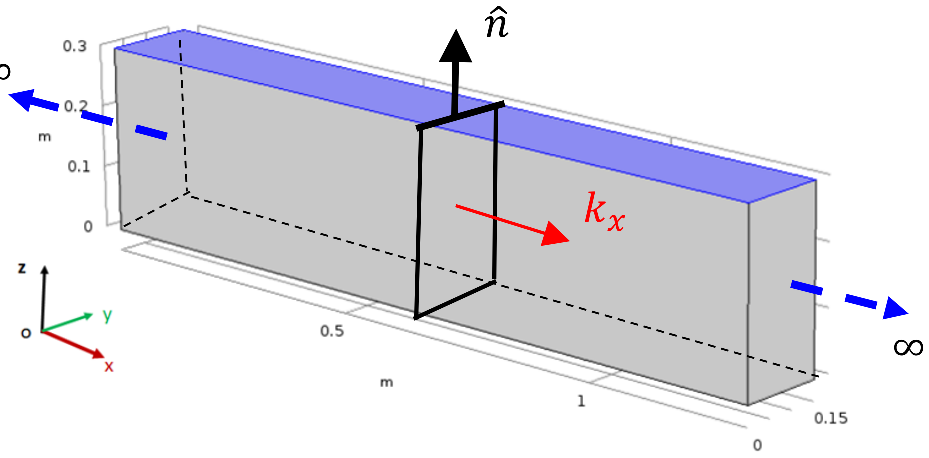

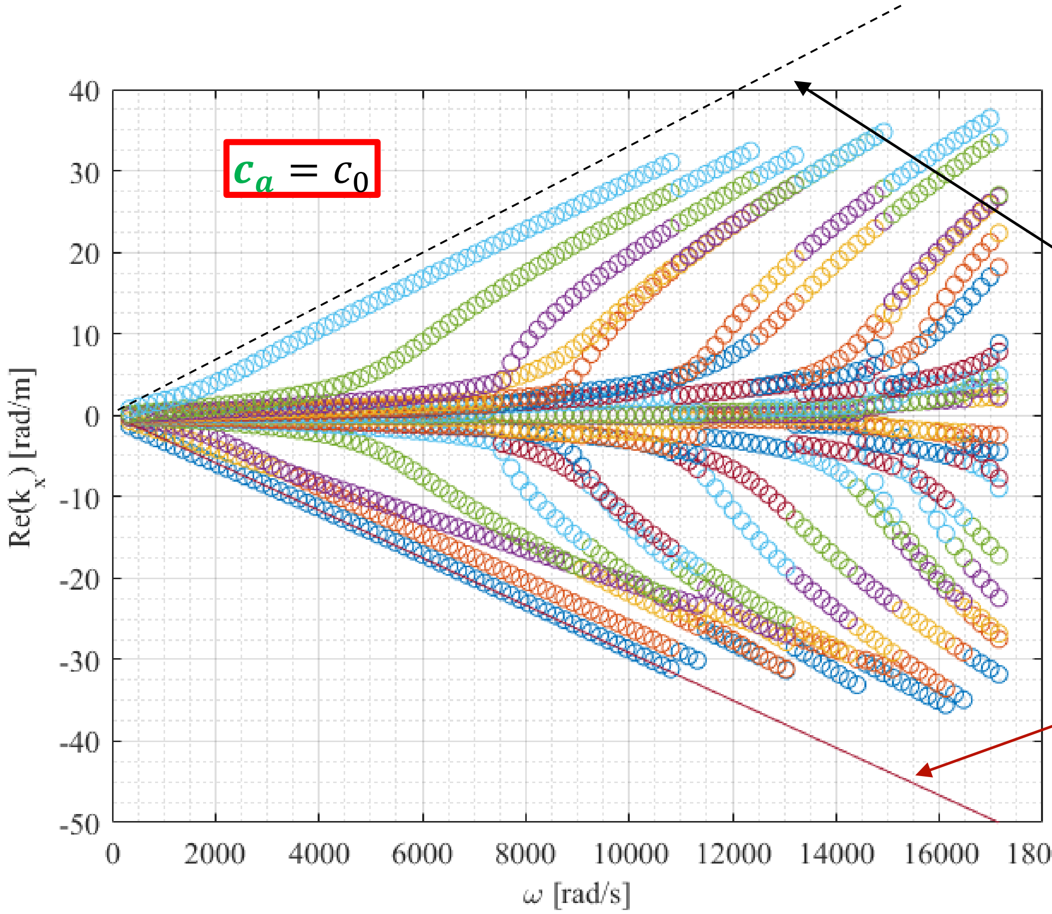

Forward Propagating plane wave *(missing)*

Backward Propagating plane wave

A distributed impedance control law: the Diode Effect

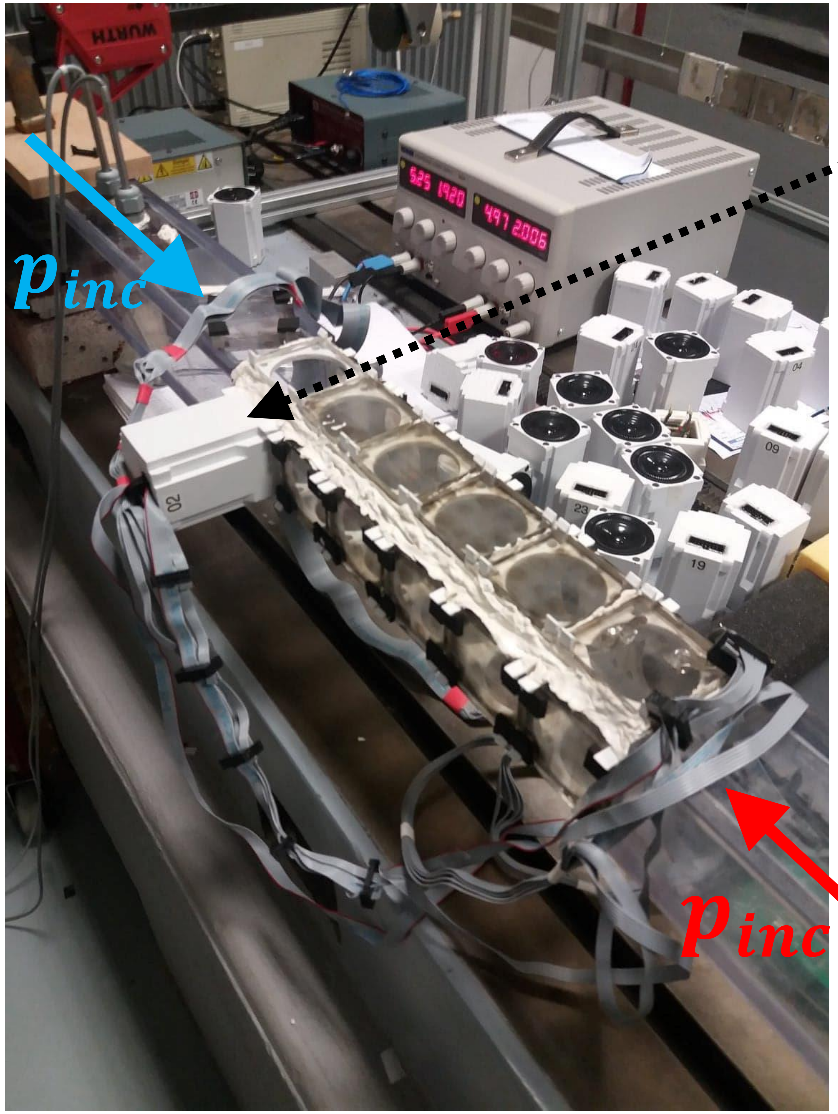

Acoustic Diode effect
WITH JUST ONE CELL!!!

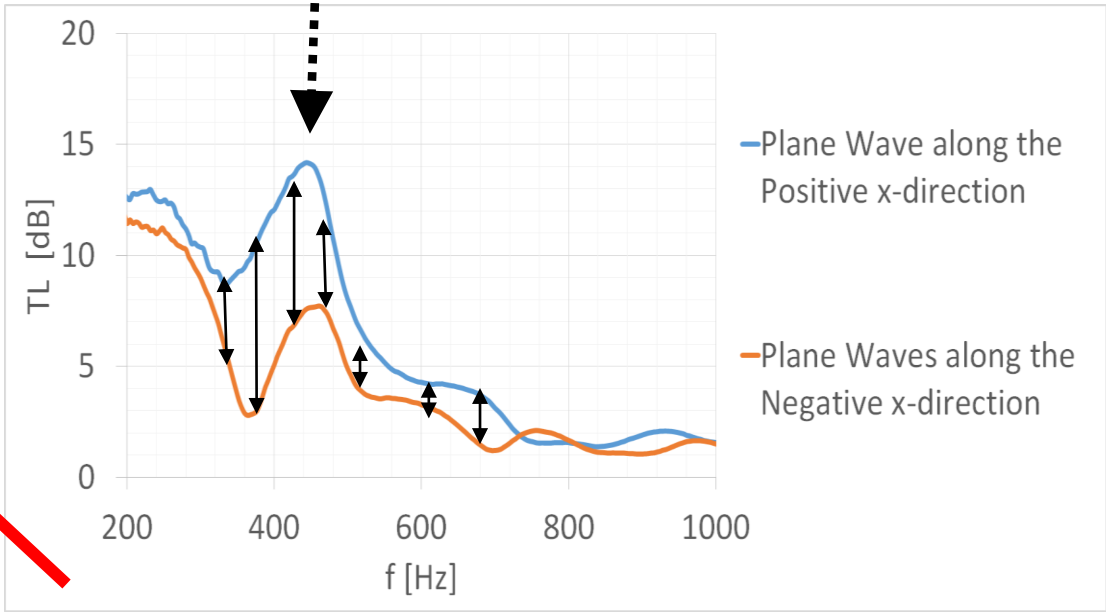

UNEXPECTED INSTABILITY
in the EXPERIMENTAL APPLICATION

- Increasing the number of cells easily brought about instability... ☹

- We need to do a step back… we need to take into account the time delay in the application of the control itself.

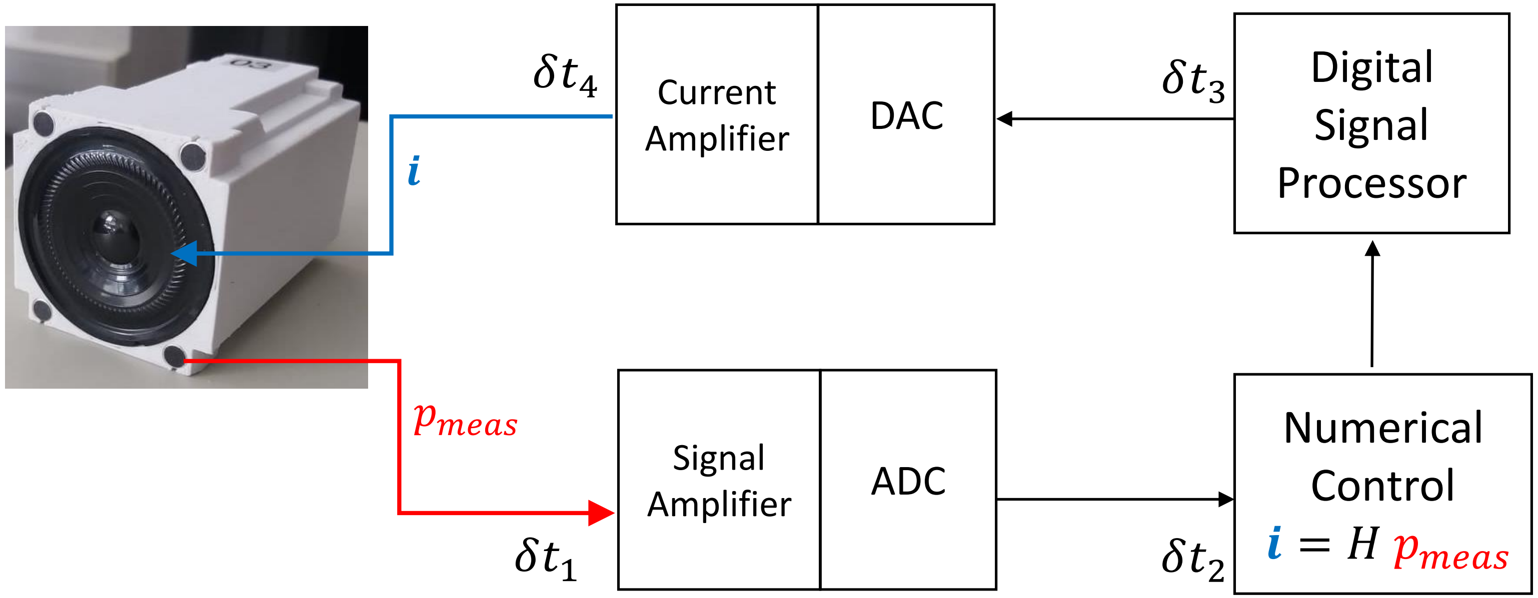

$$\tau = \sum_i \delta t_i$$

Summary

- The distributed impedance control law:
  - Theoretical stability.
  - The diode effect.

- Local Impedance Control: stability issue.

- Conclusions.

- Current work

Local Impedance Control: STABILITY ISSUE

- We will analyze now the Local Impedance Control, which the Distributed Impedance Control idea stems from. The Distributed Impedance Control is just an extension of the Local Impedance Control.

$$i(\omega) = \boxed{H_{loc}(\omega)}\, p + H_{dist}(\omega)\,\frac{\delta p}{\delta x}$$

- Therefore, first thing is to analyze the Stability of the ***Local Control***. If the Local Impedance Control is not stable, the Distributed Impedance Control has no chance to be stable!!!

Local Impedance Control: STABILITY ISSUE

- What happens if we consider a delay in the application of the Local Impedance Control?

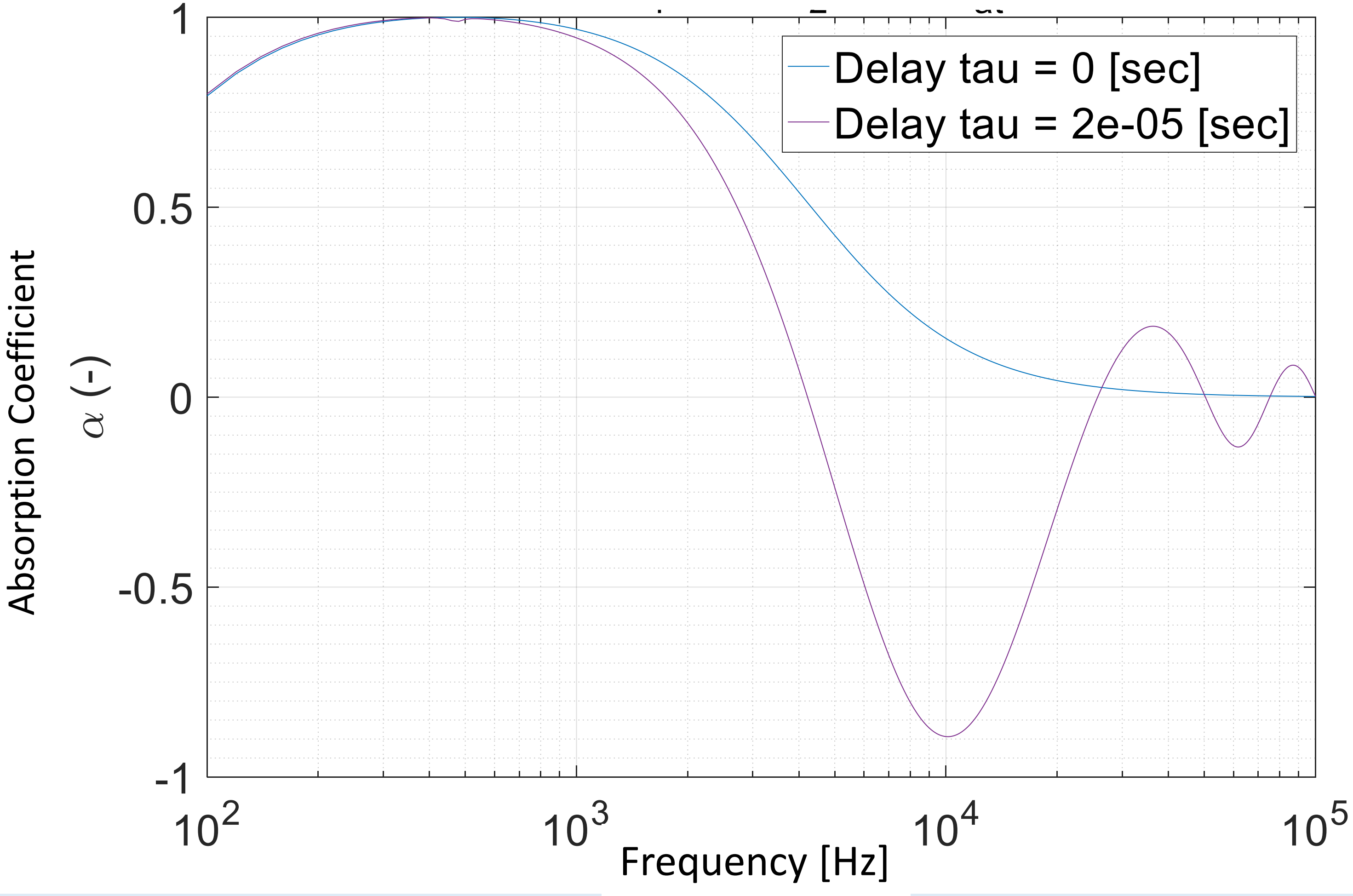

$$\tau = \sum_i \delta t_i$$

Normal Absorption Coefficient negative above 3kHz!!!!

Local Impedance Control:
STABILITY ISSUE

- What happens if we consider a delay in the application of the Local Impedance Control?

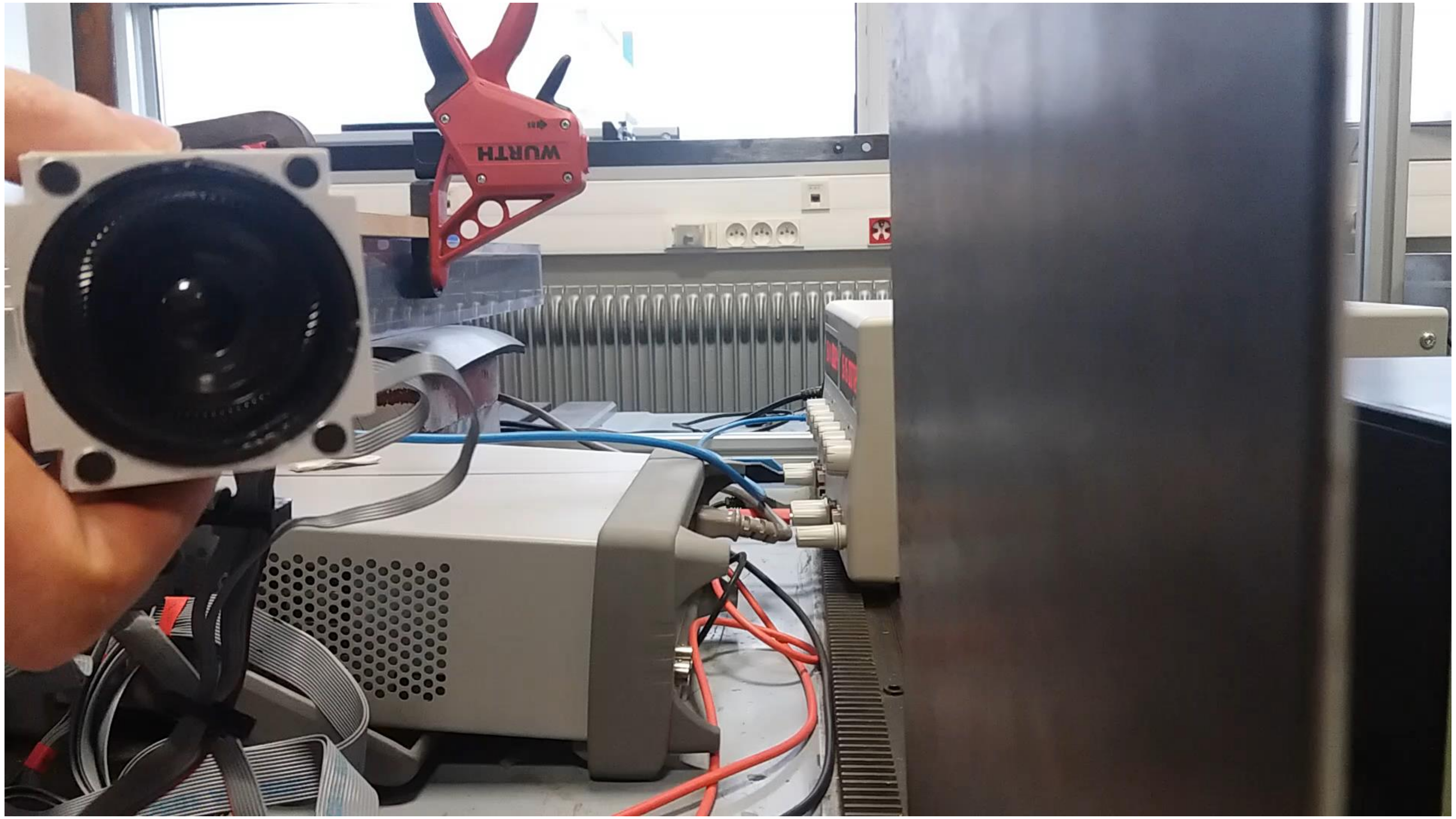

Local Impedance Control:
STABILITY ISSUE

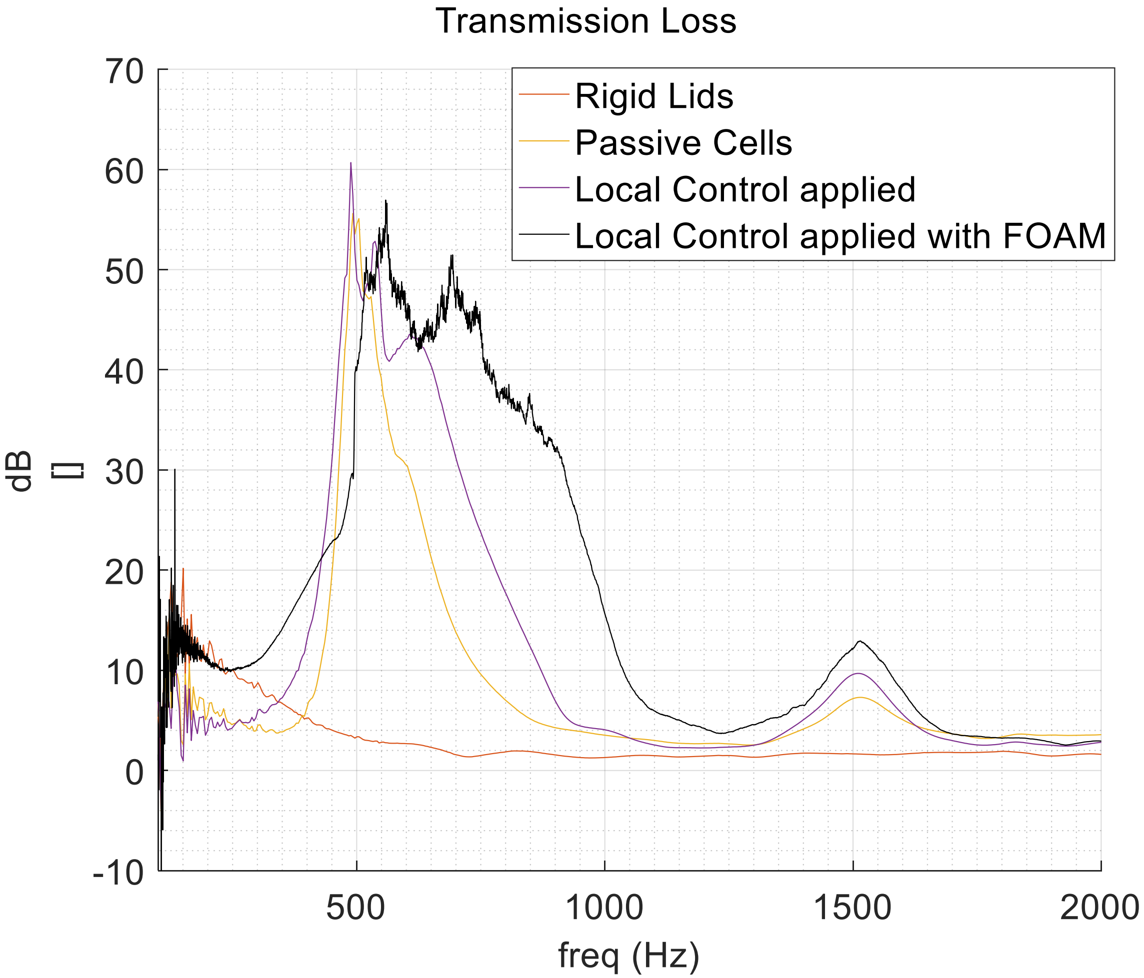

Summary

- The distributed impedance control law:
  - Theoretical stability.
  - The diode effect.

- Local Impedance Control: stability issue.

- Conclusions.

- Current work

Conclusions

- The condition for the Acoustic domain to be stable if coupled with a Distributed Impedance Controlled liner, has been assessed through analytical and numerical analyses. They retrieved the same result: a limit on the artificial celerity coefficient $c_a \leq c_0$.

- The diode effect has been shown numerically and experimentally, but the tests have shown clear instability.

- The first reason of instability has been found in the application of the Local Impedance Control, on which the Distributed Impedance Control is rooted.

- The instability of the Local Control has been explained numerically by the delay in the digitally-implemented Control chain. Experimental tests have confirmed the validity of this conclusion.

Current Work

- Test and optimize different Control Law, stabilizing the system by the application of a porous layer in front of the cells.

- Synthesize a robust Control Law through Advanced Automatic Control techniques based upon the H_∞ method. It will take into account the delay from the beginning of the Control design.

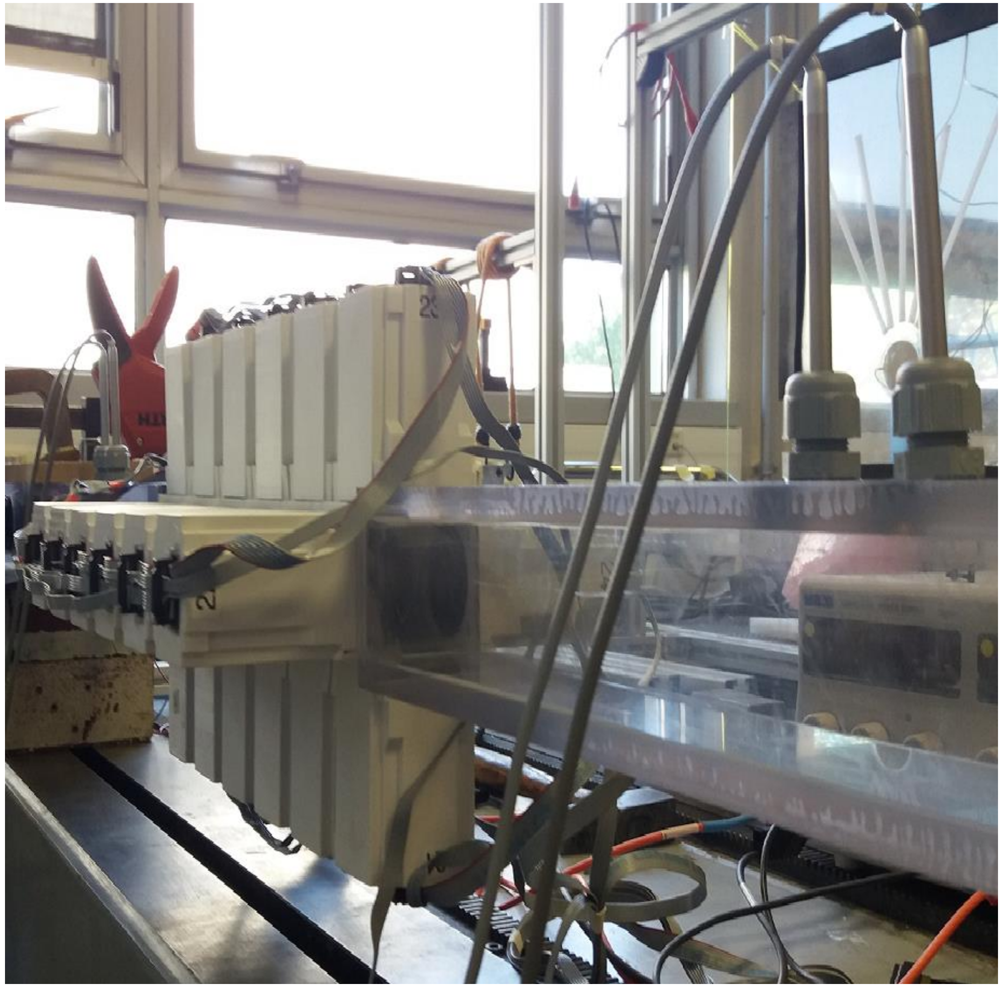

Part 3: Gradient metamaterials, MDOF oscillator and wave-conversion liner

Thomas LAURENCE

H2020 MARIE SKŁODOWSKA-CURIE ACTIONS

Generalities about interfaces

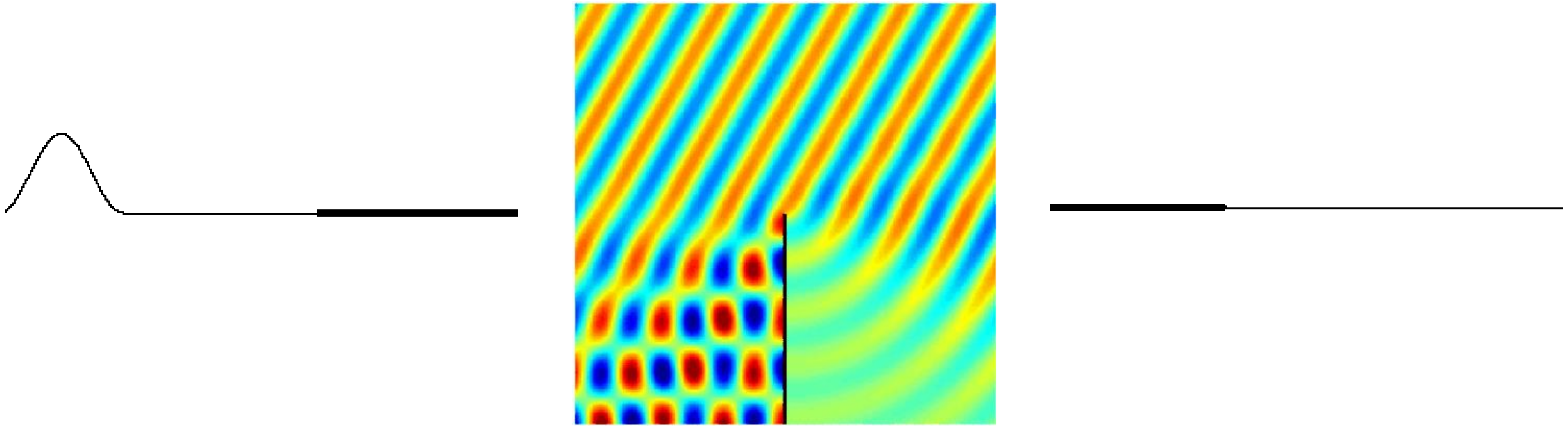

Generalities about interfaces

- Interaction with an interface of specific impedance :

$$Z_s = R_s + jX_s = \frac{p}{v}$$

compared to the specific impedance of the fluid $Z_c = \rho_0 c_0$

- Reflection coefficient in normal incidence:

$$R = \frac{Z_s - Z_c}{Z_S + Z_c}$$

- Absorption coefficient:

$$\alpha = 1 - R^2$$

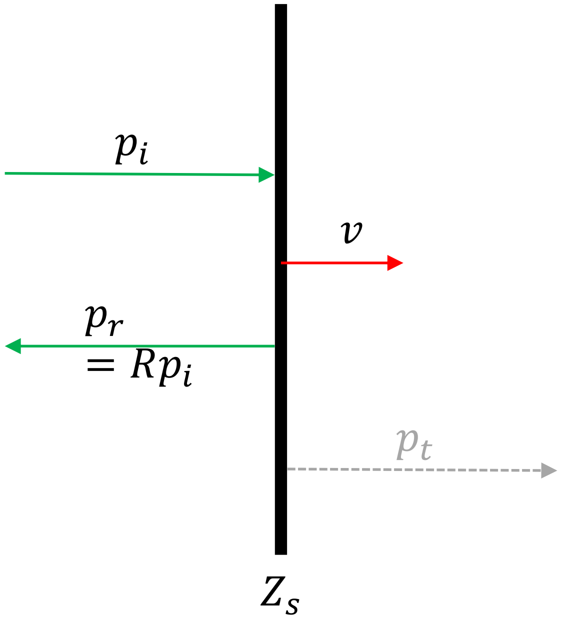

Generalities about interfaces

➢Snell-Descartes Law (SDL):

$$\sin\theta_i + \sin\theta_r = 0$$

Valid for an homogeneous impedance

- ➔ What happens for a controlled inhomogeneous impedance ?
- ➔ How can we create an inhomogeneous impedance ?

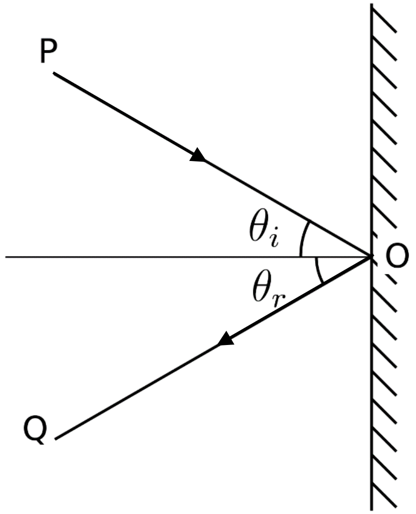

Multiple Degrees Of Freedom Oscillator

- MDOF sensor-based shunted loudspeaker

Current equation (Newton):

$$Z_m v = S_d p - Bli$$

Can be tuned to a target specific impedance
by adjusting $i = \Phi(p)$:

$\boldsymbol{\Phi = \frac{S_d}{Bl}\left(1 - \frac{Z_M}{S_d Z_s}\right)}$ gives the specific impedance Z_s

- ➔Offers the possibility to have an inhomogeneous impedance
- ➔Active resonator, can be changed on the fly
- ➔Virtually any impedance is achievable

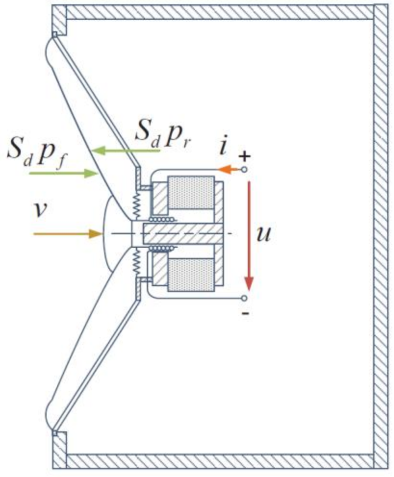

Source: [Rivet, Thesis]

Generalized Snell Descartes Law

- Gradient-based metamaterials :

Gradient property over the material (for example a surface)

- Helical wavefront generation, abnormal reflection…
- Phase gradient metasurfaces : wave manipulators.

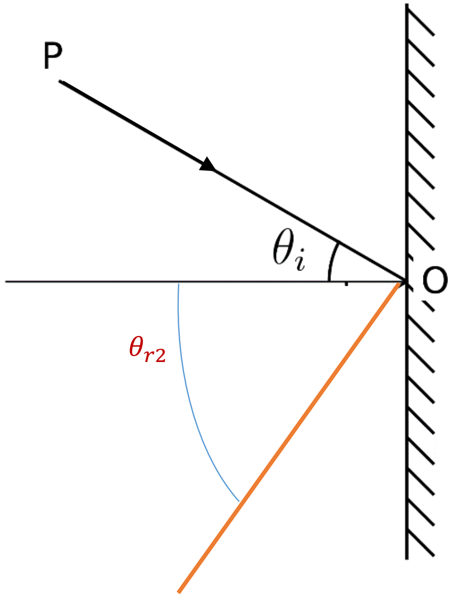

- Based on generalized SDL with a reflection phase ψ :

$$\boxed{sin\theta_i + sin\theta_r = -\frac{1}{k}\frac{\partial\psi}{\partial x}}$$

Generalized Snell Descartes Law

- Gradient-based metamaterials :

They mostly use passive cells.

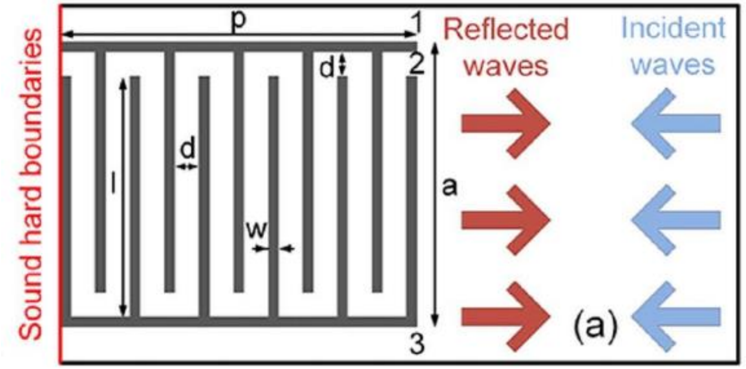

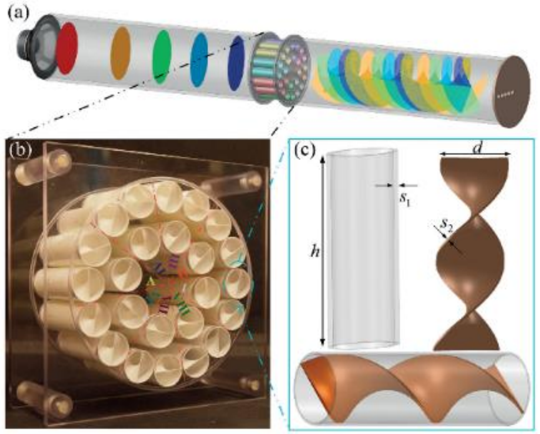

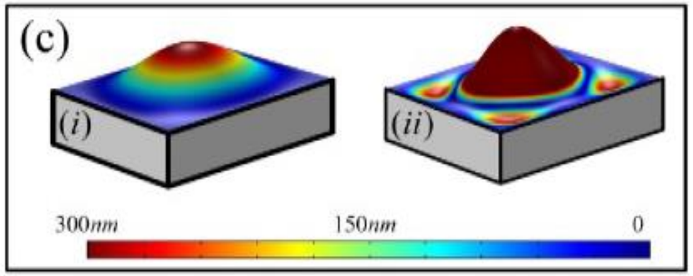

➔**Could we combine this approach and MDOF active oscillators ?**

MDOF target impedance

- Definition of the target impedance Z_s with a criteria on the reflection coefficient phase, and implementation of the control law Φ.
- Frequency shift of the resonators along the surface :

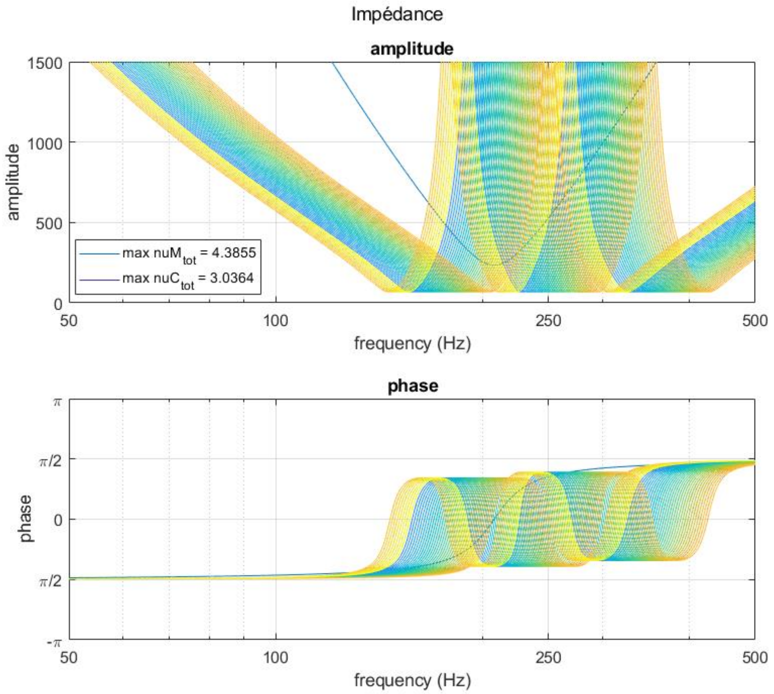

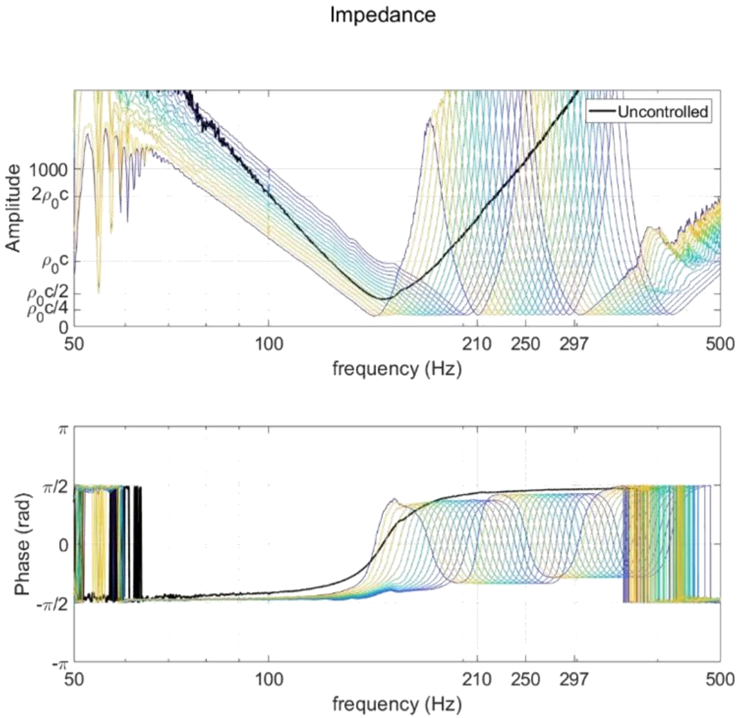

MDOF target impedance

- The phase target is exactly met !

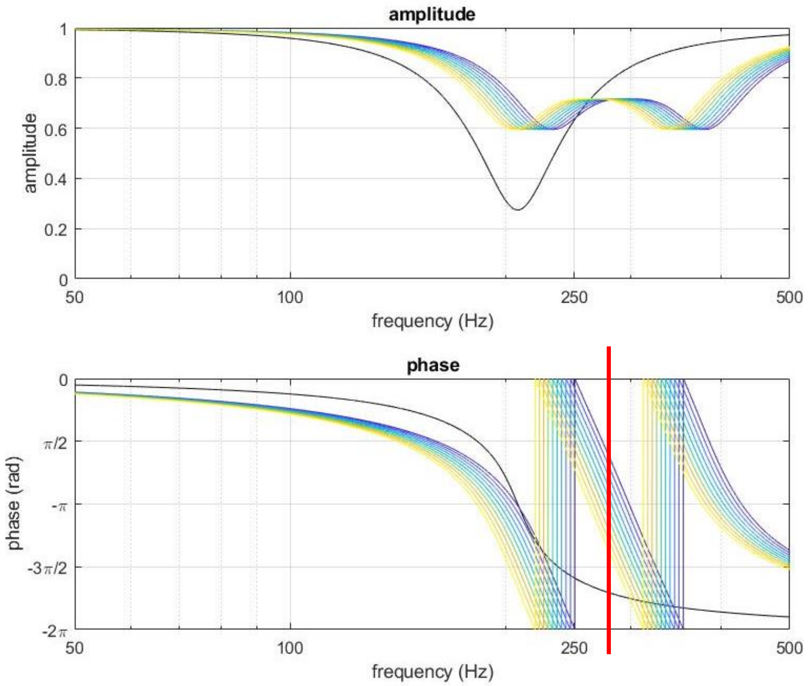

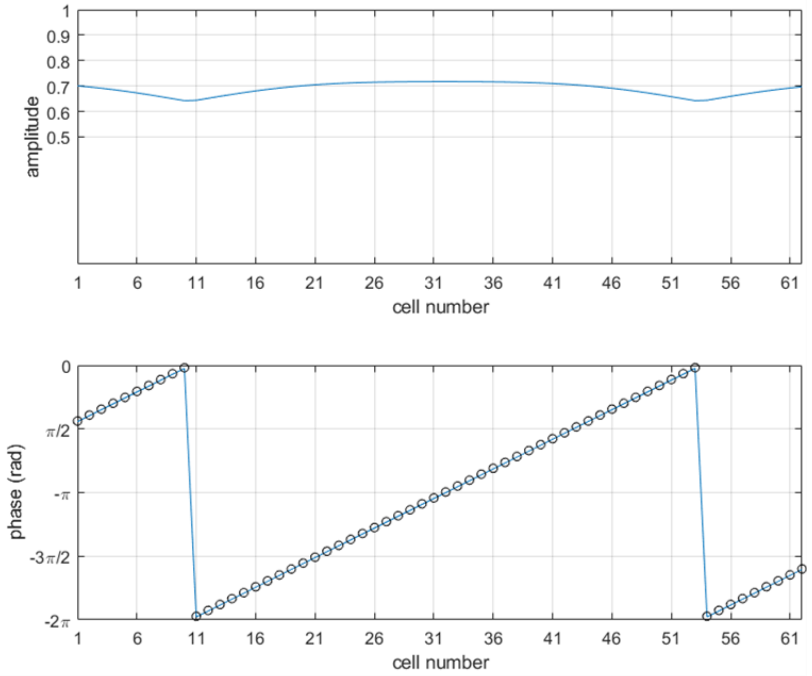

Wave redirection

- First simple application : anomalous reflection (standard application in the litterature).
- Good simulation results, over a large frequency band.
- Need for experimental results.

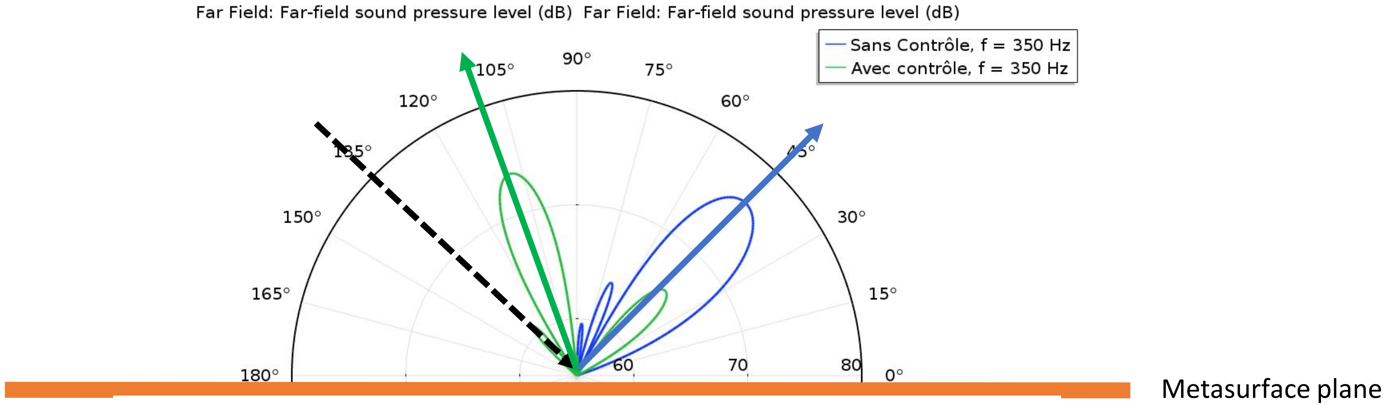

- Condition from generalized SDL:

$$\sin\theta_r \leq 1 \iff \frac{\Delta\psi_m}{kd} - 1 \leq \sin\theta_i,\ \ \theta_i \in [-90°, 0°]$$

➔ No reflection for a given incidence and a given phase gradient !

With an optimized gradient, in a duct:

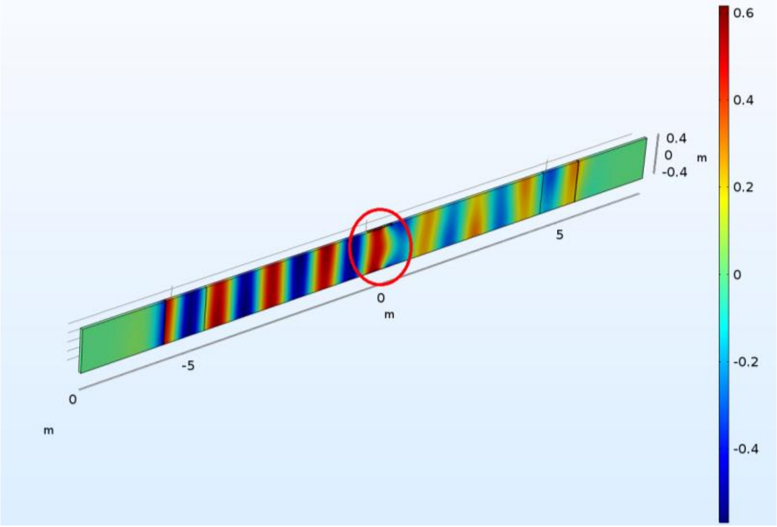

- Condition from generalized SDL:

$$\sin\theta_r \le 1 \iff \frac{\Delta\psi_m}{kd} - 1 \le \sin\theta_i,\ \ \theta_i \in [-90°, 0°]$$

➔ No reflection for a given incidence and a given phase gradient !

With an optimized
gradient, in a duct:

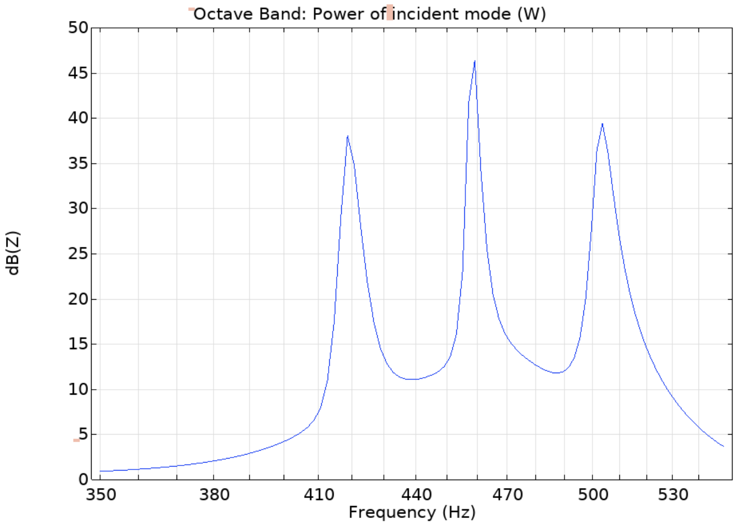

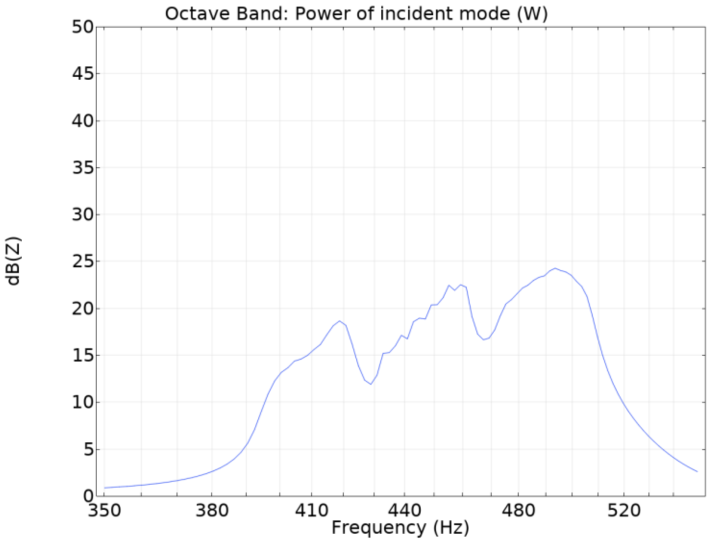

Real life applications

Smart Mitigation of flow-induced Acoustic Radiation and
Transmission for reduced Aircraft, surface traNSport,
Workplaces and wind enERgy noise

Part 4: Flow-acoustics interaction With innovative materials

Massimo D'Elia

H2020 MARIE SKŁODOWSKA-CURIE ACTIONS

Introduction

Flow-Acoustic Interaction
with
Innovative Materials

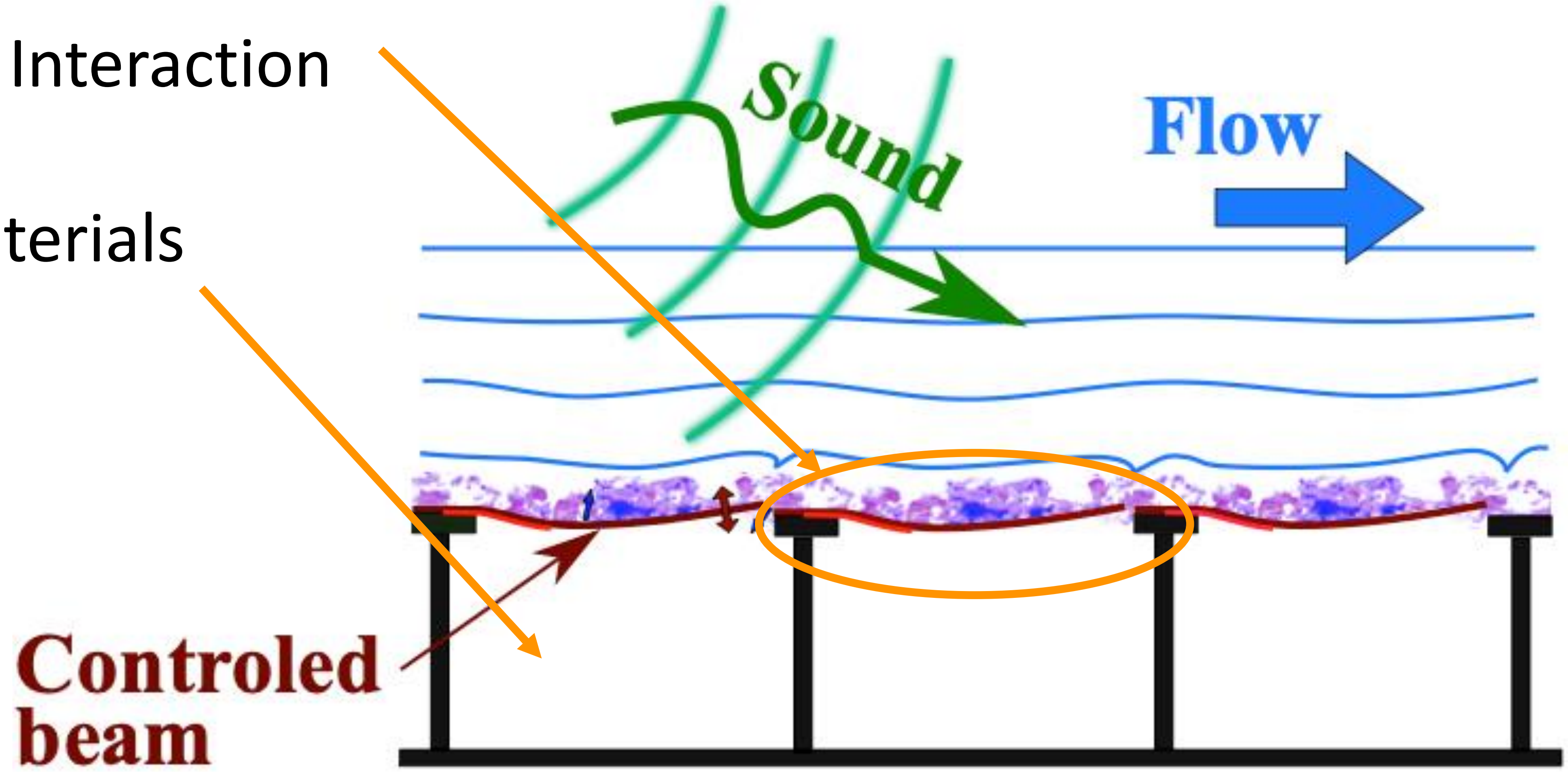

Introduction

First Step:

Flow-Acoustic Interaction

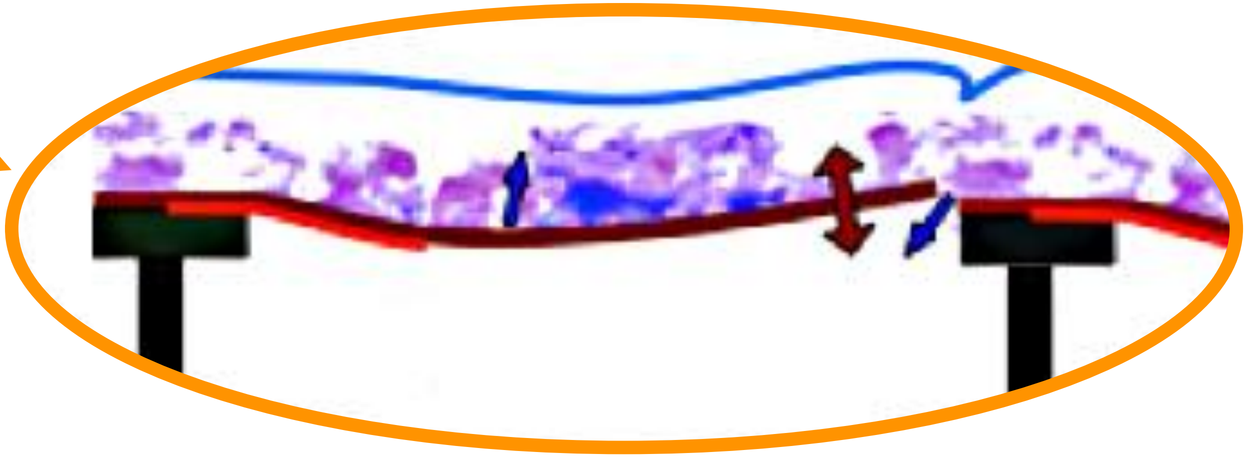

Flow-Acoustic interactions over small cavities:
Application to corrugated pipes

Industrial interest of

TNO innovation for life

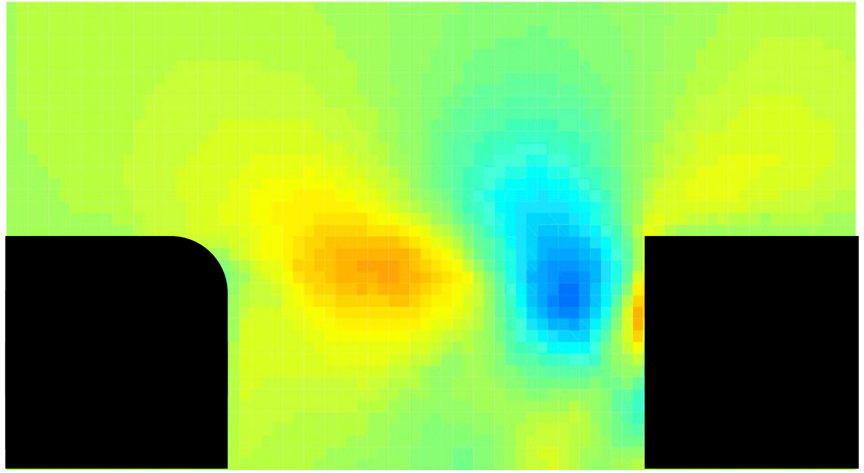

Introduction

Flow-Acoustic interactions over small cavities:
Application to corrugated pipes

- Experimental investigation: | Microphones measurement, Laser Doppler Velocimetry
- Extraction of a linear model

Acoustic Transmission

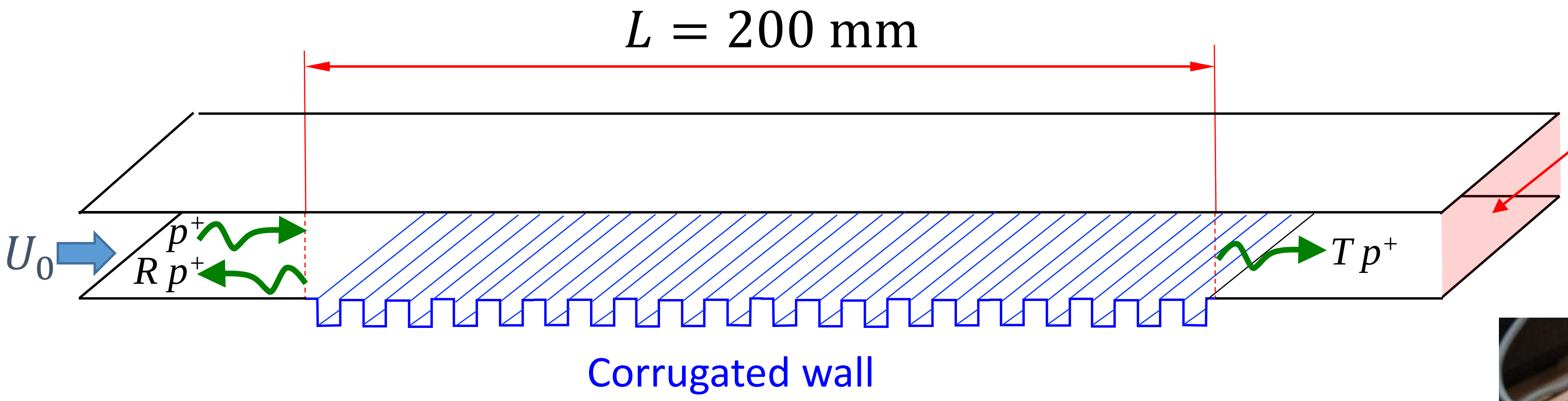

$S = 40 \times 50$ mm

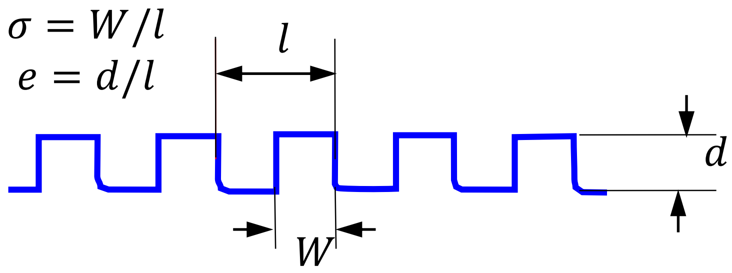

$W = 4$ mm
$d = 4$ mm, $l = 12$ mm

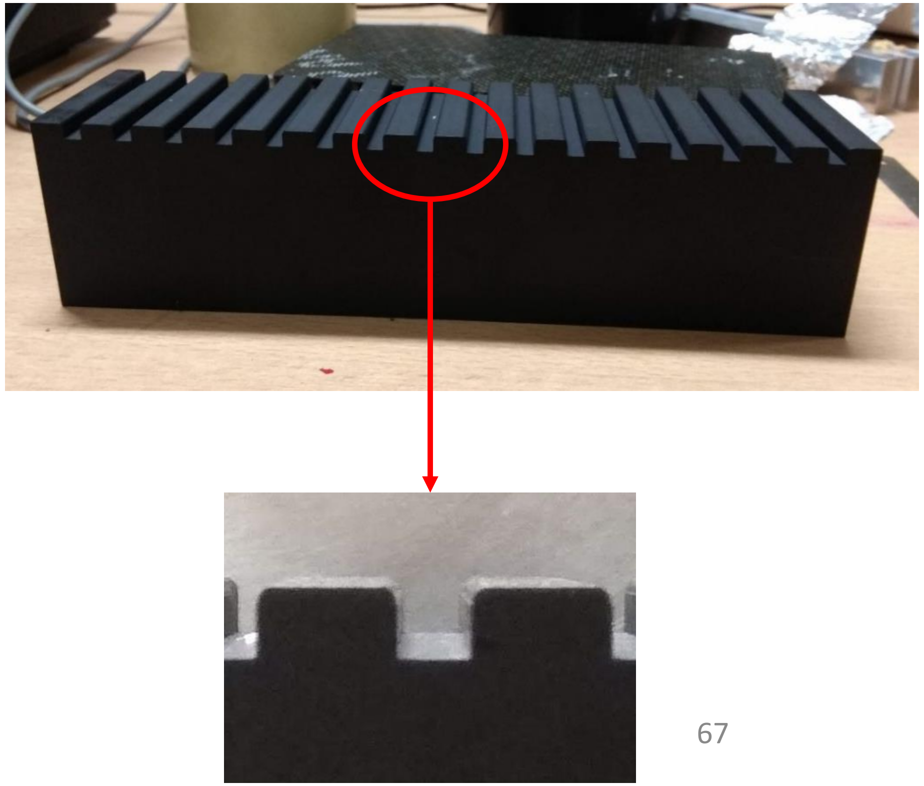

Acoustic Transmission

LDV measurement

f = 2 kHz
St = 0.4

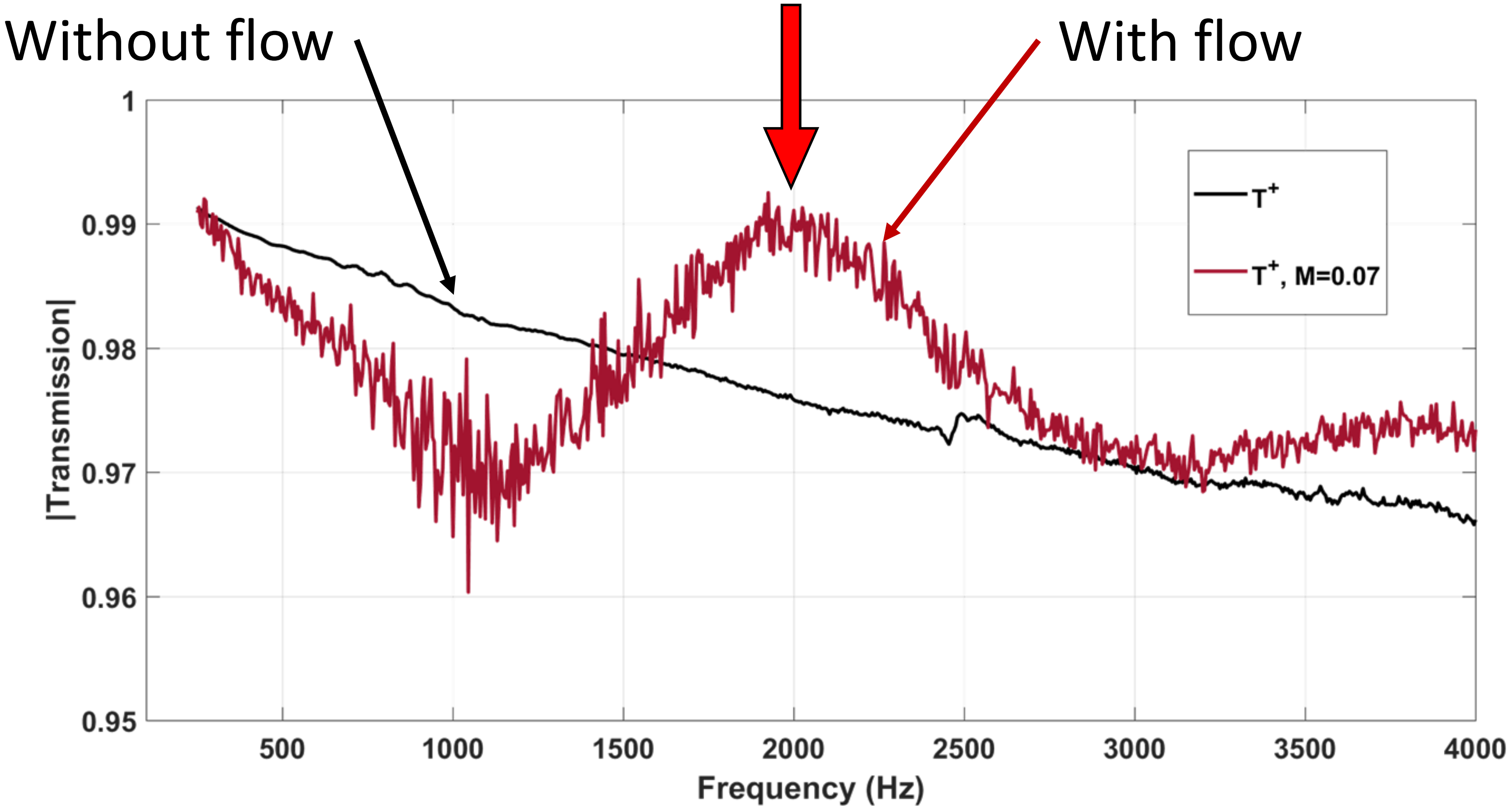

Oscillations:

- Oscillations of transmission coefficients with flow
- Frequency of oscillations dependent on flow velocity: constant Sr

LDV Setup

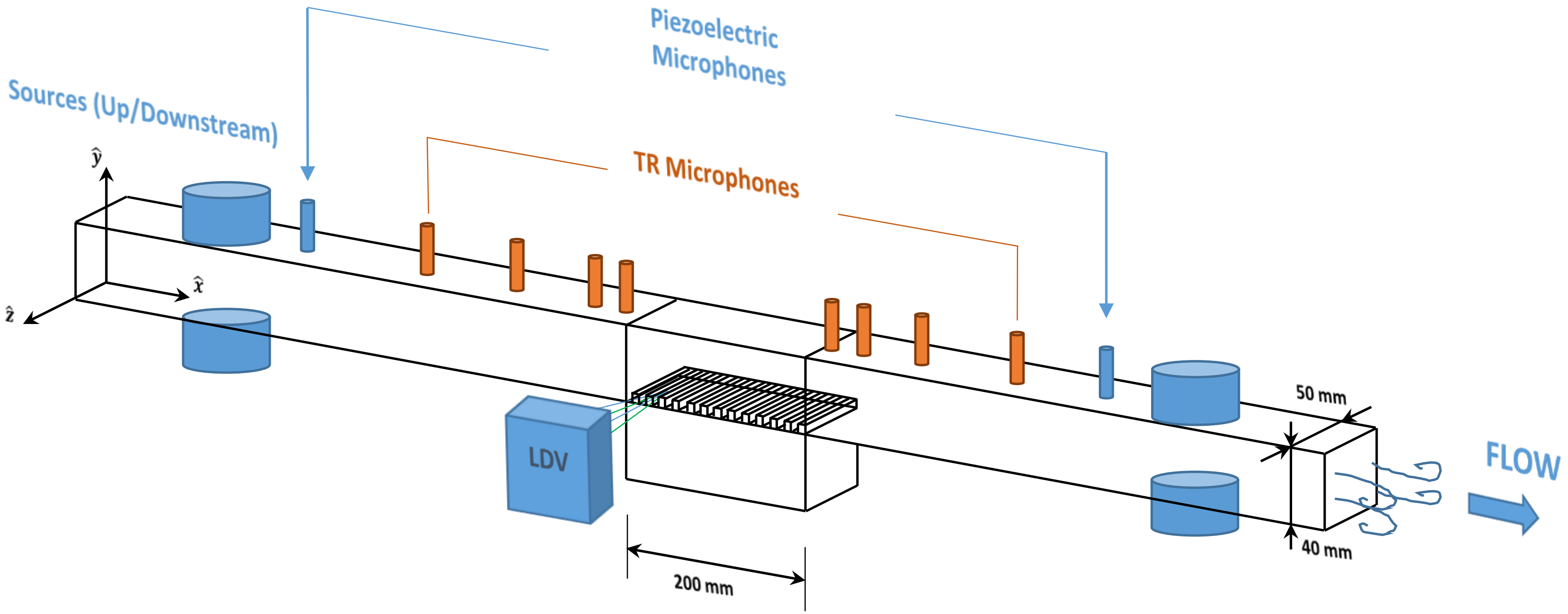
Piezoelectric Microphones
Sources (Up/Downstream)
TR Microphones
$\hat{y}$
$\hat{x}$
$\hat{z}$
LDV
50 mm
40 mm
200 mm
FLOW

LDV Technique

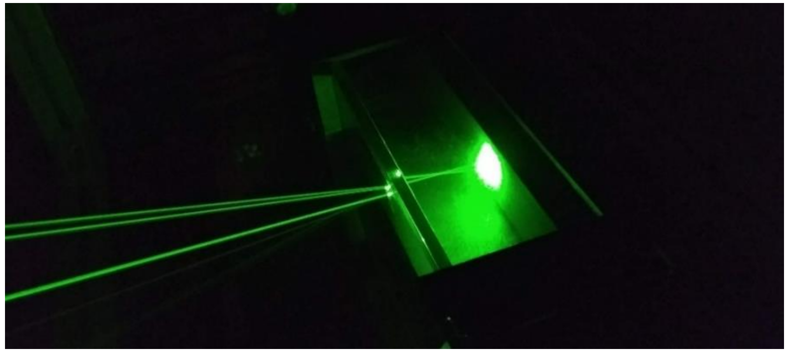

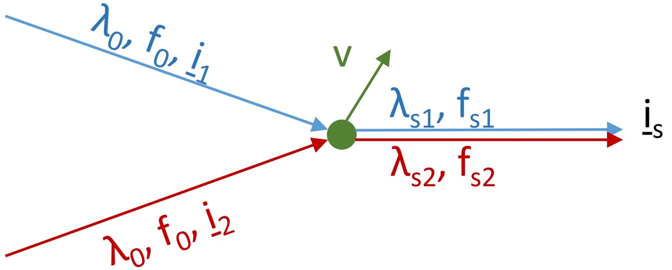

$f_{s1} = f_0 + V/\lambda_0(\underline{i}_s - \underline{i}_{s1})$
$f_{s2} = f_0 + V/\lambda_0(\underline{i}_s - \underline{i}_{s2})$ ⟶ $\mathbf{f_D = f_{s1} - f_{s2} = V/\lambda_0(\underline{i}_{s2} - \underline{i}_{s1})}$

Retrieved velocity: $V = v_{mean} + v_f + v_t$
Sum of average, fluctuating and turbulent components

Fluctuating component can be retrieved either by phase-locked measurements or by <u>least-square approach</u> (chosen method)

Corrugated pipe - LDV Measurements

As we are interested in the vorticity shed by the cavities, we measured 1 mm inside the (fourth) cavity and around 1.3 mm above, with a step of 0.10 mm (machine resolution).

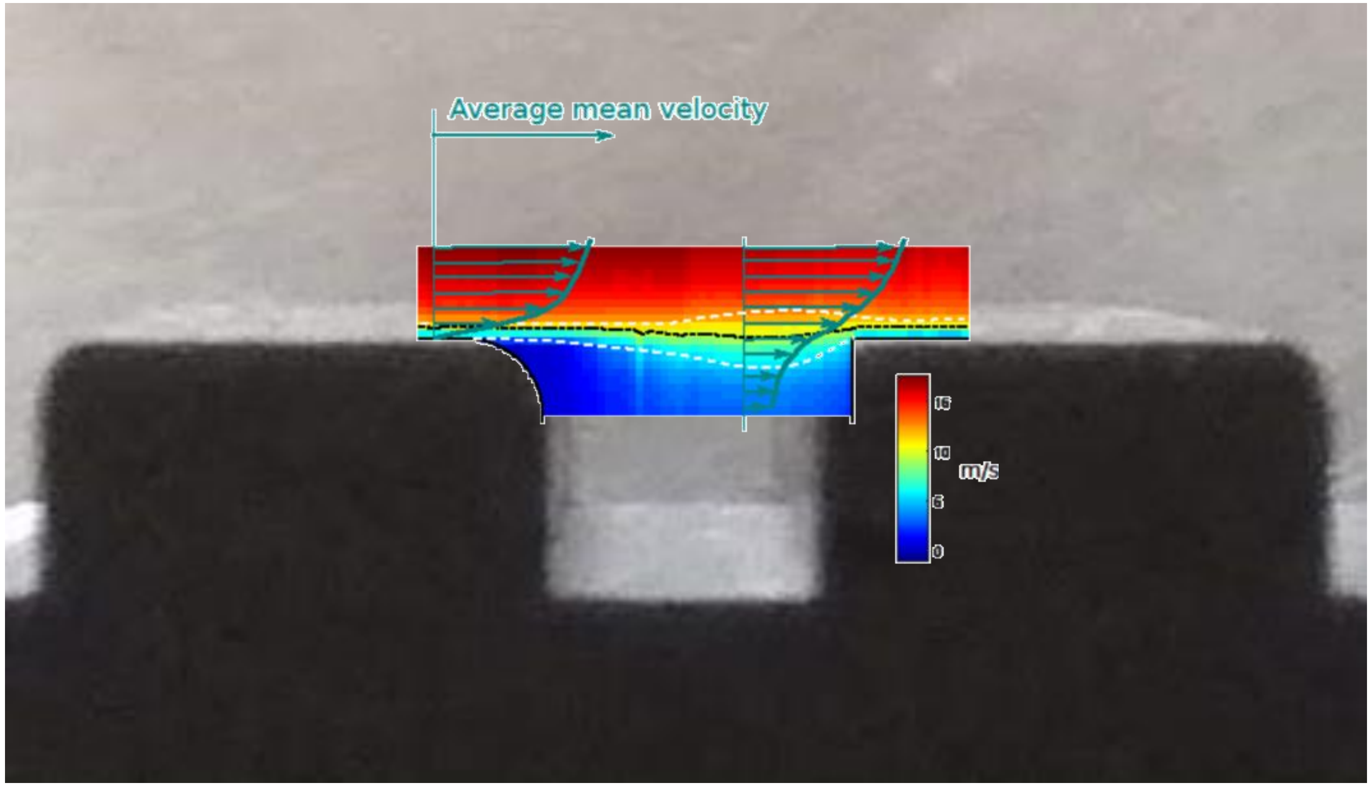

Geometrical restrictions: acquisition in two steps and tilt

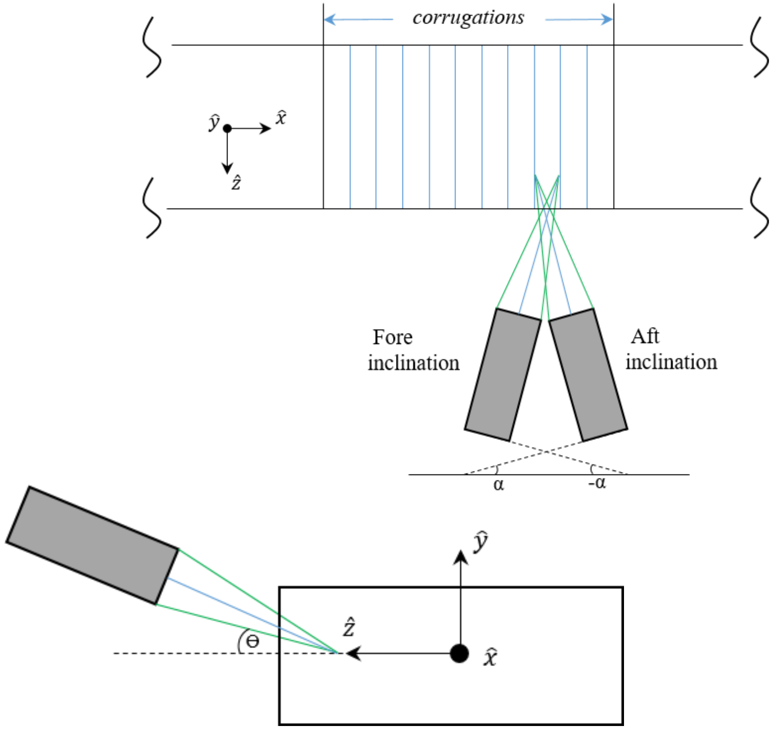

Corrugated pipe - LDV Measurements

By looking at the velocity phase right above the cavity, we can find a very clear linear behaviour.
From this, we can then obtain the shed vorticity traveling velocity, which, when traced down in black on the left figure, coincide pretty well with the vorticity core.

$$v_f = \left|V_f\right| e^{-ikW} \rightarrow \mathrm{k} = \frac{angle\left(v_f\right)}{W} \rightarrow \lambda_t = \frac{2\pi}{k}$$

$$c_t = \lambda_t f = 9.25\ m/s$$

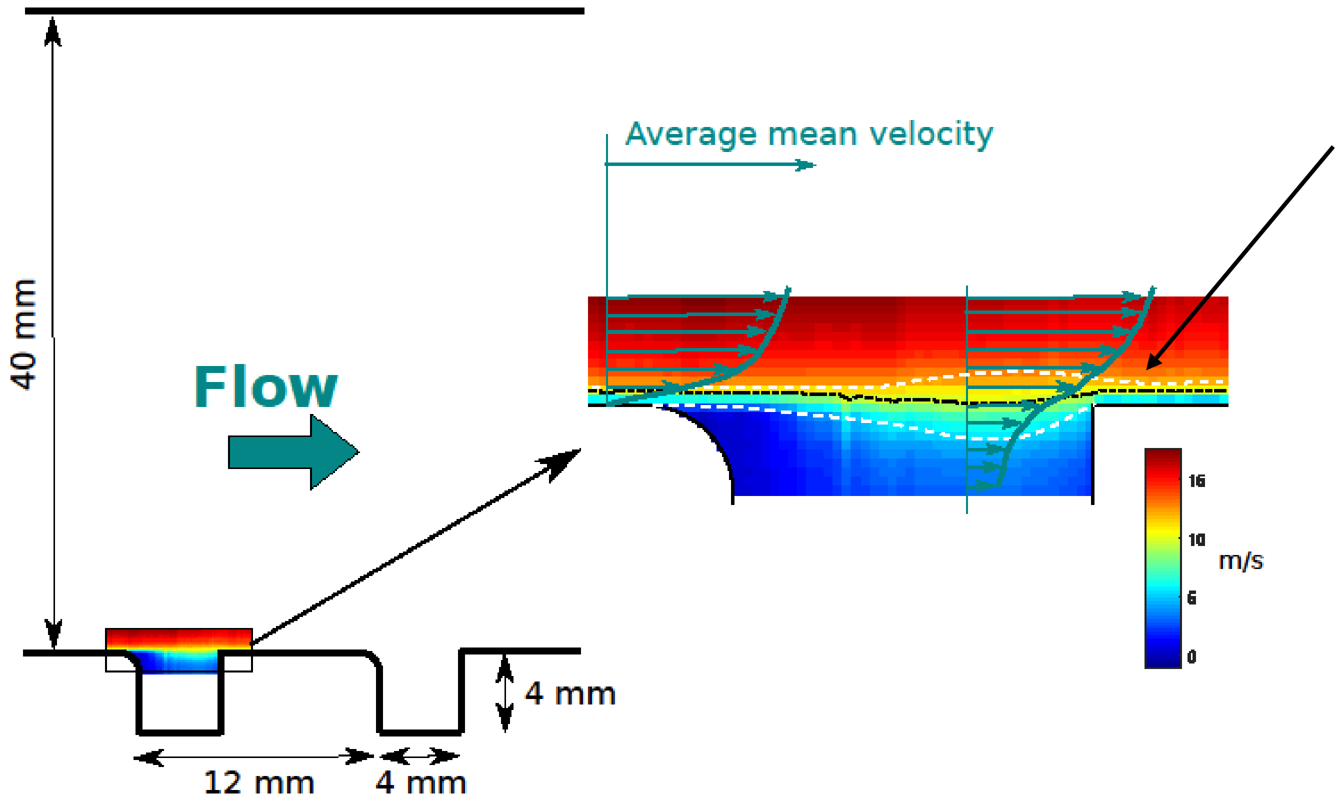

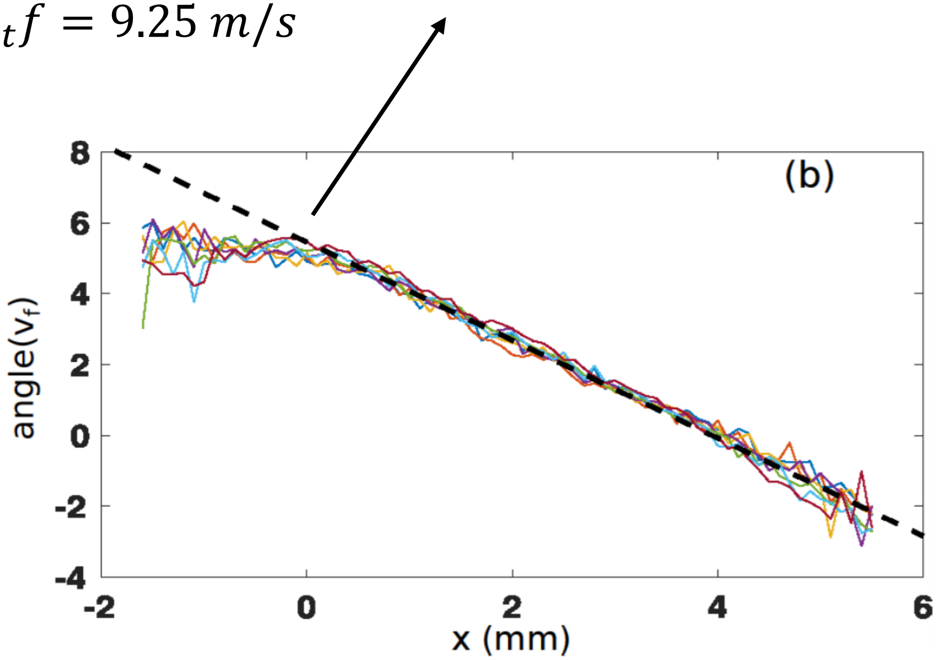

Acoustic power calculation

- In presence of Flow -> Acoustic power can be ***produced***.

This can be obtained by Howe energy corrolary:

$$\mathrm{P} = -\iiint_{\Omega} \rho_0 \langle (\omega \times V) \cdot u_a \rangle d\Omega$$

where ω is the flow vorticity, V is the flow velocity and u_a is the acoustic velocity

- First term of integral retrieved by measurements.
- As acoustic component cannot be isolated, u_a is computed numerically (and magnitude matched away from cavity, where solely acoustic component is present and measured)

Acoustic power calculation

This can be obtained by Howe energy corrolary:

$$\mathrm{P} = -\iiint_{\Omega} \rho_0 \langle (\omega \times V) \cdot u_{aco} \rangle d\Omega$$

where ω is the flow vorticity, V is the flow velocity and u_a is the acoustic velocity

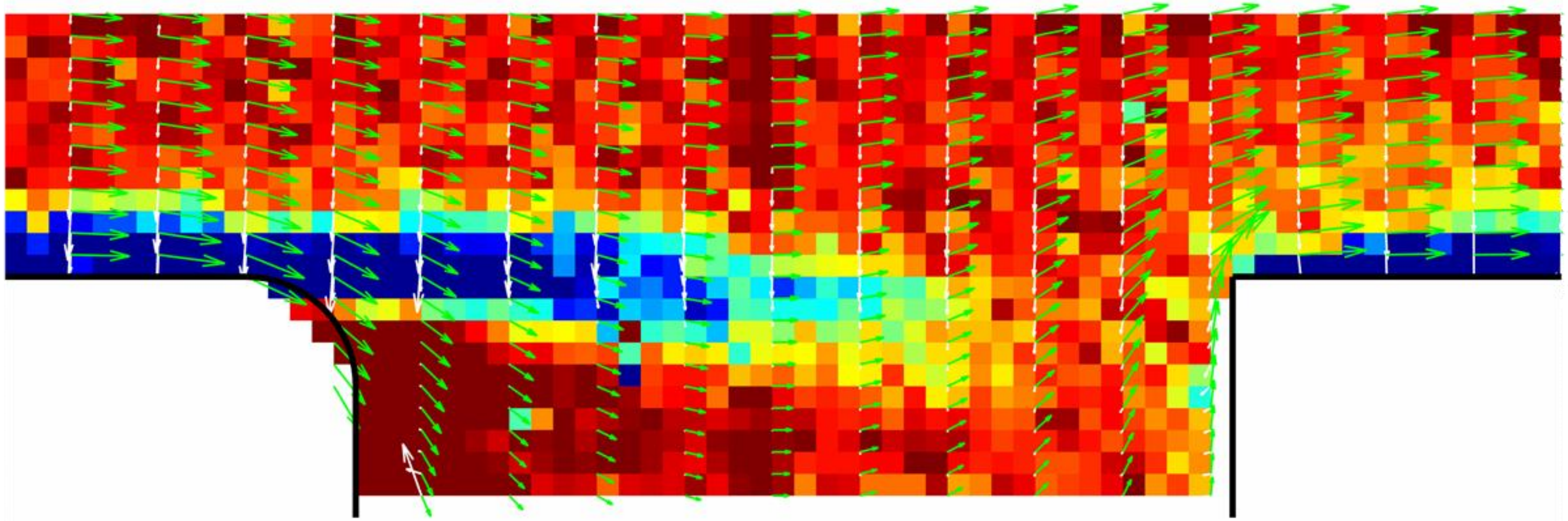

Mean vorticity + Fluctuating Vorticity

Acoustic power calculation

This can be obtained by Howe energy corrolary:

$$\mathrm{P} = -\iiint_{\Omega} \rho_0 \langle (\omega \times V) \rangle \cdot u_{aco} d\Omega$$

where ω is the flow vorticity, V is the flow velocity and u_{aco} is the acoustic velocity

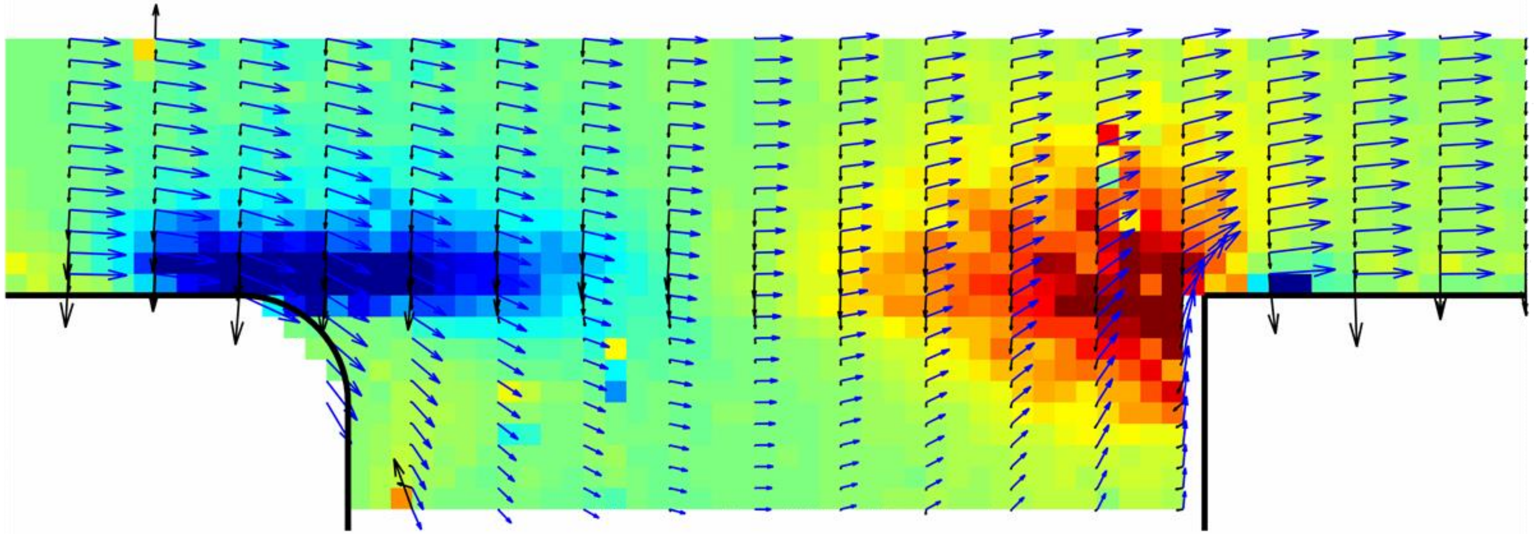

Acoustic Power

Acoustic Power Measurement: Microphone vs LDV measurements

Furthermore, such power such be related to the Transmission coefficient variations seen in the T-R measurements.

From T-R measurements, the non-dimensional acoustic power is:

$$P_{adim} = \left[(1+M)^2 + (1-M)^2\left|\frac{p_2^-}{p_1^+}\right|^2 - (1+M)^2\left|\frac{p_2^+}{p_1^+}\right|^2 - (1-M)^2\left|\frac{p_1^-}{p_1^+}\right|^2\right] S \approx \left(1 - |\mathrm{T}^+|^2 - |\mathrm{R}^+|^2\right) S$$

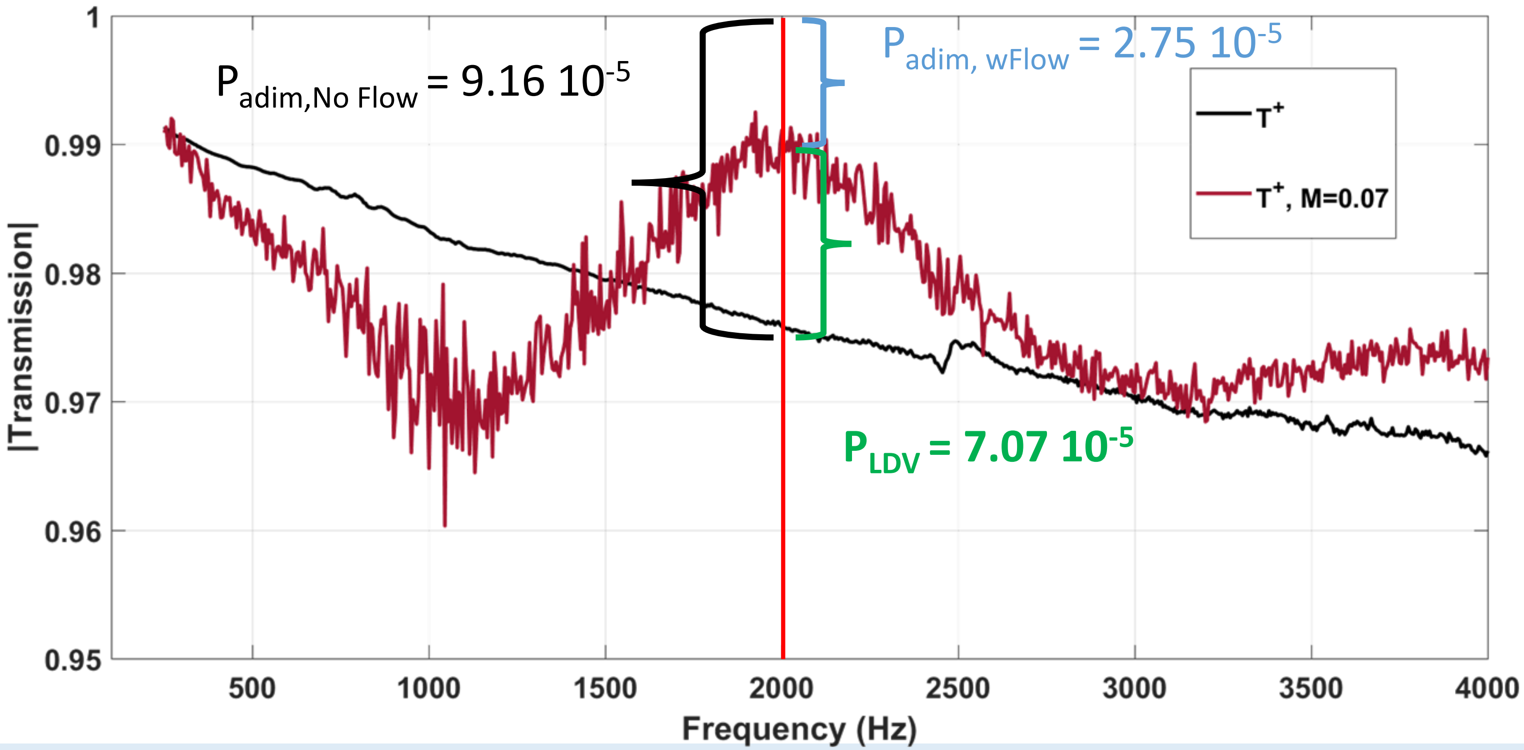

$P_{adim,No\ Flow} = 9.16\ 10^{-5}$

$P_{adim,\ wFlow} = 2.75\ 10^{-5}$

$P_{LDV} = 7.07\ 10^{-5}$

$$\Delta P_{adim} = 6.41\ 10^{-5}$$

Integrating the measured power over measurement slice (x depth and number of cavities over test section), we obtain:

$$P_{LDV} = 7.07\ 10^{-5}$$

Conclusions

In contrast to the whistling case, measurements in the linear domain of corrugations show that the vorticity is distributed over the entire opening of the corrugation.

In the linear regime, the vorticity is proportional to the sound velocity and the sound power provided by the flow is proportional to the square of the velocity.

In the linear regime, the vorticity remains approximately constant along the opening. There is no evidence of instability in the shear layer.

I have shown that it is possible to extract the sound power provided by the flow from LDV measurements.

A simplify model in the linear regime can be deduced from the LDV measurements

⇒ Interesting results that will be soon published in a journal

Future Works

Effect of flow on innovative absorbers

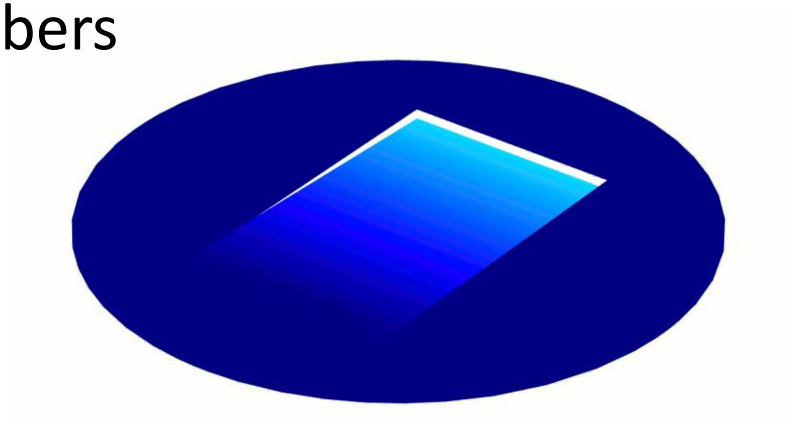

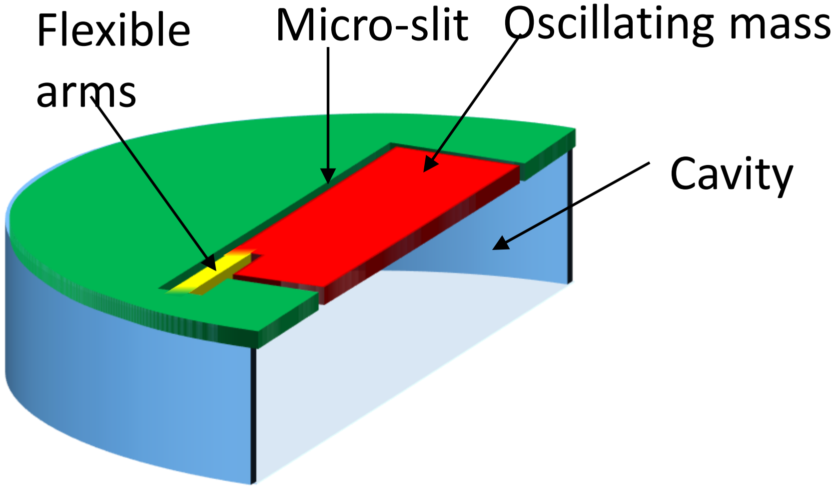

Micro-slit systems:

Leakage = Resistance

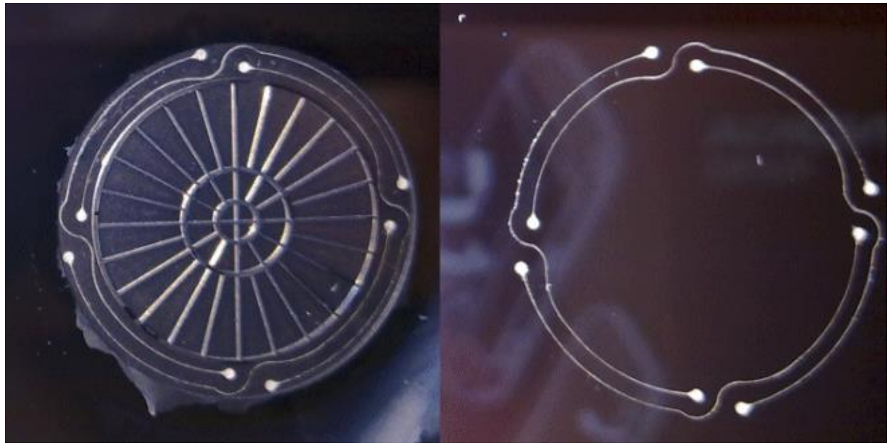

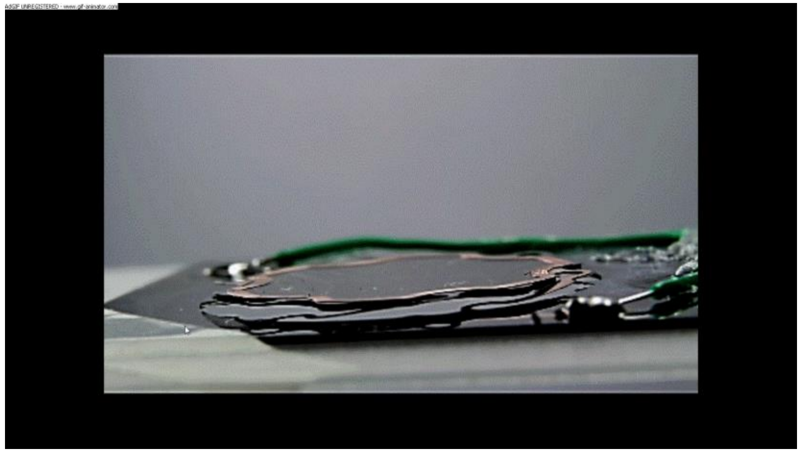

Part 5: Non-linear system identification in aeroacoustics

Niloofar Sayyad Khodashenas

H2020 MARIE SKŁODOWSKA-CURIE ACTIONS

Perforate Plate

Application of perforates

- Automotive mufflers
- Aircraft engines linear
- Combustion chambers

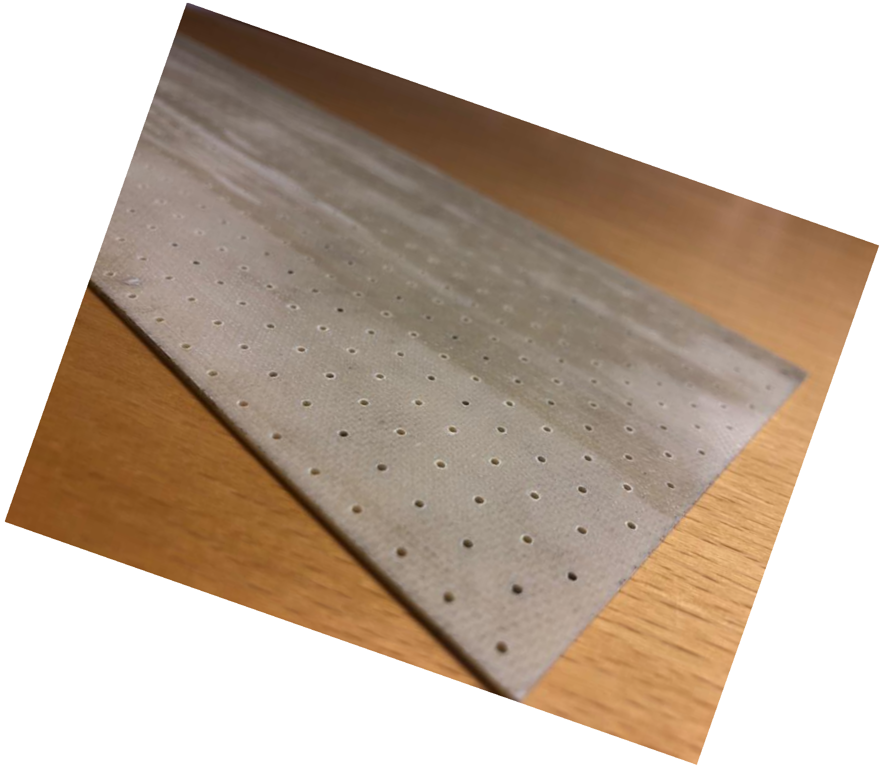

Noise control properties depend on

- Mean flow field
- Temperature
- Acoustic excitation level ✓

Perforate Plate

- Acoustic excitation level

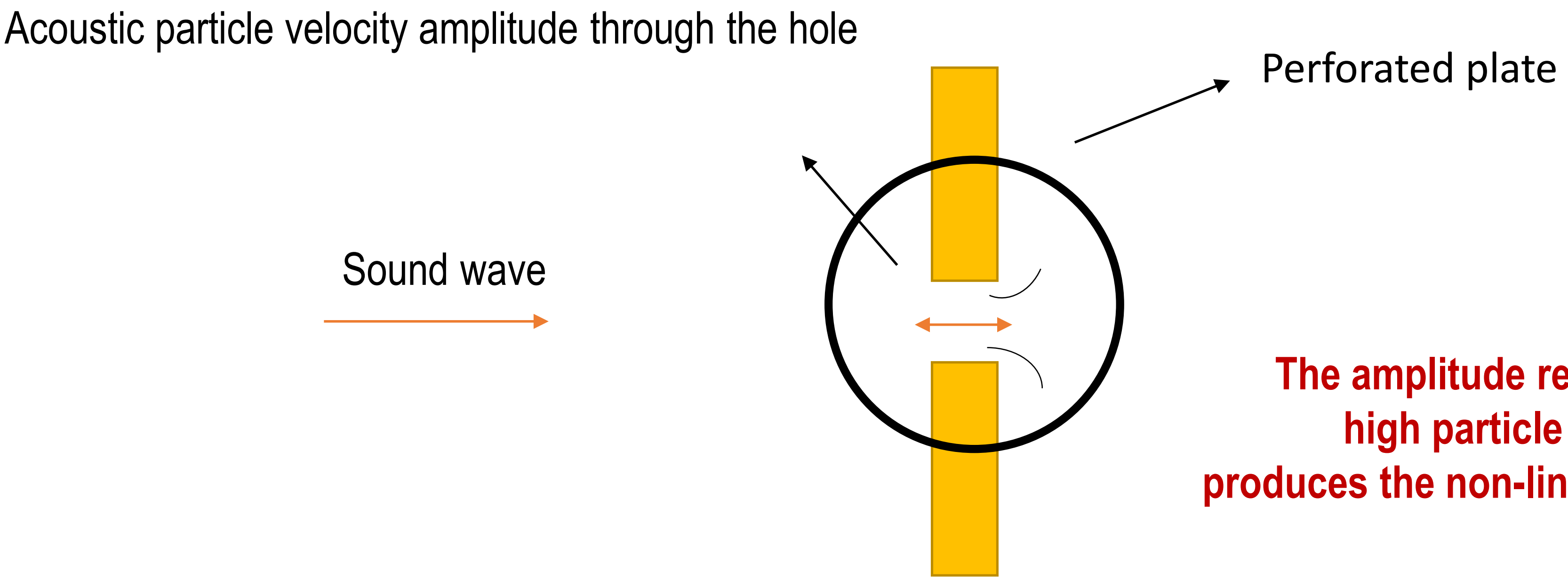

The amplitude related to the high particle velocity produces the non-linear phenomena

Main objective

- To study the non-linearity phenomenon at the perforated plate which is associated with large particle velocities.

- The non-linear acoustic properties including harmonic interaction from experiments using either random or periodic excitation

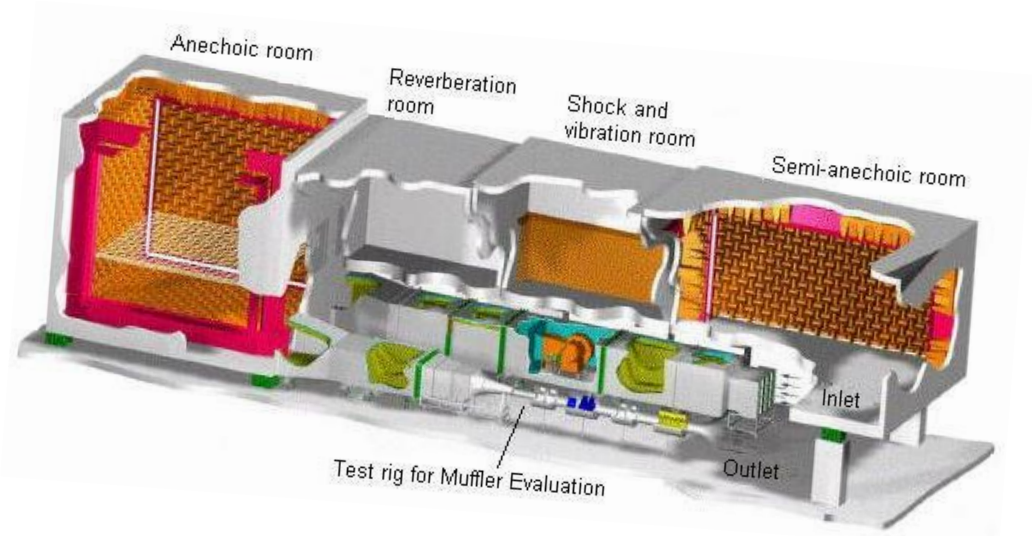

Experiment Setup

- ❖ Pipe
- ❖ Microphones
- ❖ Loudspeaker
- ❖ Perforated sample

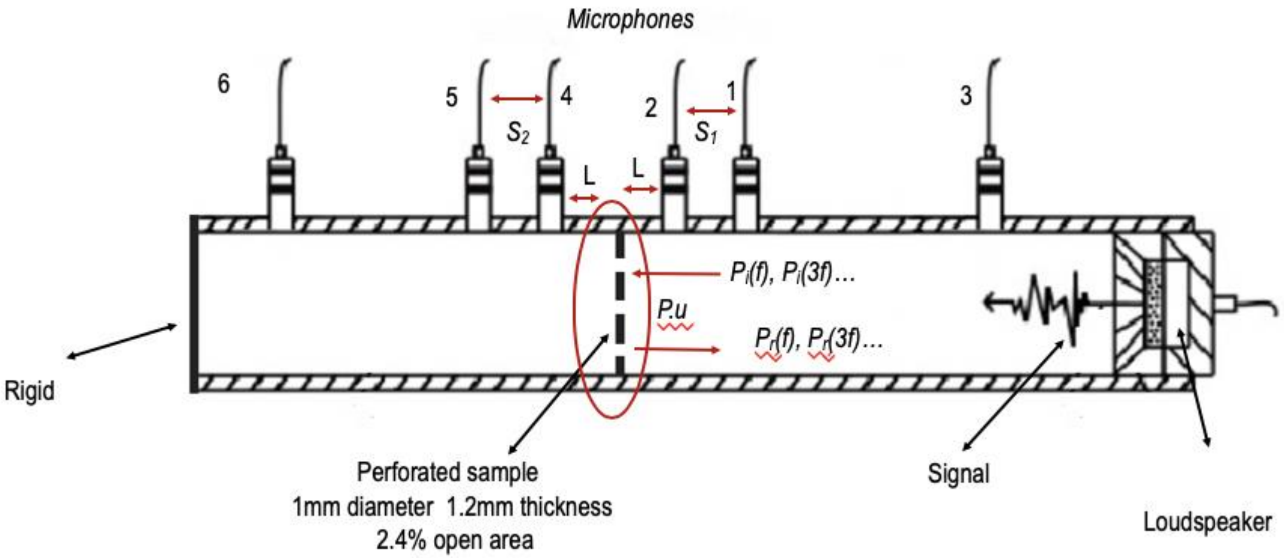

Model and Assumptions

$$\begin{pmatrix} P_r(f) \\ P_r(3f) \end{pmatrix} = \begin{bmatrix} S_{f,f} & S_{f,3f} \\ S_{3f,f} & S_{3f,3f} \end{bmatrix} \begin{pmatrix} P_i(f) \\ P_i(3f) \end{pmatrix}$$

$S_{f,3f} = 0$ ↔ **Negligible**

$S_{f,f} = R(f)$ ↔ **Reflection coefficient at *f* (non-linear)**

$S_{3f,3f} = R(3f)$ ↔ **Low level (linear) result at *3f***

$\boxed{S_{3f,f} = \dfrac{P_r(3f) - S_{3f,3f} P_i(3f)}{P_r(f)}}$ ↔ **Indication of harmonic interaction (non-linear)**

Experiment

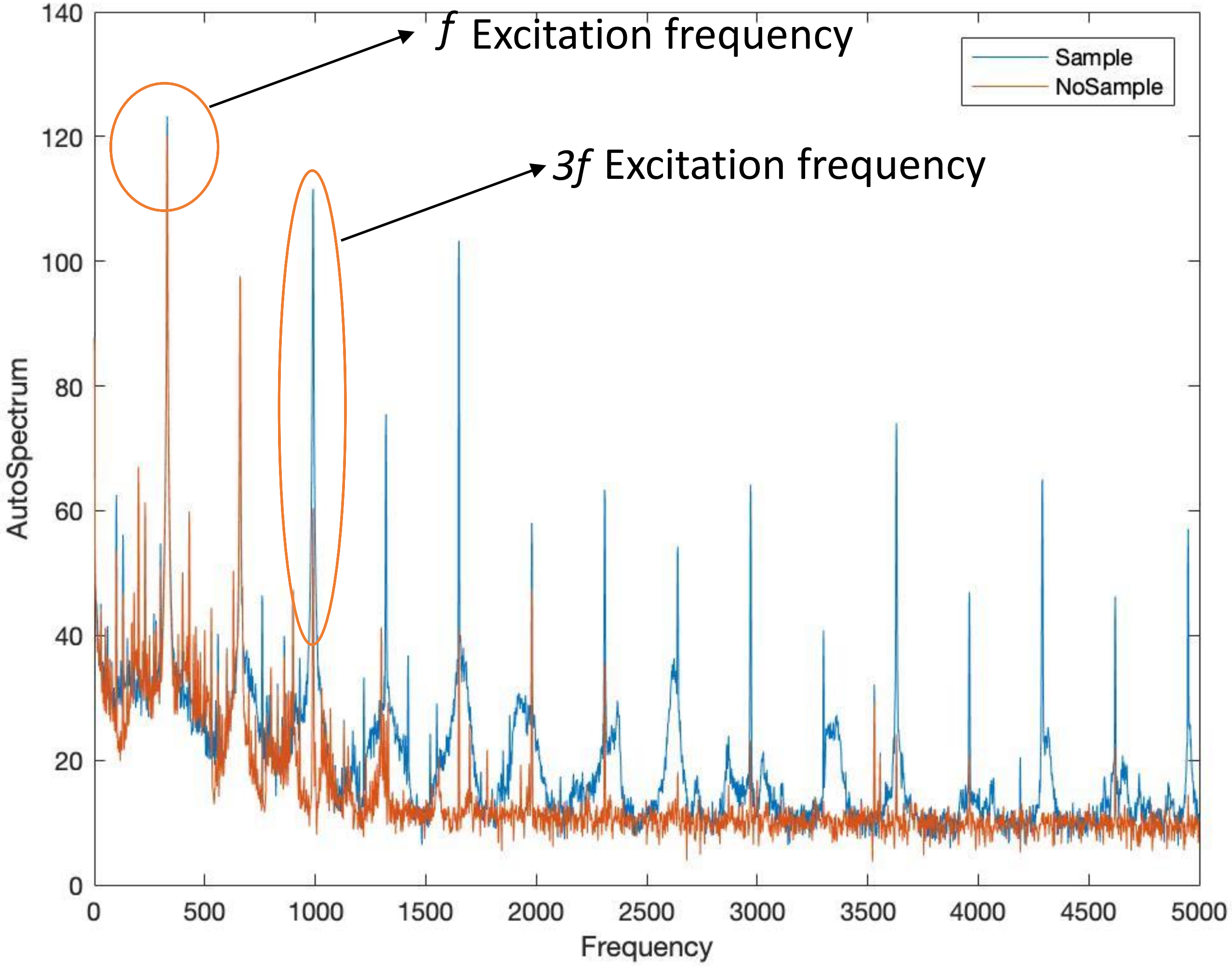

Non-linear is the
peak acoustic velocity in the hole

$$|u_H| \approx |u_N| / \sigma$$

Result

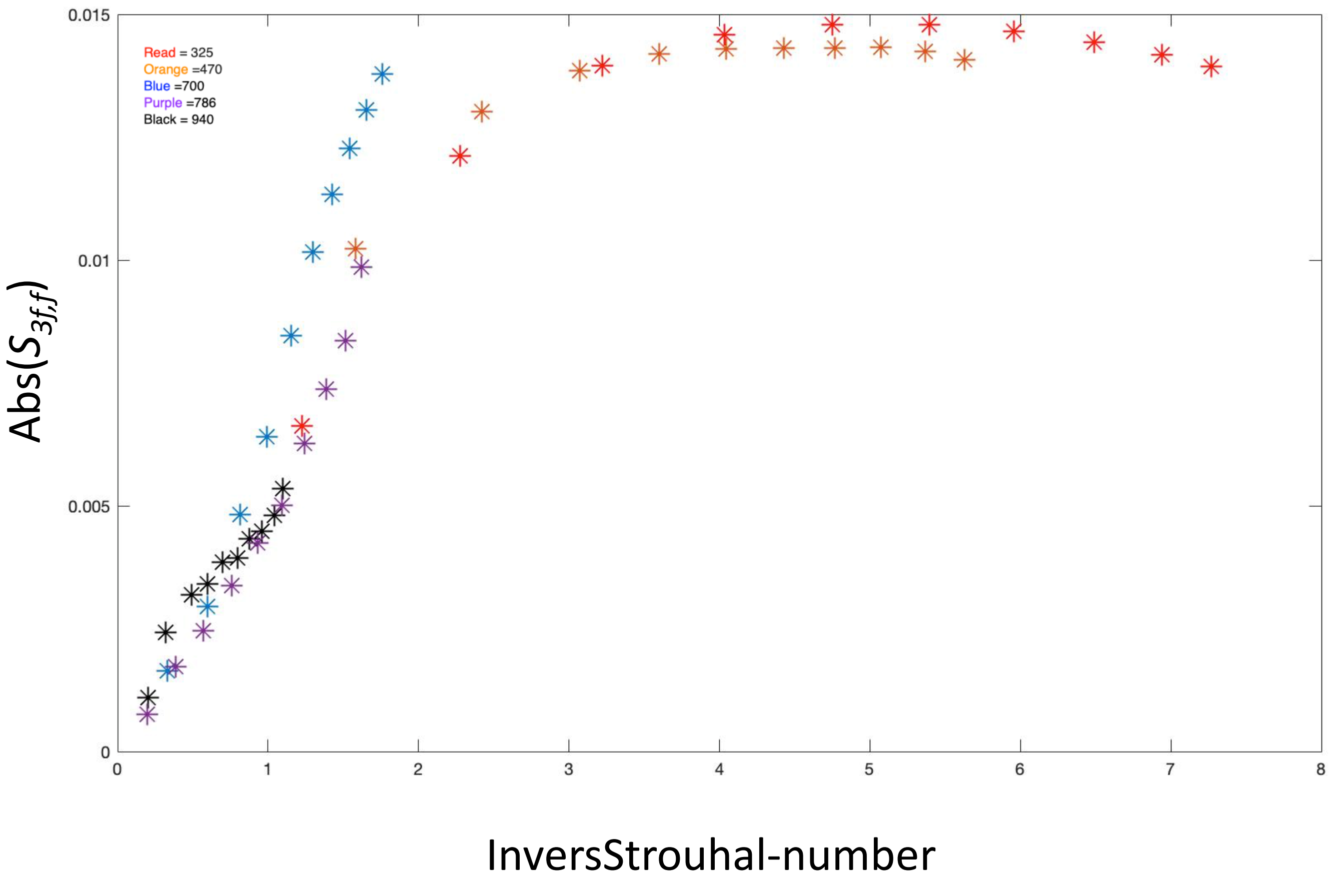

$$S_{3f,1f} = \frac{p_-(3f) - S_{33}p_+(3f)}{p_+(f)}$$

$S_{3f,f}$
is the scattering coefficient from
an incident frequency
to the third harmonic of that frequency

$$|u_H| \approx 1/\,S = u(f)/\omega/t$$

Future work

- Perform experiment
- Collect time data using both random and tonal excitation
- Analyze phase relation between harmonics for different types of excitation
- Compare non-linear scattering matrix results obtained using tonal and broadband excitation
- Analyze data using other non-linear system identification techniques

Smart ANSWER

Thank you for your attention !

THE FRAMEWORK PROGRAMME FOR RESEARCH AND INNOVATION
HORIZON 2020

MARIE CURIE ACTIONS

UNIVERSITY OF Southampton
Institute of Sound and Vibration Research

von KARMAN INSTITUTE FOR FLUID DYNAMICS

KU LEUVEN

EPFL
ÉCOLE POLYTECHNIQUE FÉDÉRALE DE LAUSANNE

TU Delft

National Technical University of Athens

CETIAT
ensemble, innover et valider

IMP PAN GDAŃSK

ÉCOLE CENTRALE LYON

LAUM

KTH VETENSKAP OCH KONST

Siemens PLM Software
SIEMENS

SIEMENS Gamesa
RENEWABLE ENERGY